AN INTEGRATED HYBRID THERMAL DYNAMICS MODEL AND ENERGY AWARE OPTIMIZATION FRAMEWORK FOR GRID-INTERACTIVE RESIDENTIAL BUILDING MANAGEMENT

by

Raheem Ariwoola

A dissertation submitted to the faculty of
The University of North Carolina at Charlotte
in partial fulfillment of the requirements
for the degree of Doctor of Philosophy in
Electrical Engineering

Charlotte

2023

Approved by:

Dr. Kamalasadan S

Dr. Chowdhury B

Dr. Cecchi V

ABSTRACT

RAHEEM ARIWOOLA. An Integrated Hybrid Thermal Dynamics Model and Energy Aware Optimization Framework for Grid-Interactive Residential Building Management. (Under the direction of DR. KAMALASADAN S)

This dissertation focuses on developing an integrated hybrid model for studying the thermal dynamic operations of passive buildings considering active power management. For this, the following methodology is designed. First, the hybrid model, including a procedure for identifying model parameters, is established. Second, the model is simulated and results compared with EnergyPlus^{TM} counterparts for validation using three different climatic zones. Third, the energy optimization framework considering all the active energy sources in the building is illustrated. Fourth, the model is utilized within Model Predictive Control (MPC) and optimization framework to demonstrate its capability for extensive applications in complex demand management programs and advanced transactive operations. For this, test cases were implemented, including energy management with Time of Use rates, power reference tracking, and demand response with load scheduling capabilities. Finally, a distributed energy resource aggregation framework that limits aggregate demand for multiple homes was formulated, to enforce grid limits and simultaneously achieve energy cost savings. The results show that the model has an average of 4% error compared with EnergyPlus^{TM} results, and the framework intuitively prioritizes natural ventilation operation while effectively coordinating building energy resources for an average of 63% reduction in peak electricity usage during the time of use event, an average of 1.2% error in power reference tracking, and a 49% to 56% gain on incentives during a load scheduling strategy in the evaluated zones. The aggregator framework proves efficient in reducing the aggregate demand of ten passive buildings from 160 kW (without aggregator oversight) to 97.5 kW (with aggregator oversight).

DEDICATION

This dissertation is dedicated to my family, who has been supporting and encouraging while navigating the challenges of graduate school and life together. To my parents and siblings; I am truly thankful for your financial and moral support. To my nuclear family, thanks for your unconditional love and perseverance. I am grateful for having you all in my life.

ACKNOWLEDGEMENTS

First and foremost, I am extremely grateful to Dr. Sukumar Kamalasadan for his constant guidance, invaluable advice, continuous support, and patience during my research course.

Next, I would like to extend my sincere appreciation to Dr. Badrul Chowdhury, Dr. Valentina Cecchi, and Dean Robert Keynton for serving on my dissertation committee and providing valuable comments and suggestions.

I would also like to thank my friends for listening to my bizarre thoughts and ideas, and for their support during challenging times.

Further, I acknowledge financial assistance, from the Graduate school for their support through the Graduate Assistant Support Plan (GASP) program and other grants from the National Renewable Energy Laboratory (NREL) and the National Science Foundation (NSF) towards my study.

TABLE OF CONTENTS

LIST OF TABLES

LIST OF FIGURES

LIST OF SYMBOLS AND ABBREVIATIONS

α Real/virtual battery self-discharge rate

α_{HVAC} Virtual battery self-discharge rate for the HVAC

α_w Virtual battery self-discharge rate for the water heater

Δ Size of the discrete time-steps

δ_T water heater thermostat deadband

$\dot{m}_i$ Zone supply air mass flow rate

$\dot{m_w}$ water heater mass flow rate

$\dot{m}_z$ Zone supply air mass flow rate

$\dot{m}_{infil}$ Zone infiltration air mass flow rate

$\dot{m}_{vent}$ Zone Ventilation air mass flow rate

$\dot{X_{HVAC}}$ Virtual battery energy state of the HVAC

$\dot{X_w}$ Virtual battery energy state of the water heater

η_a Heating Coil efficiency

$\eta_{ch,V}$ EV Battery Charging efficiency

η_{ch} Battery Charging efficiency

η_{dch} Battery Discharging efficiency

ω_s Windspeed

π_{as} Unit price of ancillary service payment

π_{grid} Unit price of electricity

ρ_{air} Air density

ρ_a Air density

A_i Zone's component surface area

A_{open} Door/Window opening area

C_D Discharge coefficient of the building component

C_h Heat capacity of the cooling or heating coil

$C_{in,z}$ Thermal capacitance of the zone air

C_p Specific heat capacity of water

c_p Specific heat capacity of air

c_T Heat capacity multiplier

C_w Opening effectiveness

C_z Zone Thermal capacitance

E_B Energy State of the Battery

$E_{max,B}$ Maximum Energy State of the Battery

$E_{max,V}$ Maximum Energy State of the EV Battery

$E_{min,B}$ Minimum Energy State of the Battery

$E_{min,V}$ Minimum Energy State of the EV Battery

E_V EV State of the Battery

F_{sch} Open Fenestration area fraction

h_i component heat transfer coefficient

J_{as} Ancillary service payment

J_{grid} Cost of electricity consumption

N_s Number of zones 's component surfaces

N_s Number of zones 's internal heat gain components

N_z Number of zones in the building

$P_{\text{non-flexible}}$ Power of non flexible loads

P_{as} power capacity for ancillary price

$P_{ch,Bmax}$ Maximum Battery Charging Power

$P_{ch,Vmax}$ Maximum EV Battery Charging Power

$P_{ch,V}$ EV Battery Charging Power

P_{ch} Battery Charging Power

$P_{dch,Bmax}$ Maximum Battery Discharging Power

P_{dch} Battery Discharging Power

P_{EV} Electric Vehicle Load

P_{grid} Incoming Utility Grid Power

P_{HVAC} Power of the HVAC equipment

P_{HVAC} Virtual battery power of the HVAC

P^{+}_{HVAC} Upper power flexibility bound for the HVAC

P^{-}_{HVAC} Lower power flexibility bound for the HVAC

P_h HVAC power

P_{le} Uncontrollable Building electrical Load

P_{load} Building Load

P_{pv} PV Power

P_{rated} Rated power of the Schedulable equipment

P_{ref} Reference Utility Grid Power

P_{sch} Schedulable loads Power

P_t Real/virtual battery power input referencing baseline profile

P_t^+ Total upper power flexibility bound

P_t^- Total lower power flexibility bound

P_w^+ Upper power flexibility bound for the water heater

P_w^- Lower power flexibility bound for the water heater

Q_{adj} Heat rate of the adjacent zones

Q_{HVAC} Coil sensible heating or cooling rate

Q_{inf} Zone Infiltration Heat rate

Q_{stack} Stack driven air flow rate

Q_{sup} Zone's supply air heating rate

$Q_{t,z}$ Convective heat transfer rate

Q_{total} Zone solar and internal heat gain rate

Q_{vent} Zone Ventilation rate

Q_{wh} Virtual battery power of the water heater

Q_{wh} Water heating element power

R Thermal resistance of the building envelope

R_{adj} Thermal resistance of the adjacent zones

R_j Thermal resistance of the adjacent zones

R_w Water heater thermal resistance

T_A HVAC equipment ambient temperature

T_a Ambient temperature

T_D Zone Determinant temperature

$T_{i,z}$ Zone's internal temperature

T_{in} Water heater incoming temperature

T_j Adjacent zones' temperature

T_{mix} Zone's mixed air temperature

T_{si} Zone's component surface temperature

T_{sp} Water heater predefined temperature setpoint

T_{sp} Zone's predefined temperature setpoint

T_s Zone's interior surface temperature

T_s Zone's supply air temperature

$T_{w,set}$ Heating hot water temperature setpoint

T_w Heating hot water temperature

T_{zi} Zone's interzonal air temperature

T_z Zone's interior temperature

U Control signal fraction for the electric heating element

u output

U_t Binary variable status of the Schedulable equipment

UA_a Thermal conductance between the heating coil and air

V Volume of the zone space

V_d Ventilation design value

V_v Ventilation volumetric flow rate

V_{wind} Wind driven air flow rate

w noise

$X_{\text{non-flex}}$ Energy states of non flexible loads

X^+_{HVAC} Upper energy flexibility bound for the HVAC

X^-_{HVAC} Lower energy flexibility bound for the HVAC

X_t Real/virtual battery energy state

X^+_t Total upper energy flexibility bound

X^-_t Total lower energy flexibility bound

X^+_w Upper energy flexibility bound for the water heater

X^-_w Lower energy flexibility bound for the water heater

y input

ASHRAE American Society of Heating, Refrigerating, and Air-Conditioning Engineers

COP Coefficient of Performance of cooling equipment

CVRMSE Coefficient of Variation of the Root Mean Square Error

DER Distributed Energy Resource

DLC Direct Load Control

DOE Department of Energy

DR Demand Response

DSM Demand Side Management

EE Energy Efficiency

EIA Energy Information Administration

EPA Environmental Protection Agency

EV Electric Vehicle

EWH Electric Water Heater

FERC Federal Energy Regulatory Commission

GASP Graduate Assistant Support Plan

GBM Generalized Battery Model

H Horizon

HVAC Heating, Ventilation, and Air Conditioning

IECC International Energy Conservation Codes

IoT Internet of Things

ISO Independent System Operator

MIP Mixed-Integer Programming

MPC Model Predictive Control

N Total Number of Buildings

NREL National Renewable Energy Laboratory

NSF National Science Foundation

PBEMS Passive Building Energy Management System

PGE Pacific Gas and Electric

PJM Pennsylvania-New Jersey-Maryland Interconnection

PNNL Pacific Northwest National Laboratory

PV Solar Photovoltaic

PV photovoltaic

RMSE Root Mean Square Error

RTO Regional Transmission Operator

SDGE San Diego Gas Electric

SOC State Of Charge

TCL Thermostatically Controlled Load

TOU Time-of-Use

TRNSYS Transient System Simulation Tool

TVA Tennessee Valley Authority

USDOE The United States Department of Energy

PREFACE

Hybrid ventilation is a key technology in modern passively-designed buildings for significant energy reductions and prevention of catastrophic grid failures. The technology ensures the building operates efficiently by prioritizing natural ventilation in efforts to simultaneously meet occupant's thermal comfort and reduce its power demands. But, due to its high sensitivity to climate, power use of hybrid ventilated buildings is intermittent, and its resulting effects on effective grid coordination are still lacking in research. Thus, this study proposed to develop efficient models, control, and optimization framework that confidently study the efficient operation of hybrid ventilated buildings in different climate regions to promote their widespread application globally.

CHAPTER 1: INTRODUCTION

The introduction to this dissertation starts with a general background about buildings and their distributed energy resources. It further illustrates the reasons why the improvement in building thermal dynamics is essential. These are followed by the motivation of the study, then the listing of the aim, objectives, and scope of the dissertation. Finally, the specific tasks accomplished and their contributions to the existing body of knowledge are provided.

1.1 Background

The current United States Energy Information Associationâs International Energy Outlook data projects that global energy consumption in buildings will have an average annual increase of 1.3% from 2018 to 2050 [1, 2]. With the alarming rate of fossil fuels depletion, the unstable fuel prices for conventional energy generation, and growing consensus about climate change's economic and social costs, US cities, institutions, businesses, and homes are operating under tremendous economic and sustainability pressures to decrease their energy consumption and set strict carbon reduction goals. With buildings inclusive, the world's energy consumption is projected to have a 50% increase by 2050 [3], and the power demand is projected to increase steadily by 5 percent annually [4], indicating a huge gap that must be met by either additional generation or energy reduction, or both. As for buildings, current developments in technology in terms of efficiency improvement, controls, and opportunities for utility microgrids integration have made them viable alternatives to accommodate such a vast and growing demand and simultaneously provide energy reduction applications, as small residences and commercial entities are continually incorporating the system

to reduce the electricity they utilize from the commercial utility grid for domestic consumption.

On another note, data has also revealed that renewable technology use in building is advancing to significant levels, and the worldwide growth of the system has increased rapidly from a niche market of diminutive applications to a mainstream power generation source [5]. This swift nearly-exponential growth has been attributed to the cost-effectiveness of the developed systems, the resilience of the system for continuous energy supply, the climate change mitigations, the innovations in renewable manufacturing such as solar PV, and the subsidies provided by the government [6]. As such, there have been increasing advantages attributable to energy use reduction in buildings, microgrid generation, and storage.

The building's design, construction, and operation significantly impact its energy use, air quality, and thermal comfort. The enthusiasm to combat the climate crisis and reduce utility bills has driven consumers and concerned stakeholders to adopt different rigorous energy efficiency strategies. Interestingly, for buildings, passive designs that work with natural ventilation principles can be explored to achieve indoor air thermal comfort. As the building sector remains responsible for the USA's highest energy utilization [7], consumers nowadays explore passive approaches to reduce or avoid the power demands necessary to operate the buildings. Unsurprisingly, thermal comforts and air quality in passive buildings rely heavily on outdoor climatic conditions, which at times can be extreme. Occasionally, for comfort, occupants need additional heating or cooling supplied by mechanical Heating, Ventilation, and Air Conditioning (HVAC) loads in severe weather conditions.

Current additions of Photovoltaics (PV) systems, Batteries, Electric Water Heaters, and other Distributed Energy Resources (DER) have driven the operation of passive buildings to a new dimension and made it more complex. There is a strong need for managing the resulting intermittent demands from such buildings for efficient and

resilient grids. Thus, this work investigates an integrated hybrid model of buildings in three different ASHRAE climate regions operating in passive, controlled-passive, and active modes. The proposed model's simulation results are then compared with a benchmark model, EnergyPlus^{TM}, developed by the U.S. Department of Energy (USDOE) to establish significant accuracy levels.

Natural ventilation allows for building air circulation from the external and internal environment by natural forces, unaided by mechanical systems resulting in less energy usage. Generally, recent, low-energy buildings have attracted significant research attention, most of which focused on building designs, construction, energy-efficient equipment, and the addition of alternative energy sources. Asides from natural ventilation, other building-science principles used by passive buildings to minimize or eliminate their building operational energy demand include super insulations, extremely air-tight envelopes, and controlled internal and solar heat gains [8].

The designs for passive buildings differ across several climates, and indoor air thermal comforts are generally challenging to achieve by natural means in severe regions. In such a harsh environment, supplementary power from the utility grid or onsite renewable is necessary to support additional heating or conditioning from efficient mechanical HVAC systems. Such systems have nowadays become significant key elements in demand management activities due to their flexibility in operations, controls, and energy uses. These inherent characteristics in the flexibility of building equipment operation can be explored to balance power supply and demand and to support the integration of onsite renewables with the utility grids [9], [10].

Buildings, primarily account for nearly 40% of all energy use in the USA [7]. Passive building requires less than 120 kWh/m^2/yr of treated floor area in primary energy demand [11]. Active buildings have unlimited demands and use mechanical systems to supply conditioned air for occupants' thermal comforts. Active buildings can share some similar features to passive buildings including extremely tight envelopes, build-

ing orientation, and thick insulations, but additionally, use automation systems or a combination of controllers to minimize energy usage. As a host to the most flexible loads and Distributed Energy Resources, the building requires an accurate and computationally efficient thermal dynamic model that precisely estimates and accurately predicts end-use electricity demands.

Contrary to the facilities operated by mechanical systems, detailed prediction of energy performance in passive buildings is often complicated due to airflow dynamics, sensitivity to weather conditions, and sensitivity to non-linear parameters originating from the controllable airflow openings in the building as windows and doors [12]. Prediction accuracy is highly essential in passive buildings because of the buildingâs slow reactions to future energy inputs, such as passive solar gains, which could subject the building to an increased chance of overheating or overcooling periods. Such occurrences bolster the requirement for sophisticated control schemes that accurately anticipate the thermal behavior of buildings and their predictable energy gains needed in the demand management analysis of energy markets.

1.2 Motivation

The residential building sector accounts for approximately 37% of the total U.S. electricity consumption [13]. Another recent report from consumer surveys indicated that approximately 90% of consumers have enthusiasm to either support or materialize advanced technologies for demand side management [14, 15]. This prioritizes residential building sector as a leading candidate for Energy management targets and Demand Response applications. As, such, to study the buildings for these services, models are required.

The models representing building thermal dynamics can generally be categorized into three distinct classes: the physics-based or white-box models, the data-driven or black-box models, and the hybrid-based or grey-box models [16–20]. The hybrid-based model is well proven as a simplified, flexible, detailed, and accurate model that

captures the strengths of the physics-based and the data-driven models [19–22], and as a result, is utilized extensively in this work. Recent studies have established that the building HVAC system and controls model is heterogeneous and complex [18, 23, 24]. Thus, as we transition to the smart energy future, building operations and the controls of its heterogeneous subsystems are correspondingly increasing in complexity.

The complexities are even more significant if the buildings are designed for residential-specific applications (such as for natural ventilation) or if any critical grid applications require clustering the buildings for an aggregated level control. As such, there are gaps in the literature on the modeling procedure that would best balance the building model's accuracy, data requirement, computational efficiency, and generalization capability [20, 25]. Proposed recommendations from literature for future modeling include breaking a comprehensive model into sub-models or using an integrated modeling methodology that enables an intuitive representation of the building system with a topology that considers the interaction between physical and intrinsic characteristics of individual building components [20, 24, 26].

In addition, modeling consistency, and building energy resources unification have been found essential in controls and grid-interactive energy management applications [27]. For a building to be treated as a single system, its thermostatically controlled load (TCL) models often include time constant parameters (such as R and C parameters) that need to be combined and represented similarly with other typical resources such as batteries and electric vehicles. For flexible characterization and coordination of these loads, the unification of the parameters using reduced-order models in the form of a generalized battery model (GBM) is essential [27].

1.3 Problem Statement

It is often difficult to obtain the exact building thermal dynamics model or parameter values that reveal accurate performance and physical reality of the buildings [18], [28], [20]. Existing comprehensive building energy simulation tools, such

as EnergyPlus^{TM} and TRNSYS are complex because they require vast amounts of well-detailed data for simulations. They are also lacking in flexibility and computationally inefficiency because mostly, they focus on a single building, have a slow run-time, and are unsuitable for simulations requiring fast-changing signals such as frequency regulations. Such reasons have made them inadequate for predictive and grid control applications, which raised the need for simplified hybrid models using discretized equations that accurately capture the building physics and simultaneously fill the gaps of the existing models including fast runtime and simplicity [29]. Although the hybrid models cannot match the details and accuracy of well-detailed simulation engines like EnergyPlus^{TM}, they, however, provide reasonably accurate results and overcome the limitations of the existing software.

1.4 Research Aim

This study aims to develop an efficient integrated building thermal dynamics model, control, and optimization framework for hybrid ventilated residential buildings that confidently study their efficient operation in different climate regions.

1.5 Research Objectives

The main contributions of the proposed work compared to the state-of-the-art are as follows:

- Identify the research gaps in parameter generation procedures, applicabilities, and implementations of the building thermal models for special applications such as hybrid ventilation operation and optimization.
- Present the current modeling challenges and requirements needed for advanced models to interoperate with the ever-developing smart grid applications.
- Develop a simplified and generalized residential building thermal model that incorporates the three distinct operational modes of passively designed buildings that have not been designed in the state-of-the-art.

- Propose a framework can use naturally ventilated building techniques as much as possible and thoroughly analyzes their comfort potential across different US ASHRAE climate zones.

- Develop a simplified functional hybrid controller using a logic-based rule to maximize the use of natural ventilation for comfort in residential buildings while simultaneously managing the building energy demands.

- Present the general performance, habitability, operability, and percentage demand reduction attributable to naturally ventilated residential buildings in three different American Society of Heating, Refrigerating and Air-Conditioning Engineers (ASHRAE) specified climate regions.

- Present a simplified functional hybrid operation mode of operation usable on residential building thermal dynamic models for aggregated level control of buildings designed to use natural ventilation.

- Present a scalable and extensible model predictive strategy that makes the building energy aware (can manage the energy consumption) for real-time control of the intermittent operation of active systems in hybrid ventilated buildings considering other large populations of building electrical loads.

1.6 Research Scope

This research focuses on residential hybrid ventilated buildings which are meant to operate by prioritizing natural ventilation in efforts to meet occupants' thermal comforts and reduce their power demands simultaneously. The process of generating their thermal dynamics was developed, and the sequential control modes were analyzed. The developed modeling techniques process was then applied to three buildings in different ASHRAE climate regions. Based on the models of these regions, demand side management through the respective distributed energy resources of one of the

buildings along with the potential utility savings were analyzed to prepare the model for more advanced studies and community-level aggregation.

1.7 Main Research Contributions

In order to achieve the aforementioned objectives, considering the scope of this study, the work is sectioned into different key tasks. Each of the tasks and major contributions accomplished with them is summarized in the next subsections.

1.7.1 Contribution 1: Develop a Hybrid Building Model Interoperable with Future Smart Grid Architecture

The main contributions are:

- Created a novel integrated hybrid building thermal model for buildings with special application requirements such as hybrid ventilation operation.
- Developed an extensible simulation framework using a Python library, consisting of a detailed house thermal model and a large population of distributed energy resource models.
- Developed a parametric identification methodological framework with Levenberg Marquardt Algorithm that accounts for a wide variation of nonlinear inputs, specifically from the weather parameters of hybrid ventilated buildings.
- Analytically Validated the developed integrated hybrid building thermal models with standards from EnergyPlus™.

1.7.2 Contribution 2: Develop Functional Hybrid Operation Modes for Residential Buildings

The main contributions are:

- Developed three distinct functional operational modes of passively designed buildings that have not been designed in the state-of-the-art.

- Developed a simplified functional hybrid ventilation controller using a logic-based algorithm to prioritize the use of natural ventilation for comfort in residential buildings.
- Developed a complete framework for implementing mixed mode operation of hybrid ventilated buildings, including load reduction potential such that zone internal temperatures are maintained within occupant's desired range.
- Analytically established percentage energy reduction attributable to the operation of naturally ventilated residential buildings in three different ASHRAE-specified climate regions.

1.7.3 Contribution 3: Develop an Optimization Framework that Further makes the Building Energy Aware

The main contributions are:

- Developed a scalable and extensible framework for implementing model predictive strategy operation of hybrid ventilated buildings for real-time control of the intermittent operation of their active systems.
- Used three distinct test cases of demand side management to gain insight into the efficacy of the model predictive optimization framework in supporting grid regulation and optimally providing reliability.
- The proposed optimization framework is validated for the correctness of operation through power balance analysis.
- Analytically established benefits such as incentives gain or percentage energy reduction attributable to the participation of the hybrid buildings on three test cases.
- The impacts of the various constraints and the operating response of DERs during Energy management events are better understood.

1.7.4 Contribution 4: Develop an Aggregator Framework using Virtual Battery Model to Unify Resources and Quantify Flexibilities of Passive Buildings

The main contributions are:

- Proposed a simultaneous optimization-based flexibility characterization strategy and aggregator oversight for a large population of passive buildings designed for special applications such as hybrid ventilation.
- Developed an MPC-based dispatched algorithm for passive building energy resources and a hierarchical coordination framework that allows aggregators for effective grid compliance.
- Analytically quantified the benefit assessments of coordinating aggregated distributed loads for grid services rather than independently.

1.8 Summary and Organization of the Dissertation

In this chapter, the general background of residential buildings, their distributed energy resources, and energy outlooks was provided. The motivation of the study, as well as the reasons why improvements in building thermal dynamics are essential, were stated. The research aim, objectives, and scope of the dissertation were highlighted. Finally, the specific tasks accomplished and their contributions to the existing body of knowledge were also provided.

The remainder of the dissertation has been structured as follows. Literature reviews relating to the scope of this study are discussed in Chapter 2. The proposed hybrid thermal model for the residential building is presented in Chapter 3, where the tested residential buildings that verify the building models based on ASHRAE climate zones were provided. Chapter 4 presents the functional hybrid operation modes for the building and the results for load reduction capability are highlighted. Chapter 5 presents the model predictive optimization framework developed for this study and

is followed by the results and discussions of the test case applications. Chapter 6 discusses aggregator formulations for grid requirements enforcement and quantifying the flexibilities of Passive buildings for other grid services. This is also followed by conclusions and future works in Chapter 7.

CHAPTER 2: LITERATURE REVIEW

The scheme of this study was discussed in the previous chapter. Working in accordance with the plan, it is important to review the current state of the art in building thermal dynamics, building energy management, smart grid architecture and services, optimization and model predictive controllers, and the research gap that eventually led us to novel ideas to accomplish the aim and objectives of this study.

2.1 Introduction

This chapter highlights comprehensive, relevant studies relating to building thermal dynamics, distributed energy resources, and their integration with smart grids. The first few sections provide relevant backgrounds on building energy use and the architecture of modern-day buildings. This is accompanied by literature reports that specifically targets the residential building sector. The later sections discussed the existing building model classifications, looking at parameters, modeling technique, and their application for smart grids. The chapter concludes by reviewing prior research works and identifying the knowledge gaps in realizing appropriate models compatible with the evolving smart grid architecture.

2.2 The U.S. Electricity System

The electricity system in the United States consists of a complex network of power generating plants, transmission lines, distribution lines, and consumers of electricity. This complex network is often termed the electric power grid. Fig. 2.1 illustrates the topology of the current state of a typical grid and how it has evolved [30].

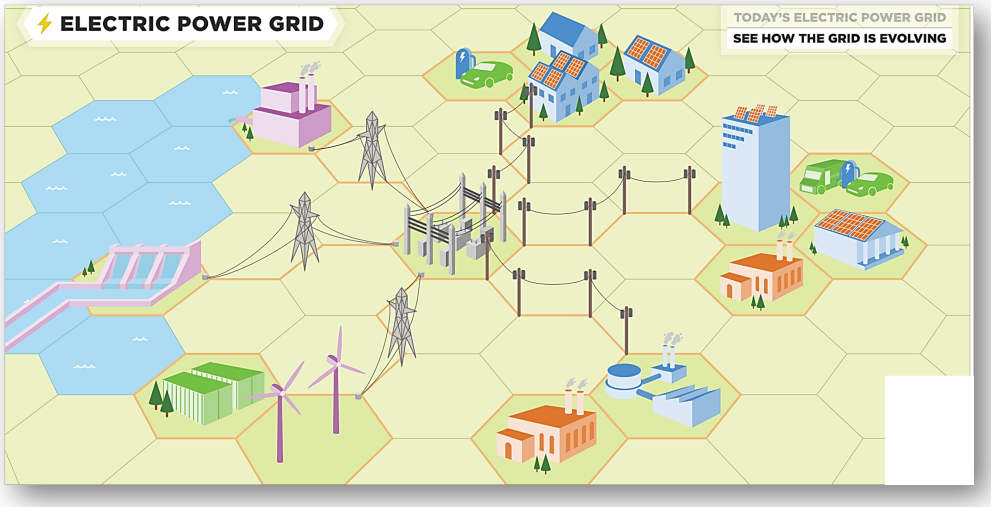

Fig. 2.1: The U.S. Electric Grid System [30]

One interesting thing about the electric power grid is that the generation by the plants and the consumption by the end-users of electricity must be continuously balanced at all times while minimizing the amount of loss in the lines. This has always been a challenge considering the modern power grids with varying levels of distributed generations. As such, both the power suppliers and end-users are key stakeholders in ensuring the reliability of the power grid.

2.3 Buildings Energy Use

The energy end users are broadly categorized into various sectors; residential, commercial, industrial, and transportation. Buildings are responsible for almost 40% of the USA's total energy consumption [7]. Residential and commercial buildings specifically are the front runners of higher electricity consumption in the United States when compared to other sectors such as industries and transportation [31]. Within the residential buildings sector, space heating and cooling, and operations of other Thermostatically Controlled Loads (TCLs) account for a significant fraction of the total electric demand [32].

2.3.1 Residential vs Commercial Buildings Energy Use Components

Even though residential and commercial buildings consume a significant amount of energy sources, what constitutes their energy uses are different. Fig. 2.3 compares the commercial and residential energy use in ENERGY STAR's building stock [33]. It can be observed that residential buildings have major appliances including washers, water heaters, refrigerators and freezers, dryers, and many more that are not prevalent in commercial buildings.

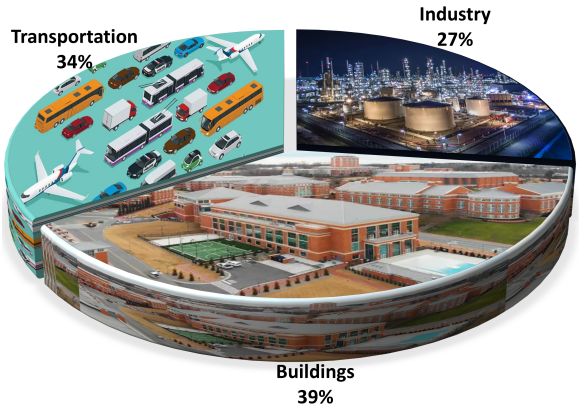

Fig. 2.2: The U.S. Energy Usage by Sector [7]

Also, the difference in residential building thermal dynamics and the commercial counterparts stem majorly from the schedule of operation and the insulating and optical properties of their building envelope, which govern how heat is stored, reflected, and radiated from the building. Table 2.2 shows the comparison between residential and commercial building envelope component properties. About 50% of the residential heating loads result from flows through the building envelopes, while this is around 60% in commercial buildings [33]. Infiltration also has a significant role in the heat gain in residential buildings.

The heterogeneity in the sources of the building's changing dynamics, including the thermal, fluid, and control system actions of the Heating, Ventilation, and Air-conditioning (HVAC) systems, has generated a requirement for a higher level of abstraction in building simulation and analysis [24]. Interestingly, buildings are becom-

ing smarter due to the way we operate, control, and integrate their resources within the developing smart grid architecture. The most recent advancement involves the increasing trends in the smart use of buildings for special applications, including hybrid ventilation for significant energy reduction [35]. However, significant challenges are limiting the development of simplified, accurate, and generalizable modeling techniques for such sophisticated special applications. These challenges are due to the complexity of the building dynamics attributable to variations in the paths and rates of the mass airflow, the presence of numerous uncertainties in the models used for performance prediction, the high sensitivity of the models to climate conditions, and the presence of control systems that have far more inputs which are either stochastic,

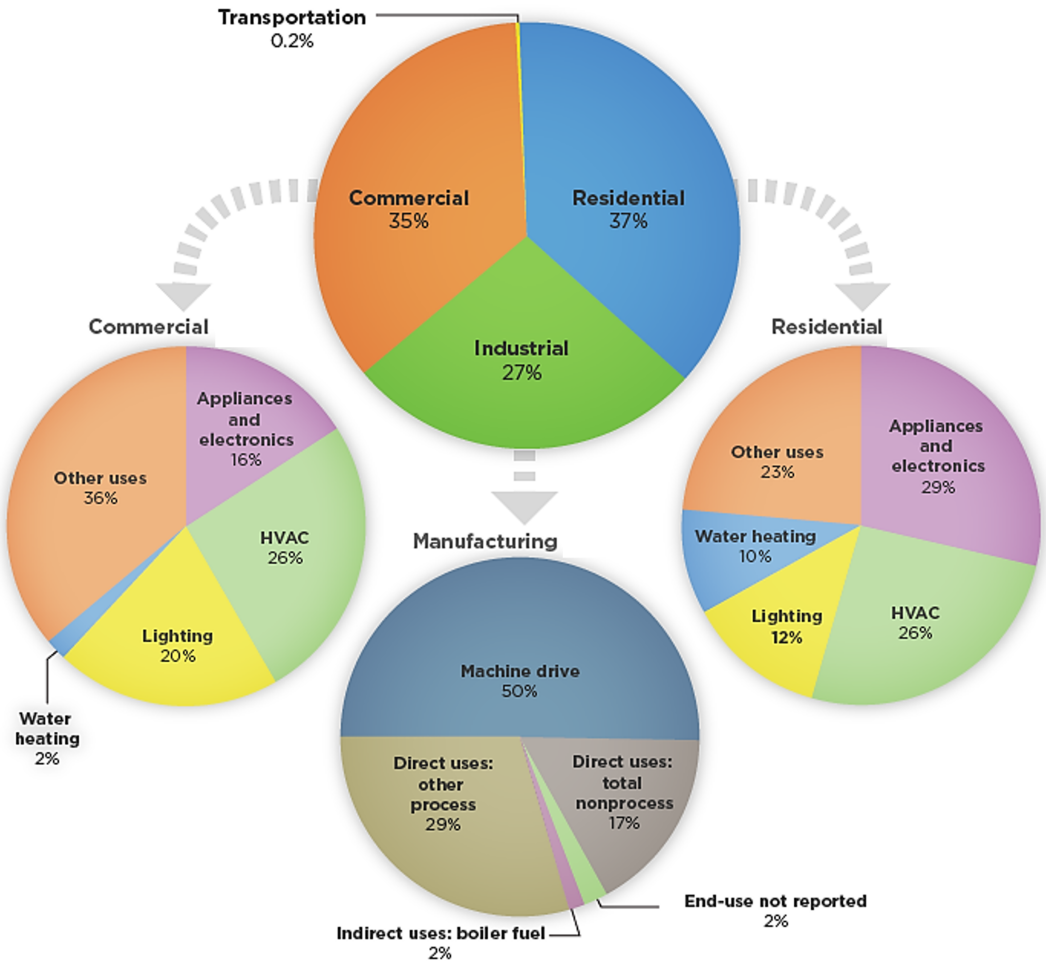

Fig. 2.3: The U.S. Electricity Consumption by Sector Energy and their End-use Categories [34]

discrete, nonlinear, and highly constrained parameters to process the models for grid applications.

2.4 Modern Building Architecture

The architecture of modern-day residential buildings is illustrated in Fig. 5.3. An increasing number of these buildings have integrated intelligence that uses Internet of Things (IoT) devices such as sensors, software, web-app, and other intelligent connectivity technology to monitor and optimize building operational activities [36–38]. Smart devices can analyze building data and use algorithm learning to identify usage patterns, trends, and potentials for operational optimizations.

Apart from the smart loads and devices, modern buildings contain other local power sources, electric vehicle charging stations, and energy storage that needs management. Through modeling, residential distributed energy resources can be aggregated to study community impacts on grid networks, and how these resources can interact with external controllers for automation, prediction, and optimization capabilities. These reasons and the supports of the transition to a smart energy future are the fundamental rationalities why building models are essential for building-grid simulation. Significant advances have been made in the past decades in model developments that can closely capture the thermal dynamic of buildings. As such simplified, accurate, generalized, and well-defined building models are required to upgrade the level of the research developments [20]. Apart from the previous reasons stated for the necessity of advanced building thermal dynamics, modern buildings with natural ventilation strategies are now in existence as many of them have been designed, constructed, and are fully operational [8, 11]. These types of buildings use passive strategies in conjunction with pressure and wind effects to supply fresh air to the internal building environment and remove air from an indoor space without the aid of any mechanical systems. According to [39] The listing of buildings in the U.S. and Canada, projects completed and verified between 2016 and 2019 rose 53%, and projects that are in

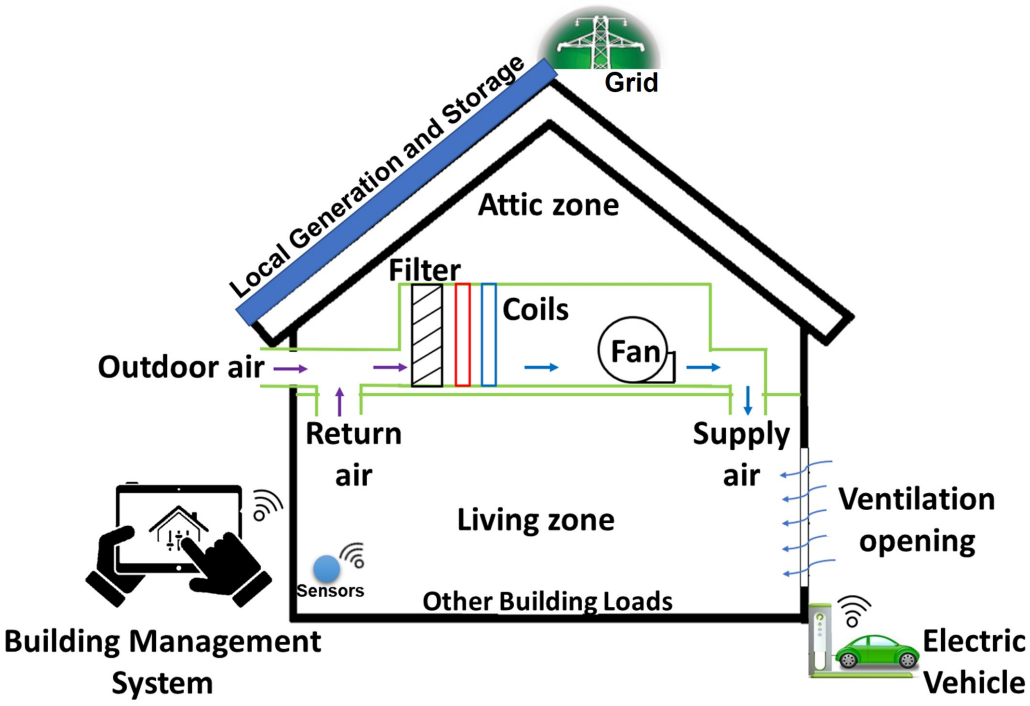

Fig. 2.4: Schematic of the Building with HVAC Equipment

planning or construction rose 79% [40]. These data confirm the idea that naturally ventilated buildings will continue to grow and become a larger percentage of the building stock over time. While these buildings are ground-breaking and highly efficient, for the most part, they rely on electricity supplied by the electrical grid, especially during inclement weather periods. Thus, comes the study of how they interact with the emerging smart grid architecture.

2.4.1 Passive Building with Hybrid Ventilation Technology in Comparison with other Modern Technologies

Modern building technologies are generating numerous opportunities for energy efficiency improvements. The use of smart devices has revolutionized the way we manage energy in our homes, however, the impact of hybrid ventilation technology in passively designed house construction cannot be overemphasized and how it compares with other forms of modern technology is stated in the following subsections.

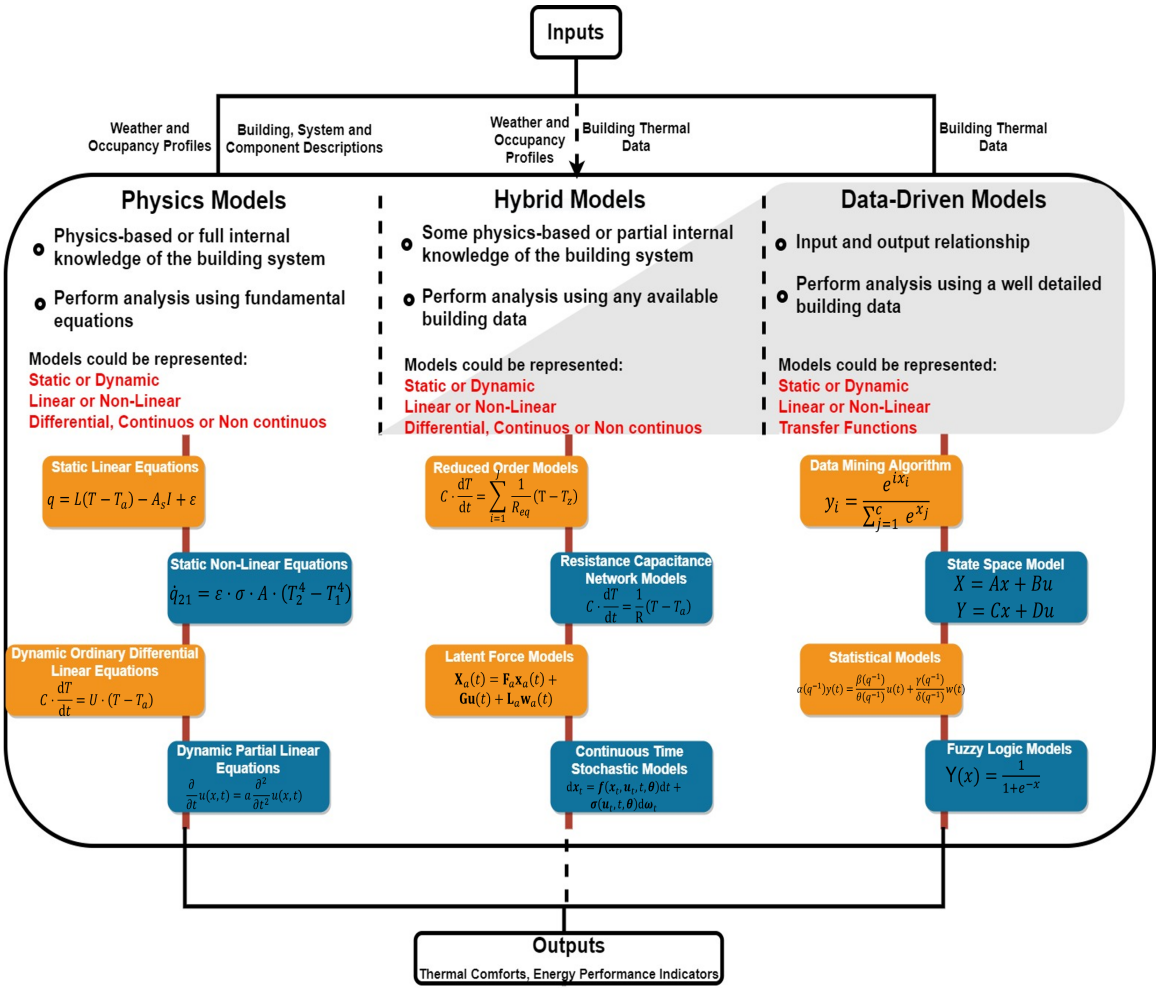

Fig. 2.5: Building Thermal Dynamic Models at a Glance.

2.4.1.1 Thermally-Heavy Building Advantage

A key benefit of the design is being able to economically heat and cool buildings without trading comfort. Most modern buildings still using smart technology alone require integration with the building's active systems, which are sometimes perceived as invasive. Various studies and tracked metering data show that buildings have been reported to consume 75% to 95% less energy than traditional counterparts when passively designed with hybrid ventilation technology [41–45]. An example of such a study is illustrated in Fig. 2.6. Similarly, Fig. 2.7 shows the apparent improved thermal quality from the surface temperature of a building after passive refurbishment, thus, visibly reinforcing the significant efficiency improvement of the technology.

Also, higher air quality and uniform indoor temperatures have also been reported to be significant in passive-designed buildings.

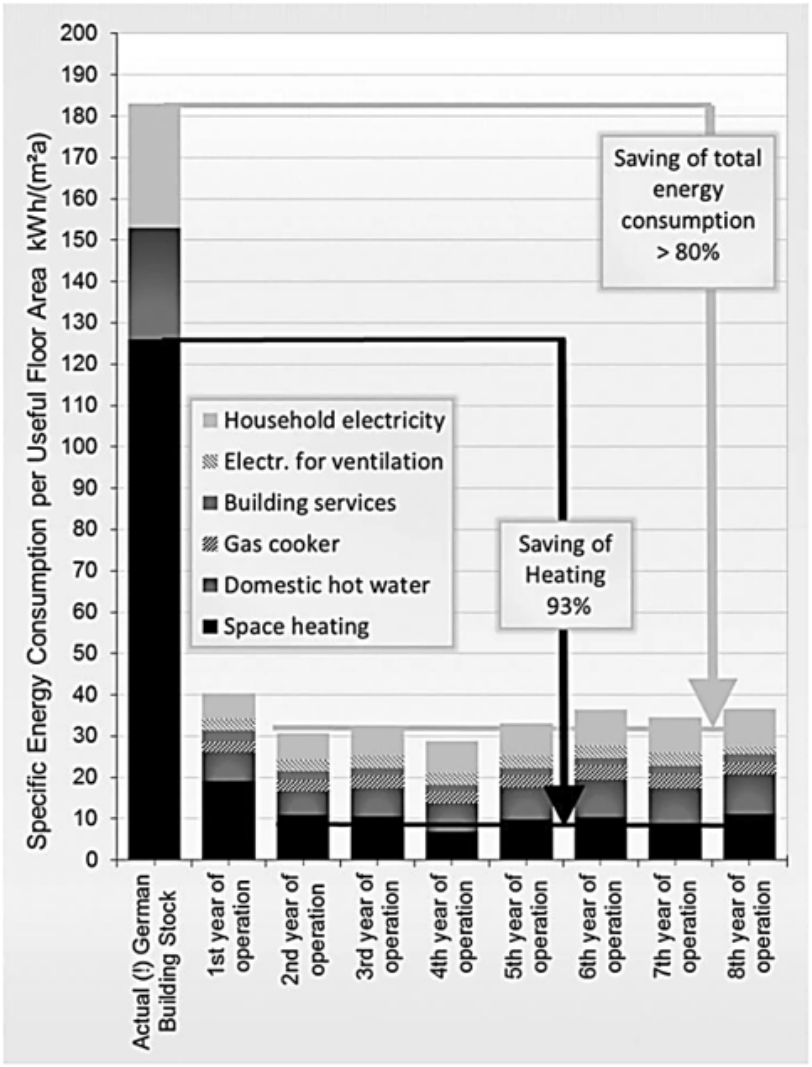

Fig. 2.6: Passive House Energy Use Comparison with Traditional Building [41]

2.4.1.2 Nested Energy Efficiency

Designing or configuring buildings to maintain superliner energy efficiency critical in advanced demand management. With basic controls, only passively designed buildings are able to achieve this level of efficiency. This is possible because, in addition to their base design which has already incorporated a significant level of energy reduction solutions, like other smart controlled buildings, the technology has the option to

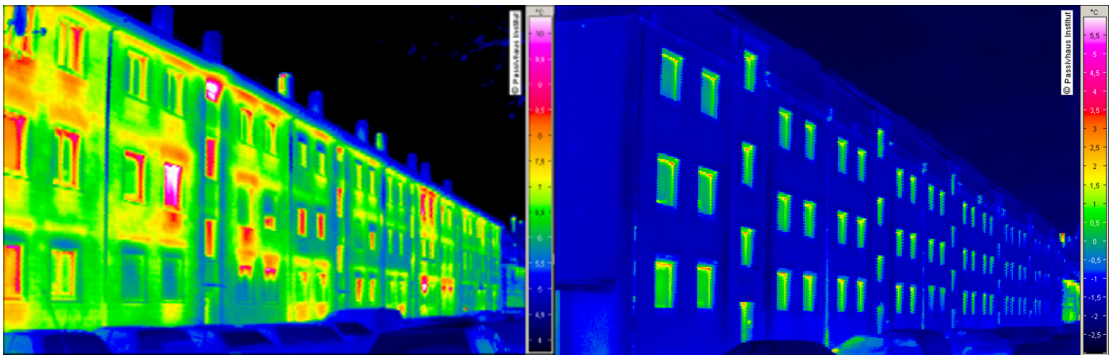

Fig. 2.7: Infrared Thermographic image of a traditional building before(left) and after (right) the passive refurbishment [46]

also accommodate the use of smart sensors, controllers, and optimization frameworks for a higher level of optimal energy efficiency operation.

2.4.1.3 Economically Viable Operation under extenuating Circumstances. (Covid-Ventilation)

Recent health and safety concerns have increased ventilation air usage. The recirculation of air is normally deployed to HVAC systems as energy saving strategy, however, this has resulted in increased infection risks, and ASHRAE proposed bringing in 100% of fresh outside air for conditioning [47, 48]. Significant operational variations of the HVAC systems occur during the pandemic [49, 50]. Studies have found that an average of 15% ventilation was increased across the board due to mechanical overventilation of buildings - a protocol that should largely have been supplemented with the use of hybrid ventilation technology.

The US EPA reports that an increased air rate from 2.5 L/(s.person) to 10 L/(s.person) will almost proportionately increase the HVAC systems operation costs by 2 to 10% [51]. Authors of [52] also presented that the energy use intensity of buildings would significantly increase by 150% if the ventilated air rate were to be raised from 0 to 200%.

The author of [53] quantifies the natural ventilation performance according to the window opening conditions and the infection probability during that operation. It was

reported that infection probability is less than 1% with the use of a mask and when windows are more than 15% open. However, the power used by HVAC for ventilation during the window openings increases by 10%. This reinforces the need for a controller that delivers the natural ventilation necessary for comfort while simultaneously keeping the HVAC demand very low.

2.4.1.4 Operational Generalization - Security/Optional Dependency on IoT

The hybrid ventilation technology is not exclusive to a certain building type. However, other smart technologies may be exclusive to operations in certain sectors due to their vulnerability to security attacks thereby limiting their functionality in certain applications. Examples include a targeted international hack at Penn State University through Wireless thermostats [54] and another international hack at an unnamed University through Smart bulbs, metering, and other wireless devices [55]. Finally, a similar hack from sophisticated foreign hackers gained significant remote access to lighting controllers in the operations networks through the snatching of a California universityâs housing files [56]. The aforementioned occurrences reinforced the necessity to keep our optimal energy efficiency operations out of smart devices from networks vulnerable to attacks with the evolving smart building technology.

2.4.1.5 Challenges

The challenges facing the technology however include a lack of consumer knowledge of how the financial works. Basically, these projects are designed with the main goal of reducing energy bills and improving occupants' comfort, even when this leads to initial higher construction costs. Typically initial costs of a passive house project are 3-5% higher than those of traditional construction [57] but worthwhile considering 75% to 95% in annual energy reduction.

2.5 Demand Side Management

The demand side management involves planning, monitoring, and controlling the activities relating to the electricity usage of consumers to maintain grid reliability [58]. It is an alternative way that electric system planners and control operators uses to balance the energy in the grid by altering load flexibility to suit available supply, rather than providing additional generation to meet the demand.

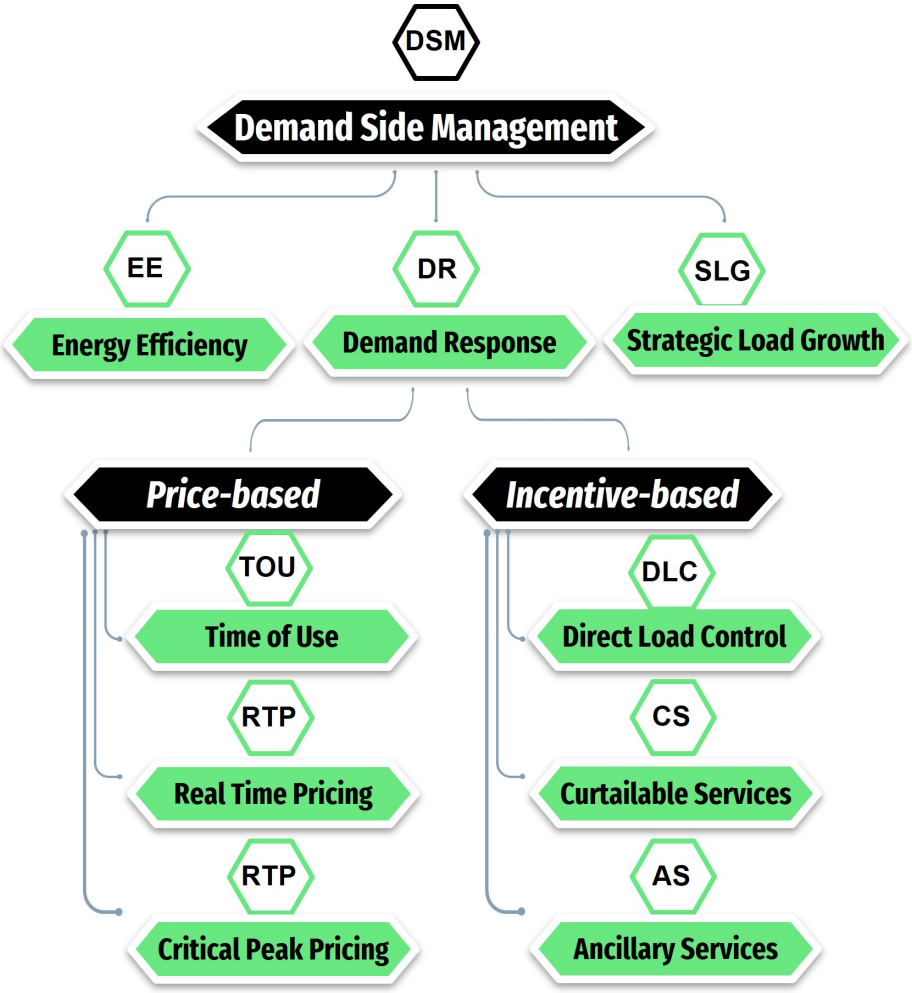

Fig. 2.8: Demand Side Management Chart

2.5.1 Demand Response in Residential Buildings

Demand response is an element of demand-side management and in the residential sector follows the retail level classification that can either be price-based or incentive-

based depending on the techniques being used to achieve or execute the program [59]. Demand response in the residential sector gives home owners a significant opportunity to reduce or shift their loads during peak periods in response to specific time-based rates or any other form of economic or incentive signal. Depending on the market structure, the demand response task is overseen by either the utility or Independent System Operators (ISOs) or Regional Transmission Operators (RTOs) that are classified as non-profit organizations. A report of electricity savings, and impacts specific to demand response is monitored by FERC [60]. A sample snapshot from USEIA is illustrated in Fig. 5.6.

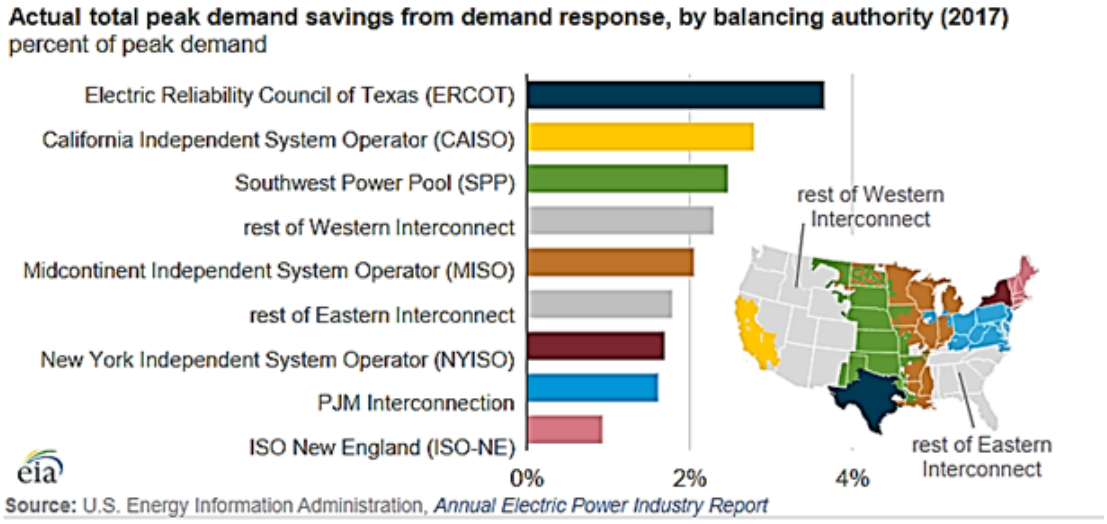

Fig. 2.9: Demand Response Savings by Balancing Authorities [61]

Demand response activity is widely spread across multiple sectors as entities prioritize economic savings on utilities. Fig. 5.6 highlights the Demand Response Savings by various Balancing Authorities in the United States. The PJM data in Fig. 5.7 illustrates the significant contributions from the residential sector till 2018/2019. Both charts of Fig. 5.7 compare the contribution of the residential sector from the PJM Demand Response report. According to the charts, it can be observed that the residential sector captured 18% of the total Demand Response market in 2018, while the number has reduced significantly in 2021. While it is impossible to neglect the

effects of nationwide pandemics, among other factors, on the reduction. It, however reinforces that other demand-side management can be prioritized for considerable electricity savings. Future projections show favorable expectations that demand response still continues to grow. Duke Energy expects the contribution from energy efficiency and demand response initiatives to hit 2050MW by 2035 [62].

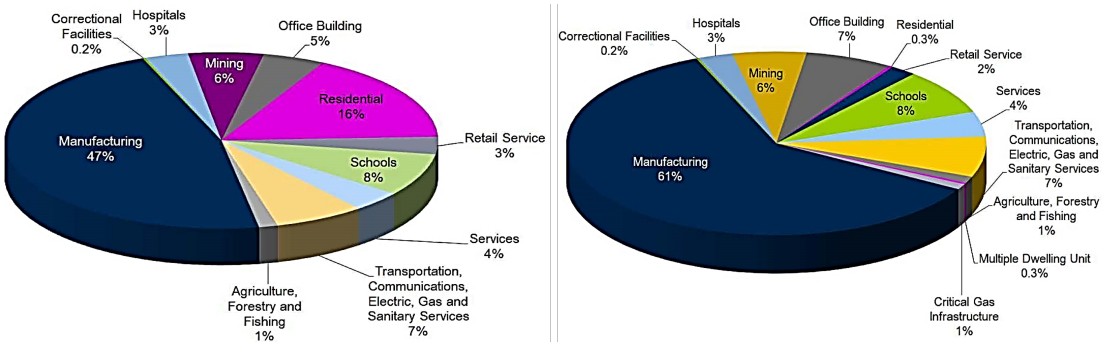

Fig. 2.10: Residential Load Management DR Registrations in 2018 [63] compared to 2021 [64]

In either the wholesale market or retail market, economic benefits and reliability drive the participation of consumers in demand side management events. Several previous works have studied wholesale DR, including; direct load control, emergency, capacity markets, ancillary services market, interruptible/curtailable loads, and demand bidding as listed by [38, 65–67], while in the retail market, efforts have been directed towards majorly price-based strategies that provide energy reduction benefits.

In price-based DR, allow consumers to exercise flexible consumption pattern through variable pricing mechanism with the aim of saving on utility bills. The common forms include Real-time Pricing (RTP), Time-Of-Use (TOU) Rates, and Critical Peak Pricing (CPP) [68, 69]. On the other hand, with the incentive based DR consumers are provided incentives for agreeing to participate in DR. The common forms include Direct Load Control (DLC), Interruptible/Curtailable Load, Emergency, and network. The differences between the pricing methodologies is explained in Table **??**

Table 2.1: Price-Based DR opportunities [70–76]

	TOU	CPP	RTP
Program	price and time periods are fixed in advance	Exercised during a few annual critical hours	Neither the price nor the time period is fixed in advance
Utility Benefits	reduce system costs	significantly reduce peaks	eliminates the necessity for expensive power plants
Consumer Benefits	flexible customer bills	flexible bills especially with Base load program	more control over utility bills
Pricing Type	Static	Intermediate	Dynamic
Practiced By	PG&E, PSE	Gulf Power, SDG&E, AEP Ohio	CommEd, Georgia Power, Duke Power, TVA

2.6 Building Energy Simulations

Building simulation engines help users understand building energy use categories, key performance indicators, generation and integration capabilities, and other analysis essential for research [77]. It takes multiple inputs such as building including geometry, lighting, water heating, HVAC, refrigeration, and renewable generation details. It integrates the aforementioned inputs with the local weather conditions, and the system configurations, operation and occupancy schedules, building component efficiencies, equipment setpoints, and control strategies to estimate the energy requirements for comfortable building operations.

A well-established and accurate building simulation models are currently in existence. Examples include EnergyPlus, BEopt, TRACE, DesignBuilder, eQUEST, TRNSYS, among others [78–82]. Yet, they are characterized by limitations inflexibilities, computational efficiencies, aggregation development capabilities, and many more [26]. These have made them unsuitable for most studies, including optimal

control implementation and smart grid applications involving frequency regulations, which require fast-changing dynamics. As adapted from [26]., Fig. 5.8a shows the architecture of a well-detailed simulation engine. In comparison, this work provided an architecture of a simplified building thermal dynamics model illustrated in Fig. 5.8b meant to perform similar functions as 5.8a

Table 2.2: Energy Flows in Building Envelopes (Quads) [33]

	Residential		Commercial	
Building component	Cooling	Heating	Cooling	Heating
Roofs	1.00	0.49	0.88	0.05
Walls	1.54	0.34	1.48	−0.03
Foundation	1.17	−0.22	0.79	−0.21
Infiltration	2.26	0.59	1.29	−0.15
Windows (conduction)	2.06	0.03	1.60	−0.30
Windows (solar heat gain)	−0.66	1.14	−0.97	1.38

It is important to acknowledge the insightful reviews that have been performed on building thermal dynamic models [17–19, 23]. For the benefit of the broad research audience, rather than discussing extensively the low-level classification of the models, structures, equations, strengths, and weaknesses, this study prioritizes reviews based on research gaps in parameter generation procedures, applicabilities, and implementations of the models for special applications such as hybrid ventilation operation and

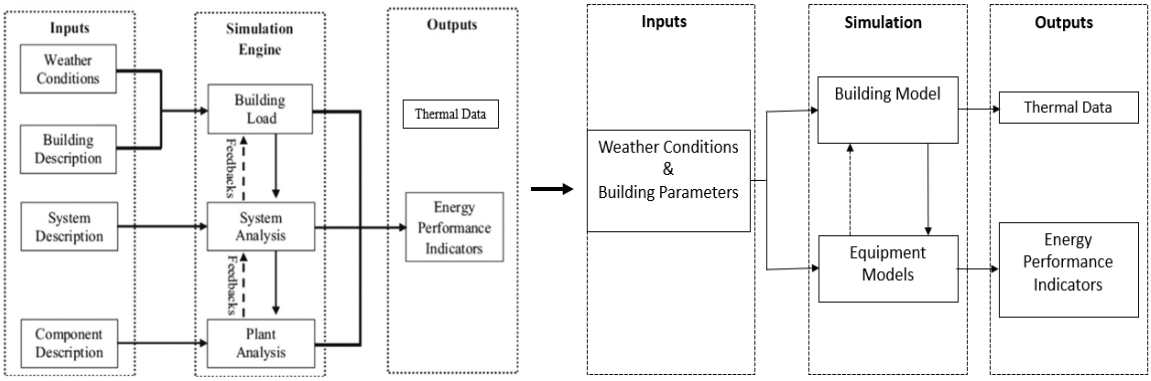

Fig. 2.11: (a) Sample Detailed Simulation Engine Architecture [26] (b)Sample Simplified Building Model Simulation Architecture

optimization. This study also examines the current modeling challenges and requirements needed for advanced models to interoperate with the ever-developing smart grid applications. Finally, this study investigates the necessity for further research efforts in the models for building thermal dynamics

2.7 Building Thermal Dynamics Models

The models for representing building thermal dynamics are extensively classified into physics (white box) models, data-driven (black box) models, and hybrid (grey box) models [16–20]. Their categorization depends on input parameters, structure, sophistication in computations, output details, and design purposes.

2.7.1 Physics Models

The Physics Models require a comprehensive knowledge of the various sub-systems and energy balance of the buildings. Current gaps in physics models are present in the subsections

2.7.1.1 Parameters

The physics model contains hundreds or thousands of input parameters usually obtained from the physical design characteristics, building components, and equipment nameplates. However, these parameters need to be obtained from onsite experiments especially, for an older building, and when the parameters are not readily available.

The parameters such as the heat transmission coefficients and heat capacities have physical significance in the modeling equations of the building. For example, in EnergyPlus, the transmission heat transfer occurs between the building zone internal space and the ambient environment is governed by the convective heat transfer rate between the two regions. The rate also depends on the component heat transfer coefficient, and the surface area of the building component, as represented in (1). The building zone interior heat capacity in (2) indicates how much heat is stored in a building and it is a function of the building zone volume.

$$Q_{t,z} = \sum_{i=1}^{N_s} h_i A_i (T_{si} - T_{i,z}) \tag{2.1}$$

$$C_{in,z} = V \rho_{air} c_p c_T \tag{2.2}$$

The accuracy of the physics model depends on the accuracy of these parameters. Building material deteriorates, and as a result, some of their parameters such as thermal resistance values change. The degradation is usually due to environmental conditions, active material deterioration, aging, building modifications, and usage patterns. A report from the U.S. Department of Energy test results has verified that thermal resistance (R) values of building components performance can decline as much as 50% over time [83]. Fig. 5.9 corroborates that notion by illustrating the degradation of the R-values of major insulation manufacturers when subjected to American Society for Testing and Materials (ASTM) C1303 standards tests [84].

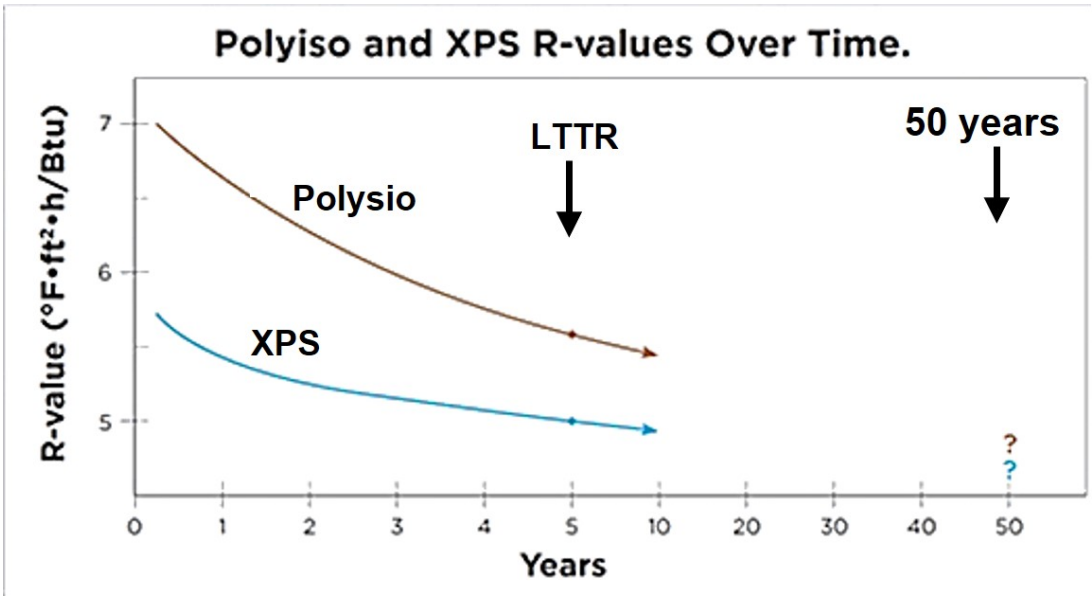

Fig. 2.12: Decline of Building Thermal Parameter Values Overtime [84]

On-site measurements using wall stratigraphy, Heat Flux Meters (HFM), and Infrared Thermography (IRT) methods, which are viable options in estimating component thermal parameters, require high expertise and are very expensive [28, 85]. Data

interpretations can also be challenging due to the influence of noise from climate conditions, shading, random reflections, or any other disturbance or extenuating circumstances affecting the procedure. Furthermore, the thermal resistance/conductance values are generally not consistent (homogeneous) throughout the area of a building envelope component [86]. As such, experiments of an area won't justify values for other areas of the building component.

2.7.1.2 Modeling Procedure

Often, physics models are characterized by design oversimplifications in characterizing human behaviours in buildings and deterministic scheduling, which eventually might introduce some errors [87]. Another example is an implicit design strategy

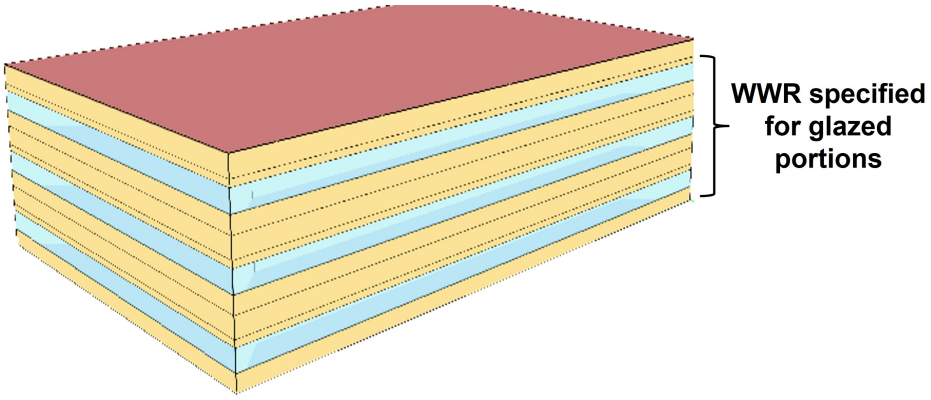

Fig. 2.13: Physics-based Building Modeling Procedure

regularly used by the developers of building models. In such a design, a Window to Wall Ratio (WWR) factor is often used to represent the glazed portion of the

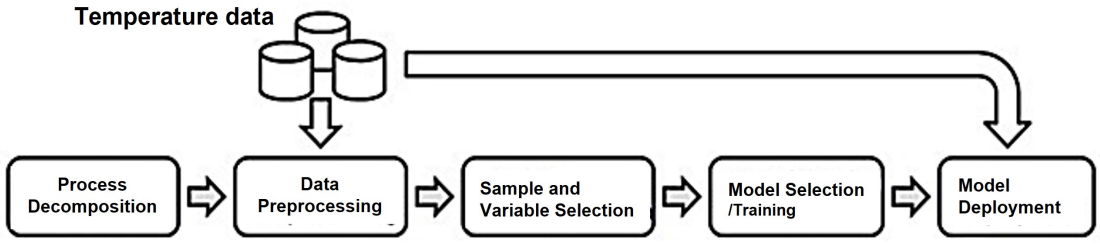

Fig. 2.14: Data-Driven Building Modeling Procedure.

building facade to reduce the set of larger windows in the designs [88]. Such implicit designs might have significant impacts inaccurately characterizing buildings designed for special applications such as natural ventilation.

Fig. 5.12 summarizes the major steps of the general physics method for building system identification.

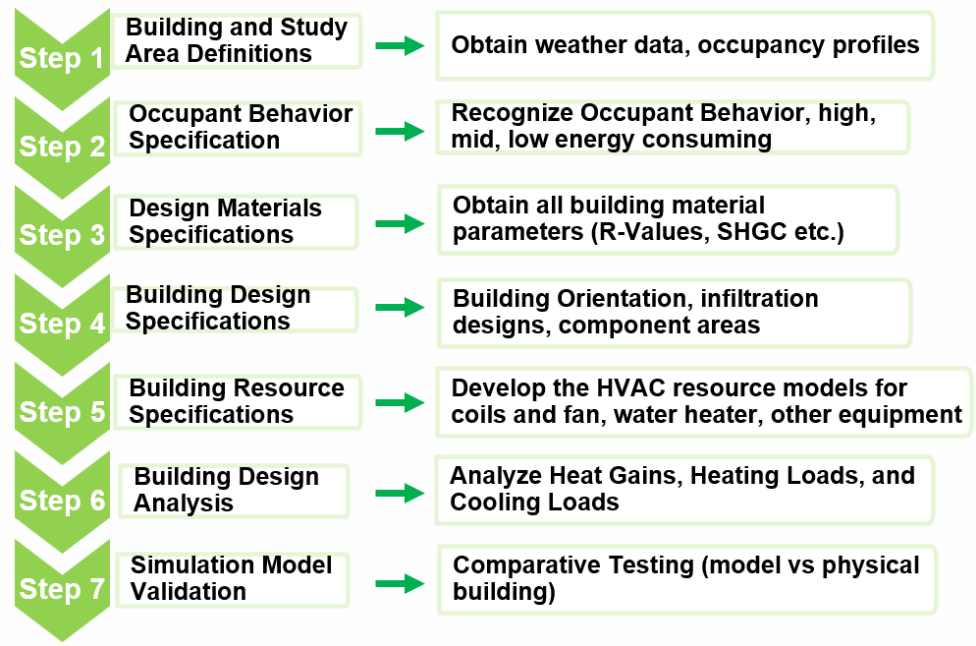

Fig. 2.15: Physics-based Building Modeling Procedure

2.7.1.3 Smart Grid Applications

The requirements for advanced controls include computational efficiency, fast-sensing, and flexibility to aggregate the models for the community-level analysis of building-grid interaction. Physics models fall short in any combination of the highlighted application requirements. In physics models including EnergyPlus, HVACSim, and TRANSYS, computations are performed on various detailed subsystems, thereby increasing their complexity. Computational efficiencies are also lower due to these comprehensive energy calculations and estimations [26]. In another context, BEOPT, BLAST, and DOE 2.1 currently do not aid high-resolution simulations lesser than an hour. These characteristics negatively impact the use of these models for several

applications involving fast-changing dynamics in power grid analysis.

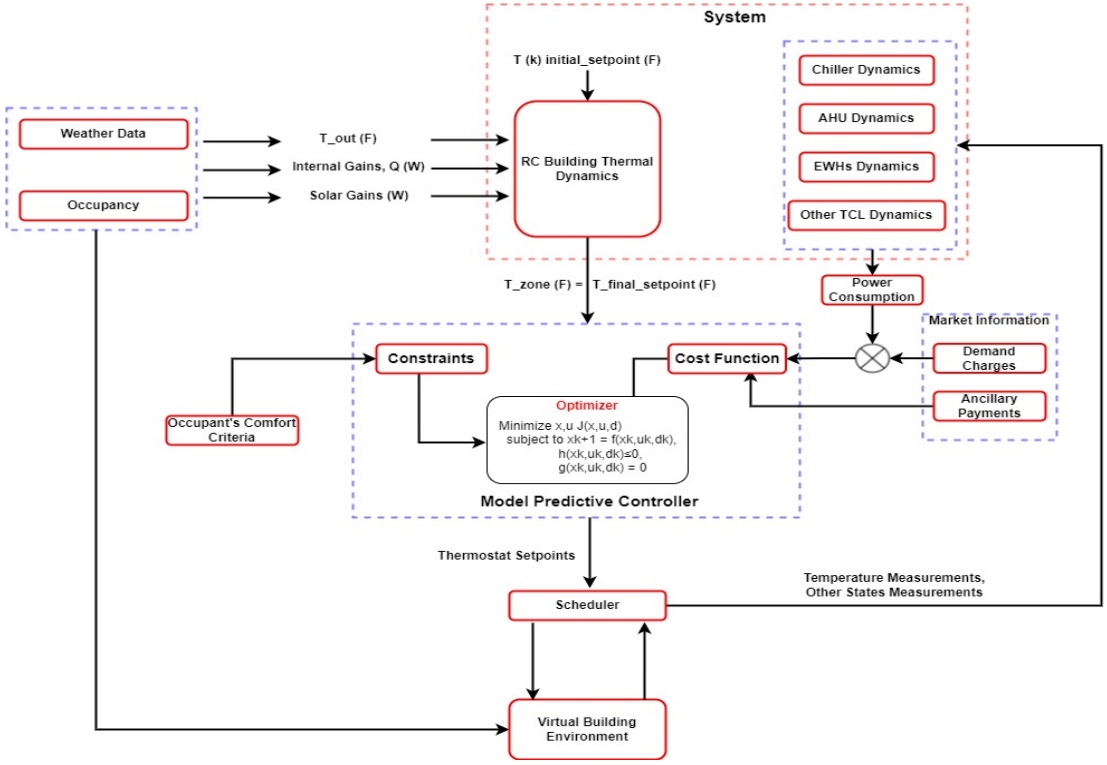

Fig. 2.16: Common Building Management and Thermal Dynamics Framework

2.7.2 Data Driven Models

The data-driven require a vast amount of high-quality data to obtain an accurate model for the building thermal dynamics [16]. The model considers the relationship between any input and output signals without involving any physical prior knowledge of the system. The most straightforward and most intuitive data-driven models are categorized under statistical models [19]. Examples of these are Auto-Regressive (AR), Auto-Regressive with eXogenous inputs (ARX), Auto-Regressive with Moving average (ARMA), Auto-Regressive with Moving Average and eXogenous inputs (ARMAX), and so on. Other linear identification are done using the transfer function representation. The complex and non-linear system dynamics involve the use of algorithms such as Artificial Neutral Network (ANN) and Support Vector Machine (SVM) for system identification. Gaps in the data-driven models are further analyzed

in the following subsections.

2.7.2.1 Modeling Process and Parameters

The parameters of the data-driven models have no meaningful significance, and the model structure is usually inconsistent with the physical reality of the building systems. Although they have high accuracy, [17,26], the non-significance of the output parameters militates the properties of the models for aggregation development and optimization analysis. A sample general representation of the system from statistical models is in (3) with only input output, and noise identified [89]. Other parameters have no physical interpretation.

$$\alpha\left(q^{-1}\right) y(t) = \frac{\beta\left(q^{-1}\right)}{\theta\left(q^{-1}\right)} u(t) + \frac{\gamma\left(q^{-1}\right)}{\delta\left(q^{-1}\right)} w(t) \tag{2.3}$$

Another example of the model using the ARX structure in a linear parametric approach and which has been used extensively to describe building thermodynamics as in (4)

$$y(k) = a_1 y(k-1) + a_2 y(k-2) + \cdots + b_1 u(k-1) + \cdots + b_{nb} u\left(k - n_b\right) + e(k)$$

2.7.2.2 Smart Grid Applications

Researchers feel skeptical about whether data-driven models can truly overperform or replicate similar physical model's counterparts satisfactorily. Recent studies have used this approach satisfactorily for certain applications with Smart grids [90, 91]. For grid analysis, building thermostatically controlled load models often includes parameters that need to be combined. For flexible characterization and coordination of these loads, unification of the parameters using reduced-order models in the form of a generalized battery model (GBM) is essential [27]. The non-physically interpretable

parameters from data-driven models generally made them unsuitable to design coordination algorithms for the building loads and associated resources. The lack of such capabilities further hinders the use of data-driven models for future smart buildings to grid applications.

2.7.2.3 Data Collection Procedures

Building Model Designs: Quality building data collection and management are challenging. In reality, most buildings are designed to collect data for metering purposes only or performance-based controls. Disaggregating the data for system identification is demanding. Further exacerbating the data collection is the lack of data for modern-day hybrid buildings, as they are still not being physically constructed in several climates. So, researchers often rely on data established from the physics models as a real building. Since the model relies on high-quality data, this would mean all the error-prone assumptions made with some of the physics models are re-ingested to the data-driven models, thereby complicating modeling errors.

2.7.3 Hybrid Models

The hybrid models bridge the gaps between the physics models and the data-driven models [92,93]. They rely on parameters of physical significance and predefined input-output relationships to establish the buildingâs dynamics. For these reasons, the hybrid models' framework provides pathways that overcome the limitations of the other two models. The implicit, oversimplification designs and onsite measurement errors from physics models can be mitigated by introducing stochastic requirements in the data to handle disturbances, constraints, and uncertainties. In simple terms, within a hybrid framework, the physics we already know can rely on tuned data to accurately unmask the physics that we do not yet know. Despite the extensive use of hybrid models, the gaps that persist are discussed further in the following subsections

2.7.3.1 Model Structure and Parameters

Hybrid building model parameters have physical significance and can exist in different forms [26]. The most challenging and important part of the model development is identifying the model order and getting the optimum parameters that agree with the physical reality of the building system [93].

2.7.3.2 Smart Grid application

The hybrid building thermal dynamics is prevalent across literature based on varying system identification methods. Generally, the widely used system identification procedures often require data generation from experiments that seek to excite the most dominant dynamics in the building being modeled [26,92–94]. Often, the pseudo-random binary sequence (PRBS), also called persistent excitation signals, is used to satisfy significant theoretical assumptions on the reliability of the generated data for statistical identification. A previous work critically established that using the experimental procedure provided better identification and simulation performance [95]. However, in reality, comfort compromise is inevitable with such experiments; turning the HVAC on and off for such experimental requirements would almost always cause discomfort to the building occupants, who are essential parts of the building's dynamics as they contribute to internal gains. Asides from that, such experiments often miss the representation of buildings for special applications such as hybrid ventilated buildings whose thermal dynamics may not necessarily depend on the operation of the HVAC system for longer periods. It is conceivable that bounding building operating conditions and disregarding special application effects would result in inaccurate predictions that are unsuitable for controllers since huge forecasting errors are unavoidable in the poorly identified model that does not represent the transient of the specific application of the system.

2.8 Gaps in Controls with Some Building Model Frameworks

The choice of the building modeling methodology have a significant impact on the ease of integration with the control architecture of the smart grid. Previous work in [96] discussed the method of hybrid ventilation with droop and optimized controls using the data-driven methodology for MPC formulations; however, for research advancements, the approach lacks the potential for the unification of all building resource models to analyze grid flexibilities as explained in [27, 97, 98].

Similarly, other works have reported the use of artificial intelligence-based models such as artificial neural networks (ANN), fuzzy systems, and hybridized methods including adaptive neuro-fuzzy inference system (ANFIS) in forecasting and prediction with high accuracy [99–101]. However, recent studies have found out that they trail behind MPC technique in realizing better building energy management even though they are computationally efficient [102]. Moreover, the intelligence-based models are completely data-driven methods that correlate only inputs and outputs, and their parameters lack significant meaning. These non-physically interpretable parameters further made them unsuitable for designing flexible coordination algorithms for the building loads and associated energy resources as explained in [27], [97]

Physics models and Data-driven morels have shortcomings that militate them against smart grid applications. Hybrid models were developed from the idea of overcoming the shortcomings of both the other two models. While the hybrid model has been applied widely in research, a closer look at its modeling architecture and procedure reveals that they are ill-suited to address modeling characteristics needed for smart energy future analysis. Most of the current hybrid building models are monolithic that intertwine data input, fundamental physics equations, closed-loop logic, and data output without making provisions for models extensions or special applications that were not initially envisioned in their framework. Rather than having an unstreamlined hybrid modeling procedure, ongoing research would prioritize

developing and performing identification on hybrid building models in an integration fashion like any other physical system. The model would have a modular platform and capture future control extensions. The advantages of such a framework would include:

- Hierarchical and realistic topological interconnection capability: The framework would allow models to be developed explicitly at individual nodes. Then interconnections can be made as new components are built up topologically and hierarchically, plugging and integrating each of the component models with clearly defined inputs, controls, and outputs, in the same way, they would be plugged and structured together in a real physical building sense.

- Interoperability and Generalization Capability: An important feature of the new modeling framework is the ability to interconnect models, subsystems, and processes causal to the main building system dynamics to exchange and access all forms of data and information. This would also guarantee easy future extension capabilities in mind where additional future functionalities would be handled as class methods during programming. It would allow different simulation modes to be enabled for standalone and co-simulation applications separately.

2.9 Summary

In this chapter, the research gaps and limitations in the current day models for residential building simulation and controls were discussed. As buildings are getting smarter, there is a corresponding increase in heterogeneous subsystems of buildings that must be analyzed for smooth transition to a smart energy future. As such, building models would require an advanced level of abstraction and modularization to manage any resulting increased complexities not currently in the state of the art. In the next chapters, this study will present frameworks that offer a path to comprehensive models, control, and optimization algorithms viable for extensive smart grid

applications.

CHAPTER 3: PROPOSED BUILDING THERMAL DYNAMIC MODEL

The research gaps in the models for residential buildings have been discussed in the literature review chapter. Next, is to present some novel ideas that help bridge the identified research gaps. Such ideas are discussed in the next sections.

3.1 Introduction

Building thermal dynamics models are of paramount importance for several controller applications in simultaneously reducing daily operational energy, and achieving indoor air quality, and thermal comfort. In this application context, controllers are required to work with accurate models that are computationally efficient, non-mathematically complex (reduced-order), and generalizable, especially considering buildings with passive designs and configured with hybrid ventilation technology. For this, an integrated and simplified model is proposed in the next subsections and extensive simulations are carried out and three out of the seven standard ASHRAE climate zones in the United States and their results are validated against standards from EnergyPlus^{TM}. A significant portion of the passive building thermal dynamics model development methodology in this chapter matches a previous publication by the same author described in [103]

3.2 Main Contributions

The goal of this chapter is to develop an integrated Hybrid Building Model interoperable with evolving Smart grid architecture. As such, the following contributions are achieved

- Created an integrated hybrid building thermal model for passive buildings usable for special application requirements such as hybrid ventilation operation.

- Developed a parametric identification methodological framework with Levenberg Marquardt Algorithm that accounts for a wide variation of nonlinear inputs, specifically from the weather parameters of hybrid ventilated buildings.

- Analytically validated the proposed integrated hybrid building thermal models in comparison with standards from EnergyPlus^{TM}.

3.3 Modeling Methodology

The EnergyPlus^{TM} heat balance equation presented in [104] provides the basic framework for developing the integrated hybrid model. As shown in Fig. 5.14, the interaction between the five basic heat transfer modes achieves the zone internal temperature for passive building. The modified EnergyPlus^{TM} heat balance equation from [104] is represented in (3.1); where the building's sensible heating and cooling components have been removed to accurately depict the thermal dynamics of a naturally ventilated building.

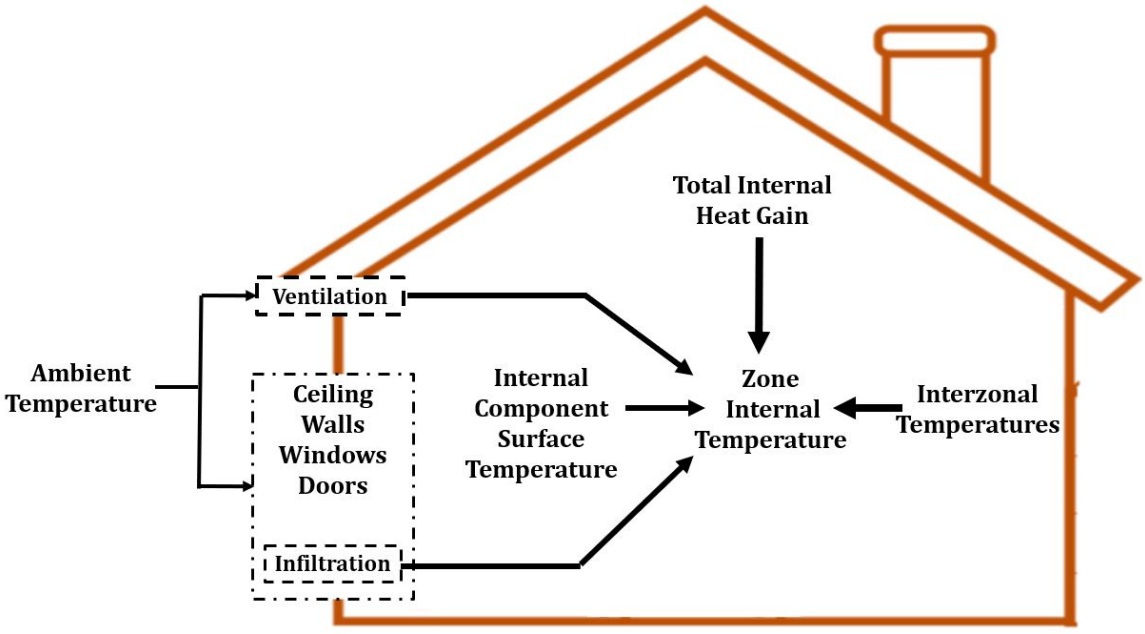

Fig. 3.1: Passive Building Representation.

$$C_z \frac{dT_z}{dt} = \sum_{i=1}^{N_s} h_i A_i (T_{si} - T_z) + \sum_{i=1}^{N_z} c_p m_i (T_{zi} - T_z) + c_p m_{inf} (T_a - T_z) + c_p m_{vent} (T_a - T_z) + \sum_{i=1}^{N_{si}} Q_{total} \tag{3.1}$$

$$C_z = V \rho_{air} c_p c_T \tag{3.2}$$

- Total Zonal Heat Gains are represented as the sum of the internal heat gains from people, equipment, lighting from the zone, and the solar heat gains directly from windows or indirectly via absorption in opaque building components
- Transmission heat transfer occurs between the zone internal space and the ambient environment governed by the convective heat transfer between the two areas.
- Another transmission and ventilation heat transfer occur between adjacent zones represented by the difference between the zone's internal temperature and the adjacent spaces' internal temperature.
- Infiltration heat transfer is governed by the difference between the zone internal temperature and the ambient air temperature through wall cracks and leaking surfaces.
- Natural ventilation heat transfer is governed by the difference between the zone internal temperature and the ambient air temperature
- Heat Storage modeled to include both the zone air thermal capacity and the effective capacitance of zone internal thermal mass (e.g., furniture, books, and partitions), which is assumed to be in thermal equilibrium with the zone air.

3.3.1 Building Model

The first step in realizing our hybrid model is to modify the convective heat transfer term from the zone component surfaces of equation (3.1) to a heat transfer term with

an equivalent resistance that constitutes a thermal barrier encompassing the zone from the outdoor area.

$$C_z \frac{dT_z}{dt} = \frac{1}{R}(T_a - T_z) + \sum_{i=1}^{N_z} c_p m_i (T_{zi} - T_z) + c_p m_{inf}(T_a - T_z) + c_p m_{vent}(T_a - T_z) + Q_{total} \tag{3.3}$$

where R is the equivalent thermal resistance of all the building envelope components and substituted for $\sum_{i=1}^{N_s} 1/h_i A_i$

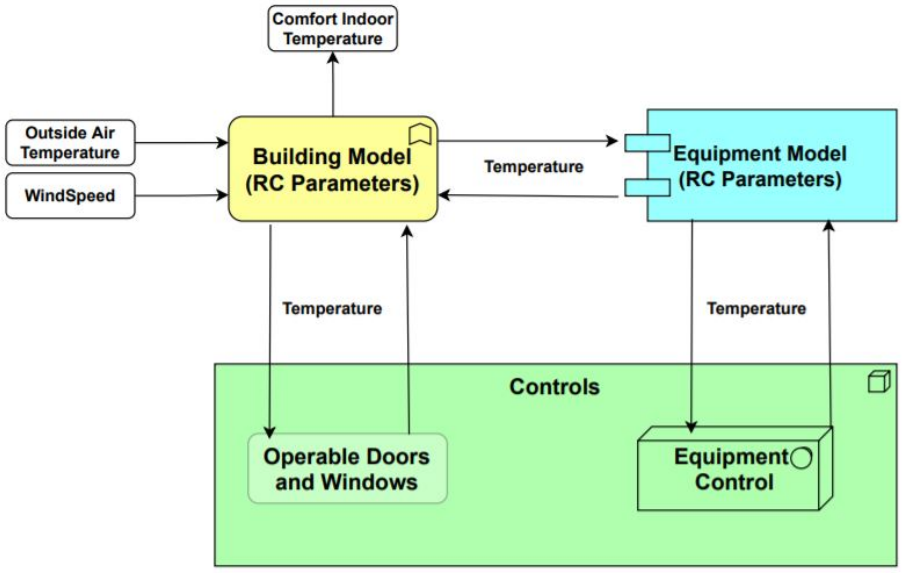

Fig. 3.2: Base Interconnection between the Building Model, HVAC, and their Controls

3.3.2 HVAC Equipment Model

The HVAC system used considers both heating and cooling and is presented as a coupled RC model as represented in (3.4). This work considers an electric heating coil and a direct expansion (DX) cooling coil to provide heating and cooling, respectively.

$$C_h \frac{dT_s}{dt} = \frac{1}{R_h}(T_A - T_s) + Q_{HVAC} \tag{3.4}$$

where Q_{HVAC} = sensible heating or cooling rate from the coils, C_h = Heat capacity of the HVAC equipment, T_A = Ambient HVAC equipment temperature, R_h = Ambient HVAC equipment resistance, T_s = Zone air temperature supply, P_{HVAC} is electric power directly associated with the coils to provide sensible heating or cooling, T_{mix} = mixed air temperature of the zone returned air and outdoor air, COP = Coefficient of Performance of the cooling unit and η = efficiency of the heating element and

$$P_{HVAC} = \begin{cases} \frac{1}{COP} \times c_p m_z (T_{mix} - T_{sp}), & \text{for cooling,} \\ \frac{1}{\eta} \times c_p m_z (T_{sp} - T_{mix}), & \text{for heating,} \\ 0, & Otherwise \end{cases}$$

T_{sp} is the intended internal temperature T_z needed to be maintained for comfort in the building zone.

3.3.3 Electric Water Heater Model

The adopted water heater model is based on a single node (1R-1C) thermal dynamics representation given in [29]. The control logic is based on the difference between hot water temperature T_w and the defined hot water setpoint T_{spt}. R_w and C_w parameters can are obtained from the water heater datasheet.

$$C_w \frac{dT_w}{dt} = \frac{1}{R_w} [T_a - T_w] - \dot{m}_{\mathrm{w}}\, C_p\, (T_w - T_{in}) + U Q_{wh} \tag{3.5}$$

The control model for the water heater is either on or off given by

$$U = \begin{cases} 0, \text{ if } T_w \geq T_{\mathrm{spt}} + \delta T/2 \\ 1, \text{ if } T_w \leq T_{\mathrm{spt}} - \delta T/2 \end{cases}$$

where T_a = Water heater equipment ambient temperature, $\dot{m}_{\mathrm{w}}$ = mass flow rate of water, C_p = specific heat capacity of water, T_{in} = Water heater inlet temperature,

and Q_{wh} is the rating of the water heating element.

3.3.4 Schedulable Electrical Loads

Users typically initiate schedulable loads in the building with an anticipated completion time. Examples include loads associated with cooking and wet cleaning appliances, such as Ranges, clothes washers, dishwashers, and dryers. According to [29], the power associated with schedulable loads can be expressed as

$$P_{sch}(t) = P_{rated}U(t) \tag{3.6}$$

where P_{sch} is the power of the schedulable loads, P_{rated} is the rated power of the load, and U_t is the binary variable representing the load status. 1 for ON and 0 for OFF.

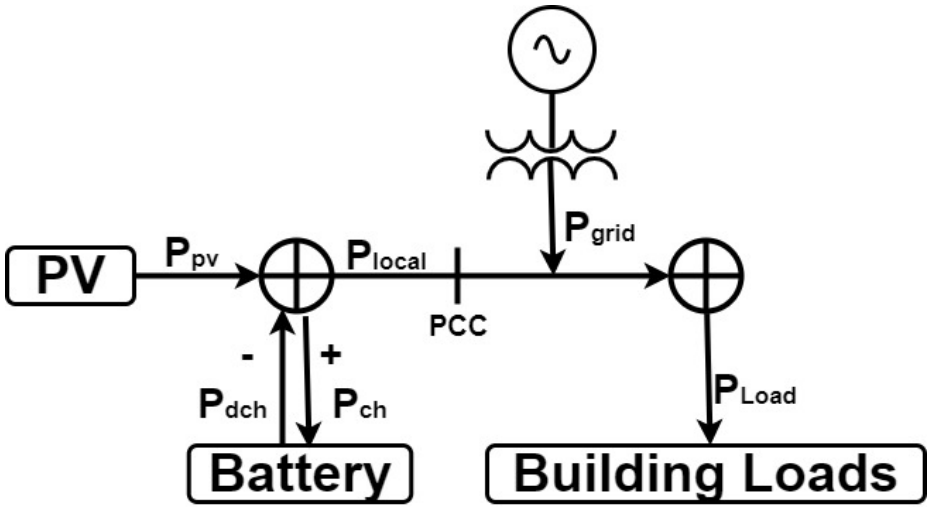

Fig. 3.3: Building Microgrid Structure

3.3.5 Energy Sources

The considered primary energy sources for the buildings are the utility grid and onsite generation. A simplified PV system model is considered according to equation (3.8)

$$P_{pv}(t) = A_{mod}(t)S(t)\eta_{pv}(1 - U_{pv}(t)) \tag{3.7}$$

where U_{pv} = the power produced by the PV system of the building η_{pv} is the efficiency of the module, A_{mod} is the total module area, S Global Horizontal Solar Irradiance, U_{pv} is the percent curtailment of the PV system.

3.3.6 Energy Storage

The battery system model is adopted from [105] and it is used to establish the energy state of the storage system

$$\mathrm{E_B(t) = E_B(t-1) + (\eta_{ch,B} \times P_{ch,B}(t) - P_{dch,B}(t)/\eta_{dch,B}) \times \Delta t} \tag{3.8}$$

$$\mathrm{E_{min,}}_{B} \leq \mathrm{E}_{B}\mathrm{(t) \leq E_{max,}}_{B} \tag{3.9}$$

$$\mathrm{P_{Batt}(t) = P_{ch,B}(t) - P_{dch,B}} \tag{3.10}$$

$$0 \leq \mathrm{P_{ch,B}(t) \leq P_{ch,B\,max}} \tag{3.11}$$

$$0 \leq \mathrm{P_{dch,B}(t) \leq P_{dch,B\,max}} \tag{3.12}$$

$$\mathrm{P_{ch,B}(t) \times P_{dch,B}(t) = 0} \tag{3.13}$$

where E_B = Energy State of the Battery, P_{ch} and P_{dch} = charging and discharging power of the battery, η_{ch} and η_{dch} = charging and discharging efficiencies of the battery. The following constraints are imposed on the battery system. Constraint (3.15) ensures the energy capacity limit is maintained, Constraint (3.17) ensures that the battery charging rate is between the minimum and maximum charging limits. Constraint (3.12) regulates the discharging rate. Constraint (3.13) prohibits simultaneous charging and discharging of the battery.

3.3.7 Electric Vehicle Charging Model

A unidirectional charging model of the battery is adopted for the EV. It is assumed that the discharging of the EV has a regular daily pattern necessary not needed in

this model, only the interaction the EV has with the building microgrid is when it is charging.

$$\mathrm{E_V(t) = E_V(t-1) + (\eta_{ch,V} \times P_{ch,V}(t) \times \Delta t} \tag{3.14}$$

$$\mathrm{E_{min,}}_{V} \leq \mathrm{E}_{V}(\mathrm{t}) \leq \mathrm{E_{max,}}_{V} \tag{3.15}$$

$$E_{V,t} \geq E_{set} \tag{3.16}$$

$$0 \leq \mathrm{P_{ch,V}(t) \leq P_{ch,V\,max}} \tag{3.17}$$

3.3.8 Power Balance

Building loads are not always coincidental with onsite generation and thus, require external power from the grid. As adopted from [105], the overall building load and the total power balance from the grid, onsite generation, and storage are represented in (3.3). Constraint (3.18) describes P_{local} as the sum of onsite generation and storage power available, and constraint in (3.20) ensures that this power is consumed locally by the building. Constraint (3.21) gives the total power balance.

$$P_{\mathrm{pv}}(t) = P_{local}(t) + P_{ch}(t) - P_{dch}(t) \tag{3.18}$$

$$P_{\mathrm{load}}\,(t) + P_{local}(t) \geq 0 \tag{3.19}$$

$$P_{load}(t) = P_{HVAC}(t) + P_{sch}(t) + P_{le}(t) \tag{3.20}$$

$$P_{grid}(t) = P_{load}(t) + P_{Batt}(t) + P_{EV}(t) - P_{pv}(t) \tag{3.21}$$

where P_{le} is the uncontrollable building electric loads

3.4 Description of the Tested Real Buildings

The tested buildings were chosen from three distinct ASHRAE climate zones to examine the performance of varying modeling structures and procedures for comfort in passive buildings. The climate variations ensure evaluations under varying terms

of building consumption, loads, use patterns, etc. which eventually shows the performance of the hybrid models under different scenarios. Each of the selected prototypes is a single-family and two-story building with 2500 square feet. They are designed with two zones; the living zone and an attic zone). The living zone is conditioned while the attic is unconditioned. The attic zone accommodates the single-duct HVAC system, but the results of the zone are not presented in this project. The building prototypes are obtained from the Pacific Northwest National Laboratory (PNNL) list of building stocks. This list gives a representation of energy-saving building design and impacts according to the recently published residential international energy conservation codes - IECC, 2021 [106]. The schematic representation of the test building is illustrated in Fig. 3.4. Before simulating to retrieve the temperature data necessary

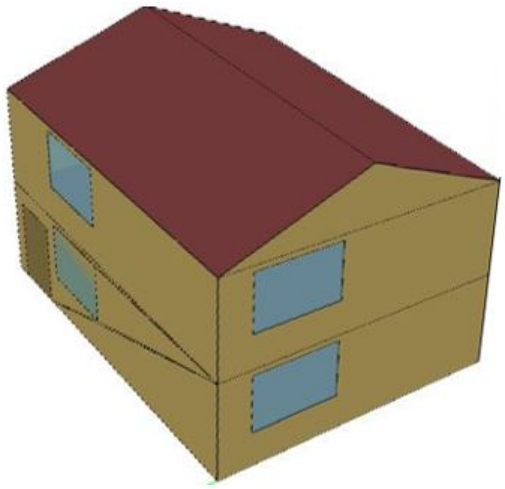

Fig. 3.4: Structure of the Tested Real Building

for hybrid parameter estimation. Each of the components of the prototype buildings was modified and configured for passive designs and is allowed to use natural ventilation according to the building operation modes described in detail in Chapter 4. It can be assumed that EnergyPlus^{TM} models of the building prototypes have been calibrated and validated to depict physically constructed real buildings. This results from the unavailability of salient temperature data and other significant parameters from physically constructed passive buildings in different climatic regions for

experimental purposes. The selected buildings feature the San Fransisco region representing ASHRAE Climate Zone 3C. Another location chosen is Cedar City, Utah, representing ASHRAE climate Zone 5B, and the third selected building location is in the Charlotte area, representing ASHRAE Climate Zone 3A. Before carrying out

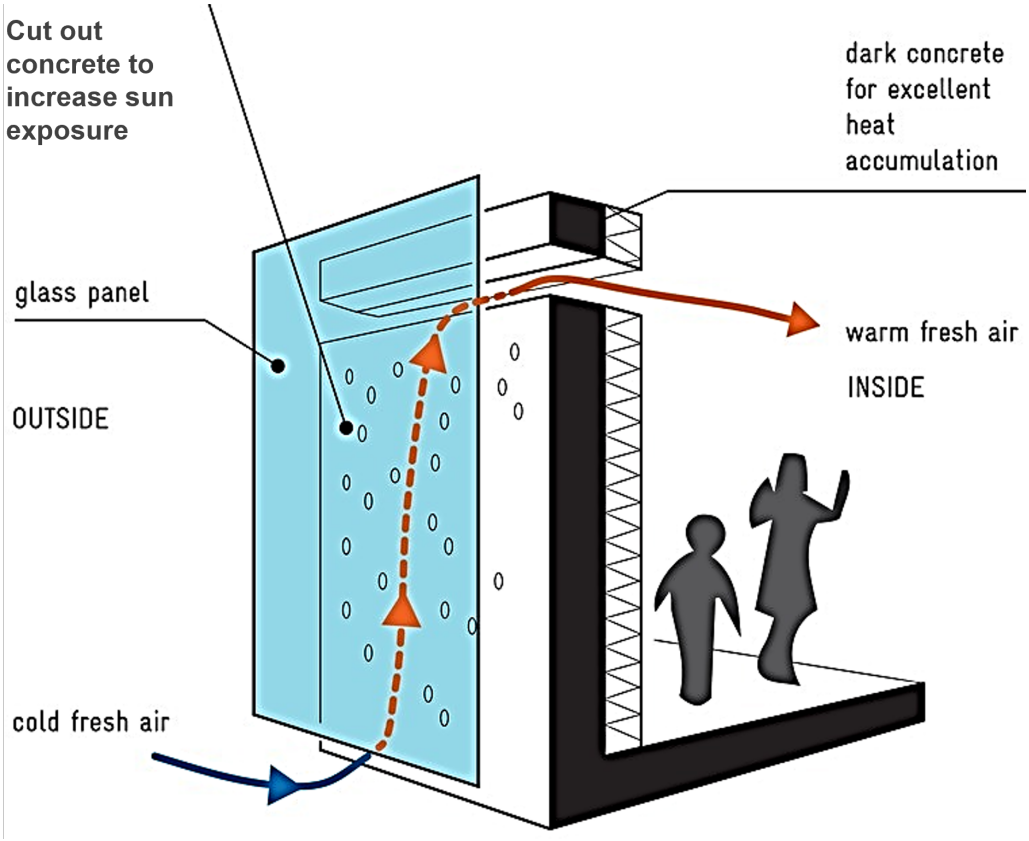

Fig. 3.5: Working Principle of a Passive Trombe Wall [107]

any EnergyPlus^{TM} simulations, the components, materials, and equipment configurations of each of the building zones were modified for passive designs. As an example, all buildings simulated in this project were configured with Passive Trombe external Walls, eco-roof vegetation, and many other passive building designs. Fig. 3.5 gives additional details on how a Passive Trombe wall works.

A strategically installed passive Trombe wall typically provides thermal storage and delivery. It stores heat for building use during the winter and rejects heat gain to the building during the summer. With the help of the eco-roof design, the passive walls

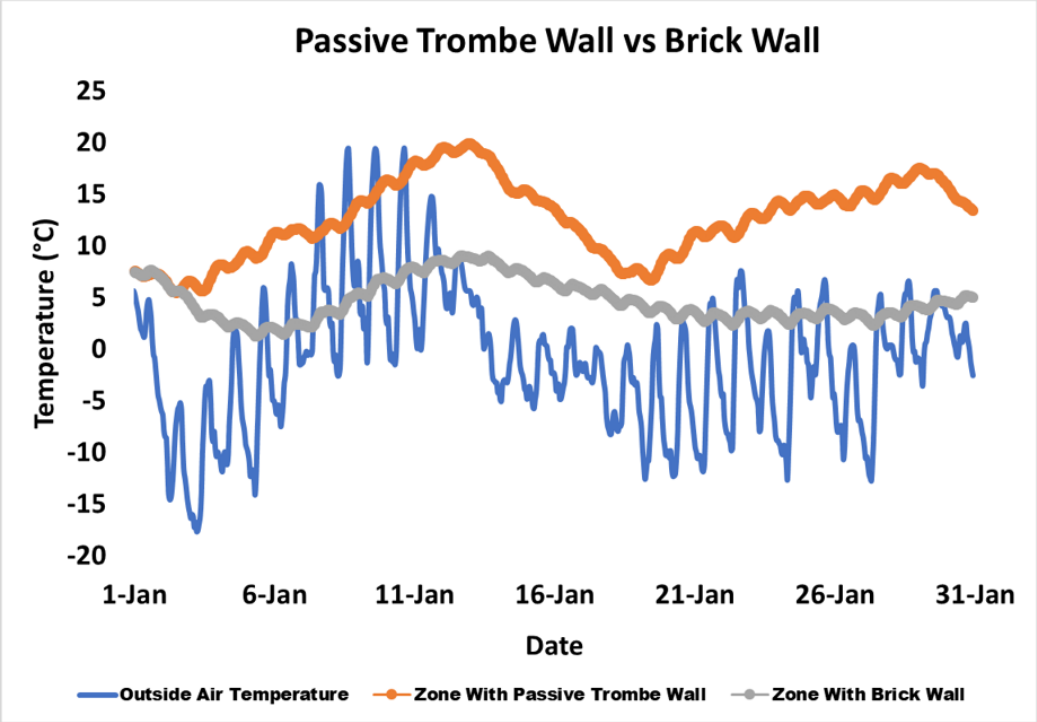

Fig. 3.6: Effectiveness of Passive Trombe Wall vs Brick Wall

can assist to keep the building's internal temperature lower during the summer. Fig. 3.6 gives a comparison of a building zone designed with Trombe walls and another with brick walls in ensuring that the building zone is provided with a comfortable temperature. A quantitative analysis of Fig. 3.6 shows that the passive Trombe wall provided a 65% better thermal energy performance when compared to a brick wall using a temperature reference of 19.5°C.

As illustrated in Fig. 3.6 for a winter simulation period, in contrast to a regular/brick wall, the Trombe wall can store heat and deliver it to the building over time. What is considered a comfortable indoor air temperature range is specified in ASHRAE 55-2017 Standard; Thermal Environmental Conditions for Human Occupancy [108]. This is known to be between a temperature range of nearly 67°F and 82°F (19.44°C to 27.77°C) provided the occupants can adapt to other contingencies such as humidity changes, wearing comfortable clothing, and other behavioral acts.

3.5 Parametric Identification Methodology for the Building Model

The output of an initial building simulation in EnergyPlus^{TM} gives the temperature data required for the parameter identifications. The passive building base model in equation (3.26) is discretized using the Euler technique given in (3.22).

$$T_z(t+1) = T_z(t) + \Delta t \dot{T}_z(t) \tag{3.22}$$

where Δt is the simulation time step, and t is the discrete-time index. Next, parameter identification was performed using LevenbergâMarquardt algorithm (LM). LM is one of the recognized standards for nonlinear curve-fitting and parameter identification methods. LM is used in this work due to its characteristic of fast and stable convergence over other methods such as Gradient Descent and Gauss-Newton solutions, considering some non-linearities in the passive building thermal dynamics equation [109].

In the course of any parameter identification procedure, LM finds out the best weights of the vector parameters that provide the best fit for the input measurement data using the following procedure [110]. Let f be an implicit functional relation that can map a parameter vector $\mathbf{p}$ to an estimated temperature vector measurements; that is, $\hat{\mathbf{T}}_\mathbf{z} = f(\mathbf{p})$. $\mathbf{p}$ contains all the parameter inputs to the zone thermal dynamics. An initial estimate of parameters from all variables $\mathbf{p_0}$ and a measured temperature vector are furnished to the algorithm and LM desires to identify new series of the vector that converges toward a local minimizer for the function f. Therefore, at every timestep, the squared error values of $\epsilon^T\epsilon$ is minimized with $\epsilon = \mathbf{T_z} - \hat{\mathbf{T}}_\mathbf{z}$. A Taylor series expansion of the parameter function can be expressed as

$$f\left(\mathbf{p} + \delta_\mathbf{p}\right) \approx f(\mathbf{p}) + \mathbf{J}\delta_\mathbf{p} \tag{3.23}$$

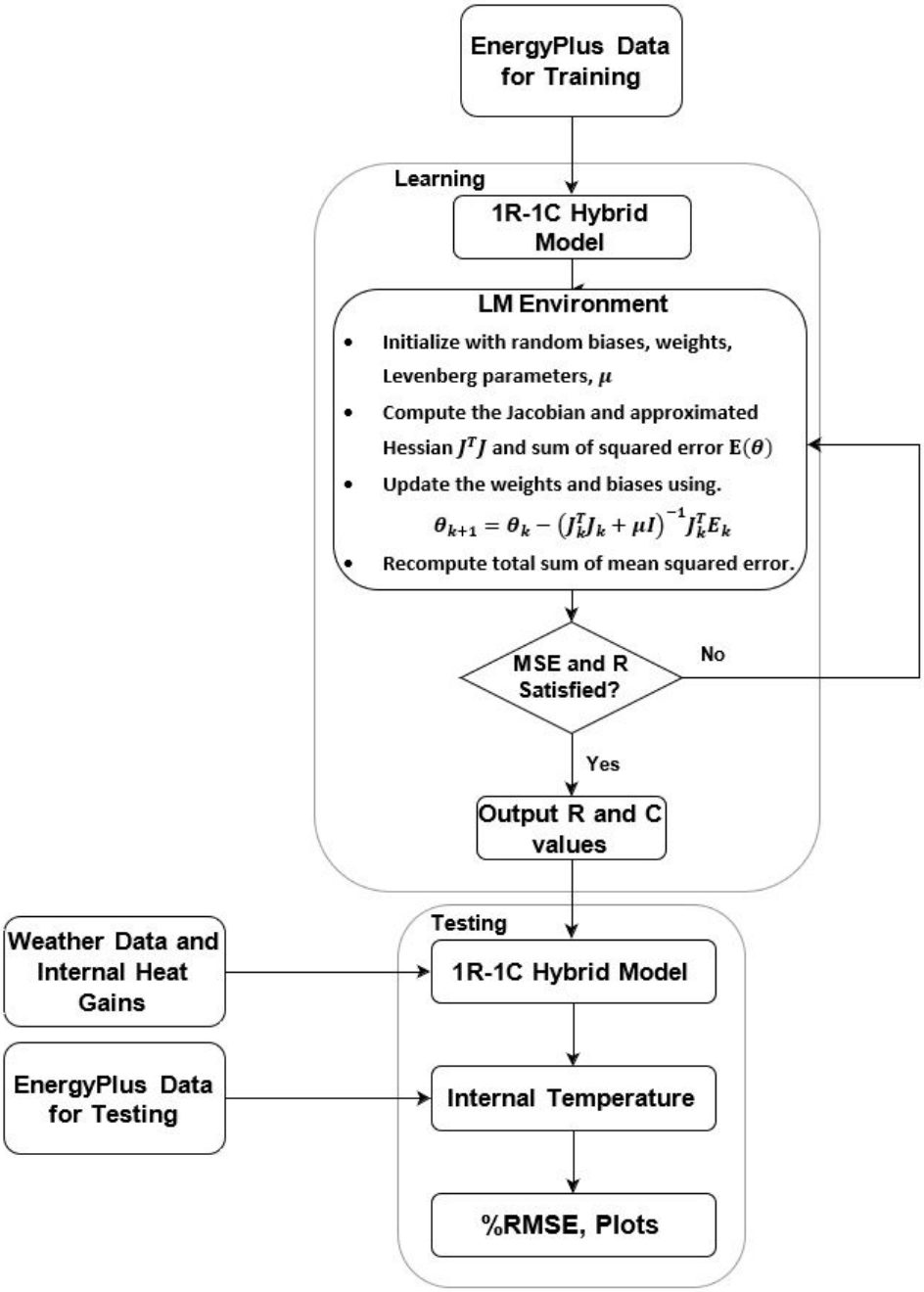

Fig. 3.7: Parameter Estimation Flow Chart

where J is the Jacobian matrix represented by $\frac{\partial f(\mathbf{p})}{\partial \mathbf{p}}$ and $\mathbf{J}^T\mathbf{J}$ gives the Hessian Matrix. Given numerous sets of inputs into the model, where T constitutes the number of the input sets and W is the total value of parameters (weights + biases), the Jacobian

matrix is expressed as

$$J = \begin{bmatrix} \frac{\partial \mathbf{f}(p_1,w)}{\partial p_1} & \cdots & \frac{\partial \mathbf{f}(p_1,w)}{\partial p_W} \\ \vdots & \ddots & \vdots \\ \frac{\partial \mathbf{f}(p_T,w)}{\partial p_1} & \cdots & \frac{\partial \mathbf{f}(p_T,w)}{\partial p_W} \end{bmatrix} \tag{3.24}$$

Thus, at each time step, the idea is to iteratively find $\delta_{\mathbf{p}}$ that minimizes $\|\mathbf{T_z} - f(\mathbf{p} + \delta_{\mathbf{p}})\| \approx \|\mathbf{T_z} - f(\mathbf{p}) - \mathbf{J}\delta_{\mathbf{p}}\| = \|\epsilon - \mathbf{J}\delta_{\mathbf{p}}\|$ until $\mathbf{J}^T\mathbf{J}\delta_{\mathbf{p}} = \mathbf{J}^T\epsilon$. A damping term μ can be introduced to adjust the Hessian Matrix for error reduction at each step. LM terminates when $\epsilon^T\epsilon$ or $\delta_{\mathbf{p}}$ falls below a specified error threshold. The flowchart describing the parameter identification procedure is illustrated in Fig. 3.7.

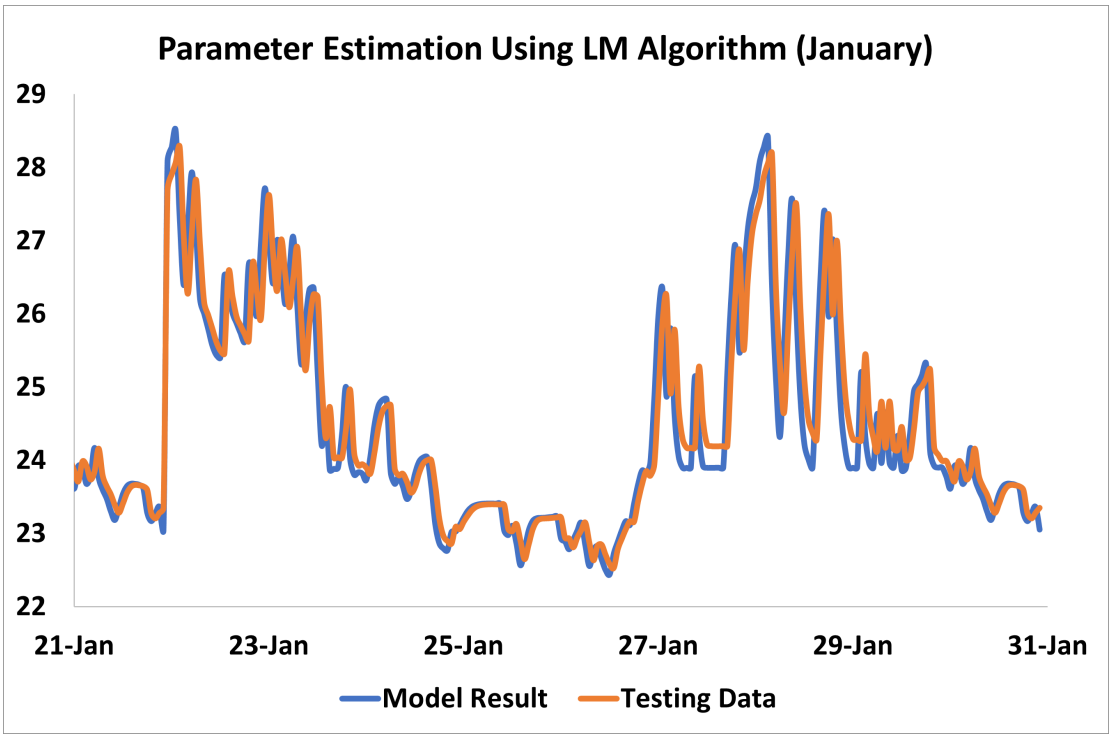

Fig. 3.8: Sample Test for LM Parameter Estimation

ASHRAE Guideline 14 criteria are utilized in this Thesis to validate the accuracy of estimations and models developed. Specifically, The Coefficient of Variation of the Root Mean Square Error (CVRMSE) values, which is a unitless percentage error value that measures the variability between actual values and the simulated results. The equation for CVRMSE is given in (3.25)

$$CVRMSE = \frac{1}{\bar{m}}\sqrt{\frac{\sum_{i=1}^{n}(m_i - s_i)^2}{n-p}} \times 100(\%) \tag{3.25}$$

ASHRAE Guideline specifies that for Hourly criteria the CVRMSE values must be less than 30% [111, 112] A lower percentage value is desirable and would mean more accurate estimations.

3.5.1 Generated Building Parameters

Table 3.1: Thermal Model Parameters for the Studied Zones

Zone	Month	R (°C/kW)	C_z (kWh/°C)	% RMSE
3A	January	34.65	2.63	3.45
3A	July	3.47	4.37	3.31
3C	January	32.29	2.95	2.58
3C	July	10.98	2.307	1.92
5B	January	49.67	2.44	2.50
5B	July	3.82	4.99	1.86

3.5.2 Other Distributed Energy Resource Parameters

The residential hybrid building have both the HVAC system, and water heating system as thermostatically controlled loads. In addition to this, the hybrid building is declared to have PV, battery, and act as a microgrid structure. The complete parameter details of various resources attached to the building are presented below

3.6 Proposed Hybrid Model and Operation Modes Development

In the model of (3.3), a network of resistances and capacitance depicts the thermal dynamics of each zone in a passive building. The network describes the evolvement of zone temperatures with different heat disturbances. Each of the passive building zones

[1] η_{ch} used generally as a square root of the Roundtrip efficiency
[2] Typical wide range setpoints of a thermostat
[3] Typical setpoint of an electric water heater
[4] Generally assumed value for uncontrollable loads in literature
[5] The battery limit are 15% and 85% of the battery energy capacity.

Table 3.2: Details of other Parameters Used for Simulations

Parameter	Value	Units
R_w [29], [113]	0.27	h°F/BTU
C_w [29], [113]	1664	BTU/°F
Q_{wh} [113]	12	kW
P_{ch}, max,P_{dh}, max [114]	5	kW
P_{pv} [115]	5	kW
A_{mod} [116]	35.5	m^2
η_{pv} [117]	0.22	
η_{ch}, η_{dch} [1]	0.95, 0.99	
T_{sp}, min,T_{sp}, max [2]	19.5, 24	°C
T_{set} [3]	132	°F
P_{le} [4]	3.5	kW
E_B, min,E_B, max [5]	2.025, 11.475	kWh

is modeled in the form of an electrical circuit containing resistance and capacitance, as shown in Fig. 3.9. Currents are represented by the heat gains entering the zones, and Voltage represents temperature states. From the circuit diagram, T_a is the external air temperature; T_z is the interior zone temperature. Q_{adj} represents the total heat gains from all adjacent zones, Q_{vent} represents the ventilation heat transfer, Q_{inf} is the infiltration heat transfer due from the outside air, and Q_{total} represents the sum of all zonal heat gains from people, equipment, lighting system, and solar irradiation.

The newly modified model is presented in (3.26) and in comparison with (3.3) replaced $\sum_{i=1}^{N_z} c_p m_i$ with $\frac{1}{R_{adj}}$ thereby eliminating bilinear states for model simplification. C_z is the effective coupled capacitance of the zone air and the total internal thermal mass from various materials, including furniture, books, envelopes, partitions, and all other interior contents. Section 8.8.2 of the ASHRAE 90.2 standard indicated that real buildings typically have larger thermal mass from their interior contents than their zone air [118]. In this study, zone air and the internal thermal

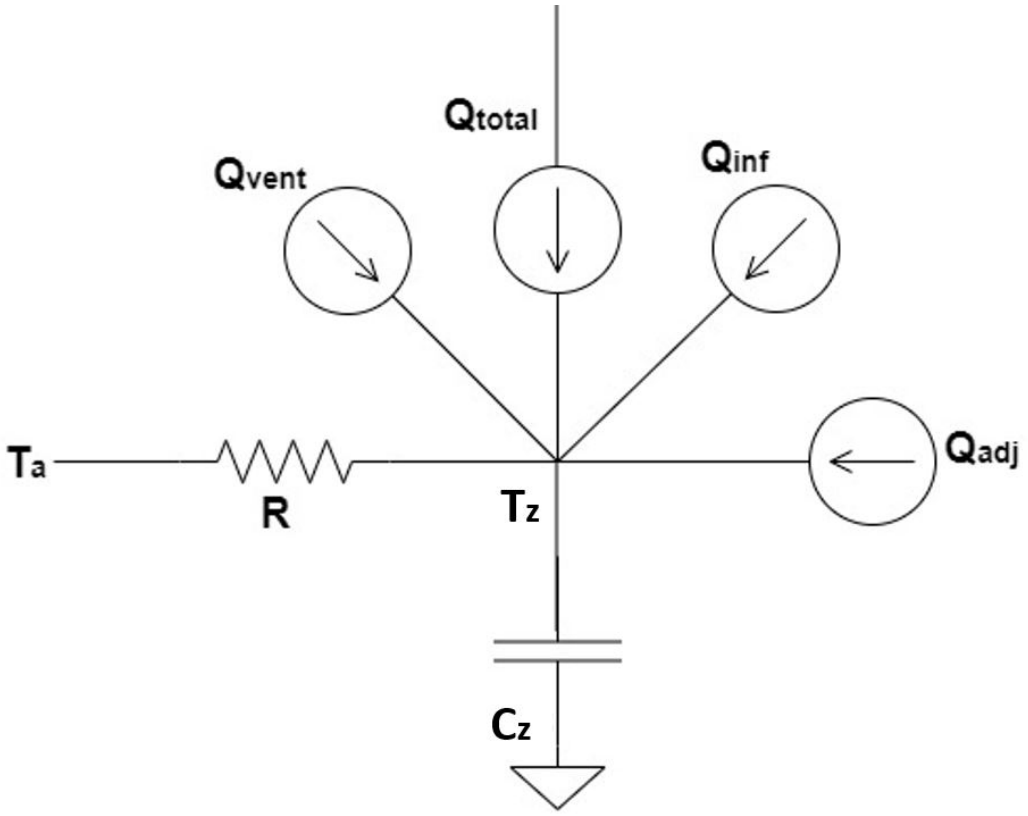

Fig. 3.9: 1R-1C Model of a Passive Building.

mass capacitance are assumed to be in thermal equilibrium.

$$C_z \frac{dT_z}{dt} = \frac{1}{R}(T_a - T_z) + Q_{total} + Q_{adj} + Q_{inf} + Q_{vent} \tag{3.26}$$

where $Q_{vent} = c_p m_{vent}(T_a - T_z)$ - Ventilation Heat Gain Rate, $Q_{inf} = c_p m_{inf}(T_a - T_z)$ - Infiltration Heat Gain Rate, $Q_{adj} = \frac{1}{R_{adj}}(T_{adj} - T_z)$ - Adjacent Zones Heat Gain Rate

Considering that this newly developed model would be used for control applications involving logic-based methods (as discussed in the next Chapter), Optimized based methods using model predictive controls as discussed in Chapter 5, and Aggregate operation as discussed in Chapter 6, where the building thermal dynamic models are represented in a unified form along other resources of the building, it is important to spell out some structure for consistency and easy understanding of the audience,

where this work has categorized the modeling perspectives into three classifications.

- Analytical Model: a detailed model representing the thermal dynamics of the passive building, including the corresponding HVAC model. This is the same as the models defined in 3.26 without any relaxation or convexification and this representation is suitable to be deployed on a test bed when evaluating the response operations of the action of the building controllers.

- Open-loop model: this represents a model developed based on the analytical model equations of 3.26 with some relaxations to achieve convexity. it also involves some integer variables to capture some HVAC system operation logic such that the operation of the system is able to work with other building energy resources with binary controls. With the open loop model, the parameter of interest is the total power consumption of the HVAC system and can be applied to optimization controllers that tend to provide some hour-ahead predictions.

- Closed loop model: involves more simplifications for more efficient computation within a control framework wherever the building thermal dynamics is deployed. In the closed-loop models, all parameters of interest are building internal temperatures and power consumption of the system. This allows our analytical model (represented as a testbed) to respond to setpoint changes generated from an optimization routine in some applications whose objective is to make the building power consumption track a given reference. Such an example is given as one of the test cases in the next chapter

3.7 Basic Control Modes

Fresh air is introduced into a building zone with the coordination of three key elements; air, an opening, and pressure. These elements are controllable for thermal stability and occupant's comfort. Based on the nature of the forces driving air into the building zones, three distinct building operation modes are formed. The following

highlights the modification to (3.26) to replicate each mode formation. The various steps to take in integrating the model and the control modes are illustrated in the flowchart of Fig. 3.10, while these next subsections further explain the modified parameters at each step.

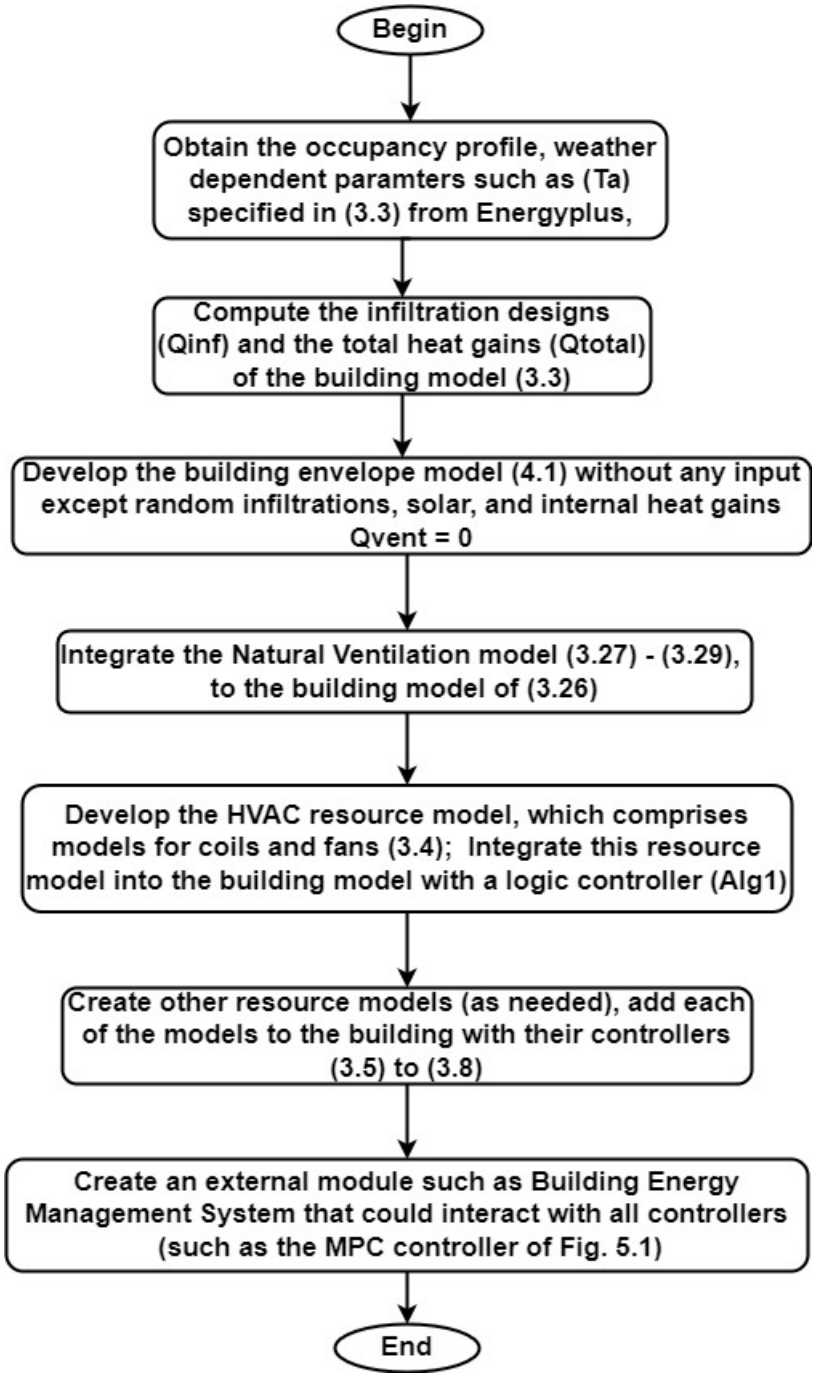

Fig. 3.10: Integrated Hybrid Building Model Development Flowchart

3.7.1 Fully Passive Mode

In this mode, the ventilation term and any air systems term driven by HVAC in (3.26) is null. Building airflows are due to random infiltration from leaks, cracks, and people moving in and out of the building. This is also not the best mode for the longer operation of the building without cycling any of the other two modes due to poor air circulation resulting in pollution for occupants. Nevertheless, this is the base model where the hybrid R and C parameters are determined through system identification under natural occurrences without any control inputs.

3.7.2 Controlled Passive Mode

A major setback of the fully passive mode is that it usually fails to satisfy occupants' comforts, particularly during the summer periods. As a result, a ventilation term that can be automatically controlled through operable windows and doors is integrated into the base model. The natural ventilation mass flow rate of the air is obtained through the combined effects of wind and stack from building component openings as described in [104]. This is represented in (3.27) - (3.29)

$$V_{wind} = C_w A_{\text{open}} F_{\text{sch}}\, V \tag{3.27}$$

$$V_{stack} = C_D A_{open} F_{sch} \sqrt{2g\Delta H_{NPL}\left(|T_z - T_a|\,/T_z\right)} \tag{3.28}$$

$$m_{vent} = \rho_{air} \times (\sqrt{V_{stack}^2 + V_{wind}^2}) \tag{3.29}$$

where V is the windspeed, V_{wind} = Wind driven air flow rate $[m^3/s]$, Q_{stack} = Stack driven air flow rate $[m^3/s]$, m_{vent} = Total ventilation mass air flow rate $[kg/s]$, C_D= Discharge coefficient of the building component, F_{sch} = Open area fraction, A_{open} = Door/Window opening area $[m^2]$, ΔH_{NPL} = ASHRAE-determined midpoint value of the lower opening to the neutral pressure position [m], C_w= Opening effectiveness. The controlled-passive mode is achieved through the windows and door's automatic

operations via simple temperature and setpoint-based logic. In this project, the values for the operable factor are assigned to modulate between 0 and 1 based on the window area to allow for necessary natural ventilation. A_{open} signal in (3.27) and (3.28) is 1, if $T_z > T_a$ and $T_z > V_{sp}$, otherwise 0 if false. V_{sp} is the ventilation set-point.

3.7.3 Active Mode

The outdoor air temperature in many climate regions gets too high or too low during the summer and wintertime, respectively. During such occurrences, the controlled natural ventilation may not satisfy occupants' comfort criteria. Accordingly, mechanical systems are required to maintain occupants' comfort. The HVAC equipment model in (3.4) was then integrated into the base model by adding a mechanical ventilation heat term, $c_p m_z(T_s - T_z)$ to (3.26) to form an active operation mode.

In this mode, all the heat gains and heat supplies to the building, including those from mechanical air systems, are fully operational. The control logic and simulation procedure for the active mode operation is described in Algorithm 1. The resulting dynamics from this integration provide a standalone or non-optimized building thermal simulation to maintain an internal comfortable temperature. The detailed process for active building operation is explained in Algorithm 1.

The next section gives details about the simulation results of each of the modes in three different ASHRAE climates and how they compared with similar simulation results from EnergyPlus™.

3.8 Results and Discussions

A sample comparison of test data and the hybrid modeling results with the LM method can be observed in Fig. 3.8. A tight fit can be observed, and the percentage RMSE is 2.5%, confirming the accuracy of the identified R and C parameters. Quantitatively, the percentage error values of each of the estimations from the three different ASHRAE climate buildings in this work were less than 5%. These R and C parameter

Algorithm 1: Residential HVAC Active Control Operation

Initialize or at every iteration, obtain $T_z(t-1)$ where, t = 1, 2, 3, ..., T. Where T is the last simulation timestep
Compute other parameters for the current simulation time step such as $T_a(t)$, $m_{inf}(t)$, $Q_{total}(t)$, etc. in (3.26)
Compute the determinative temperature $T_D(t)$ for the time step - this represents the zone internal temperature value at minimum supply temperature such that $T_D(t) = T_z(t)$ in (3.26)
Input the thermostat setpoint $T_{sp}(t)$ and the corresponding Deadband db (3.4)
for *t = 1, 2, 3, ..., T* **do**
    if $T_D(t) < T_{sp}(t) - db$ **then**
        Estimate $T_s(t)$ with (3.4) for heating mode
    end
    else if $T_D(t) > T_{sp}(t) - db$ **then**
        Estimate $T_s(t)$ with (3.4) for cooling mode
    end
    else
        $T_s(t) = T_{s(minimum)}$ - No cooling or heating is needed
    end
end
return $T_s(t)$

values are presented in Table 3.3. Next, graphical illustrations of the simulations for the passive building control modes are presented. First, without any control input, aside from random infiltrations from component leakages and cracks, then controlled natural ventilation, followed by an active phase, and finally the mixed-mode. The hybrid model simulation results show good predictions in the indoor air temperature data compared to the EnergyPlus™ results. Sample results are shown for two commonly severe annual climate periods generally tested in the literature (January and July representing the winter month and the summertime respectively). These dates were also validated through an analysis of 30-Year national average climatic data of the United States on the National Oceanic and Atmospheric Administration (NOAA) site [119].

For a region depicted by ASHRAE zone 3C. Simulation results are illustrated in Figs. 3.23 to 3.28. Identical outcomes were observed with ASHRAE climate Zone

Table 3.3: Simulation Result and Error Metrics for Zone 3C

ASHRAE Zone	Mode	Simulation Period	% CVRMSE
3C	Passive	January	5.28
3C	Passive	July	4.06
3C	Controlled Passive	January	4.41
3C	Controlled Passive	July	3.74
3C	Active	January	1.38
3C	Active	July	4.96

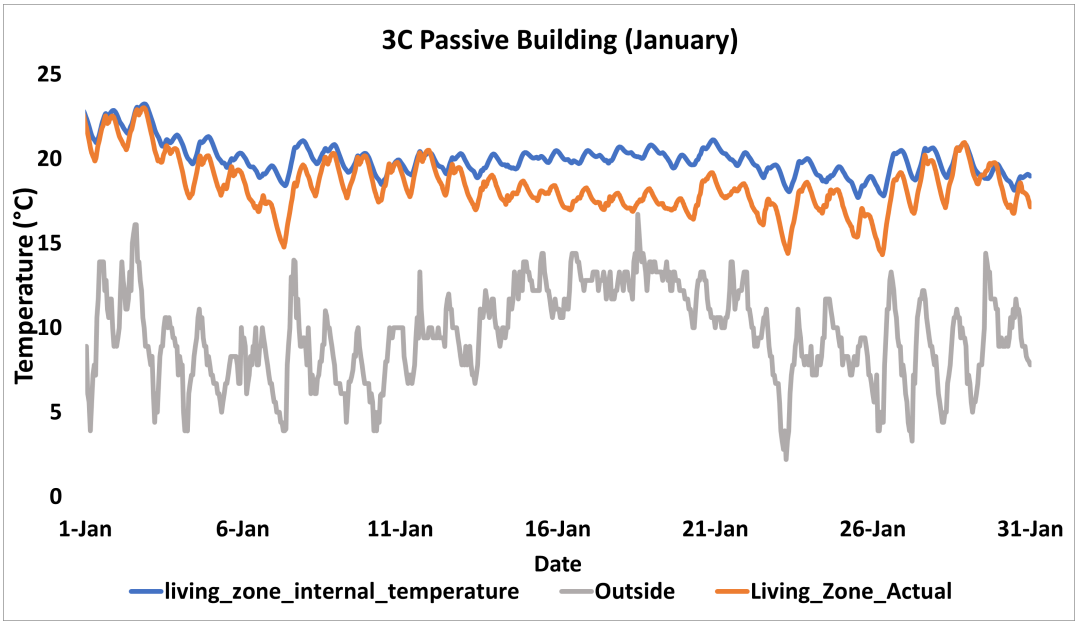

Fig. 3.11: Proposed Model vs. EnergyPlus^{TM}(Actual) for 3C Passive (January)

3A and climate Zone 5B. The obtained error metrics for these climate zones are given in Tables 3.4 and 3.5.

Table 3.4: Simulation Result and Error Metrics for Zone 3A

ASHRAE Zone	Mode	Simulation Period	% CVRMSE
3A	Passive	January	6.52
3A	Passive	July	3.06
3A	Controlled Passive	January	6.17
3A	Controlled Passive	July	4.24
3A	Active	January	1.21
3A	Active	July	3.9

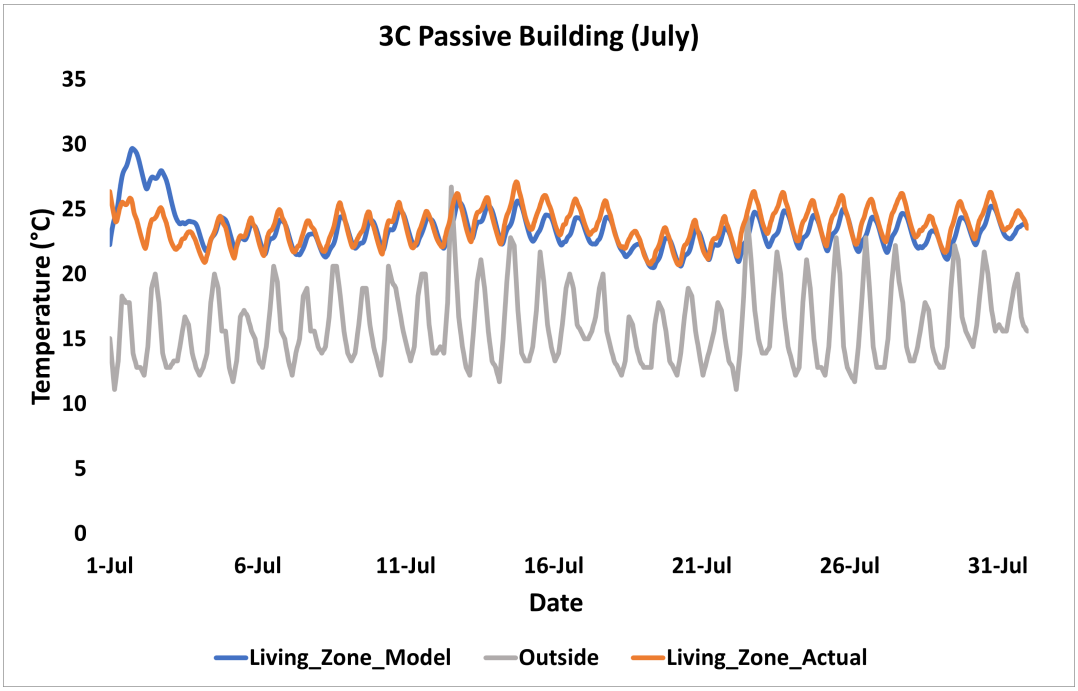

Fig. 3.12: Proposed Model vs. EnergyPlus^{TM}(Actual) for 3C Passive (July)

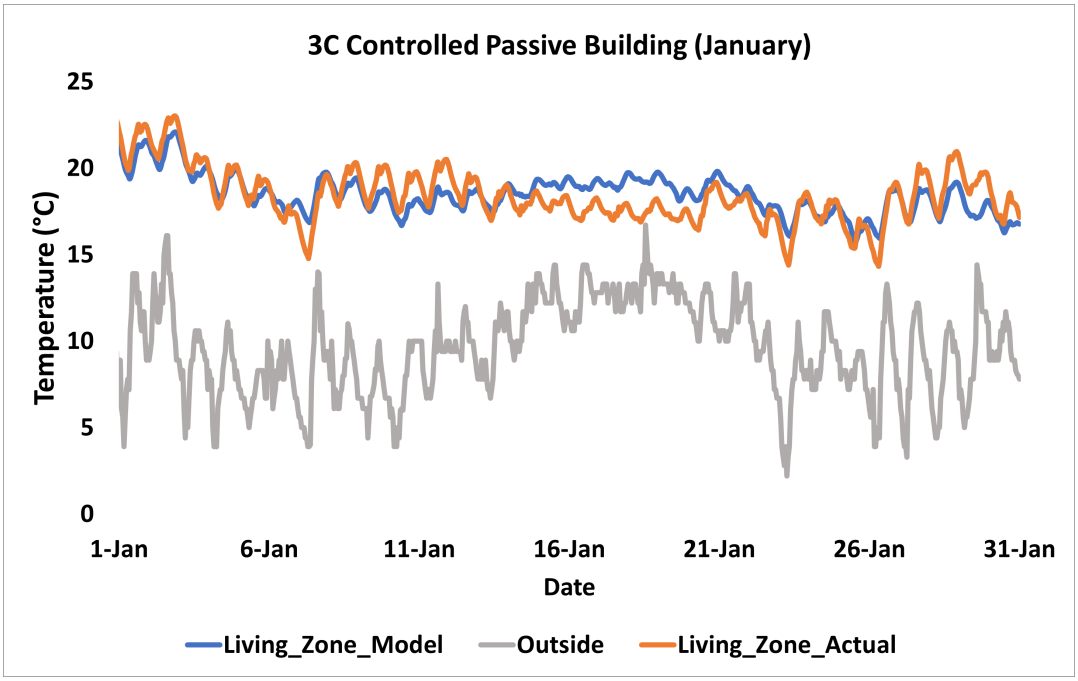

Fig. 3.13: Proposed Model vs. EnergyPlus^{TM} for 3C Controlled Passive (January)

Generally, the identified R and C parameters for the integrated hybrid model parameters vary widely. The developed model gives satisfactory results when the temperature plots are compared with the energy plus counterpart. For all three zones,

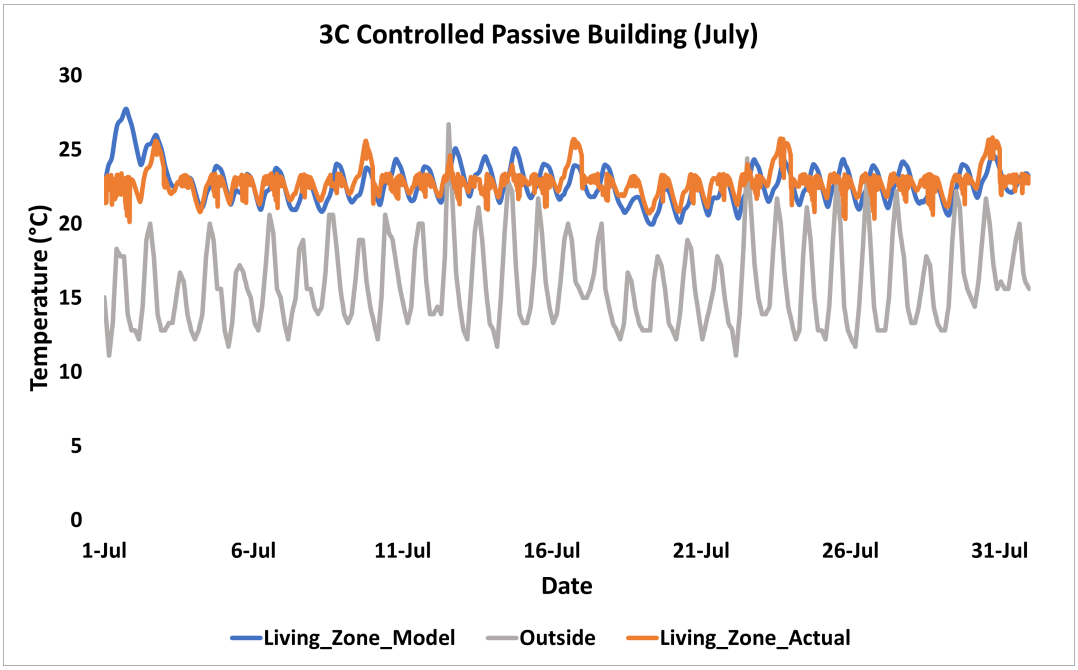

Fig. 3.14: Proposed Model vs. EnergyPlus™ for 3C Controlled Passive (July)

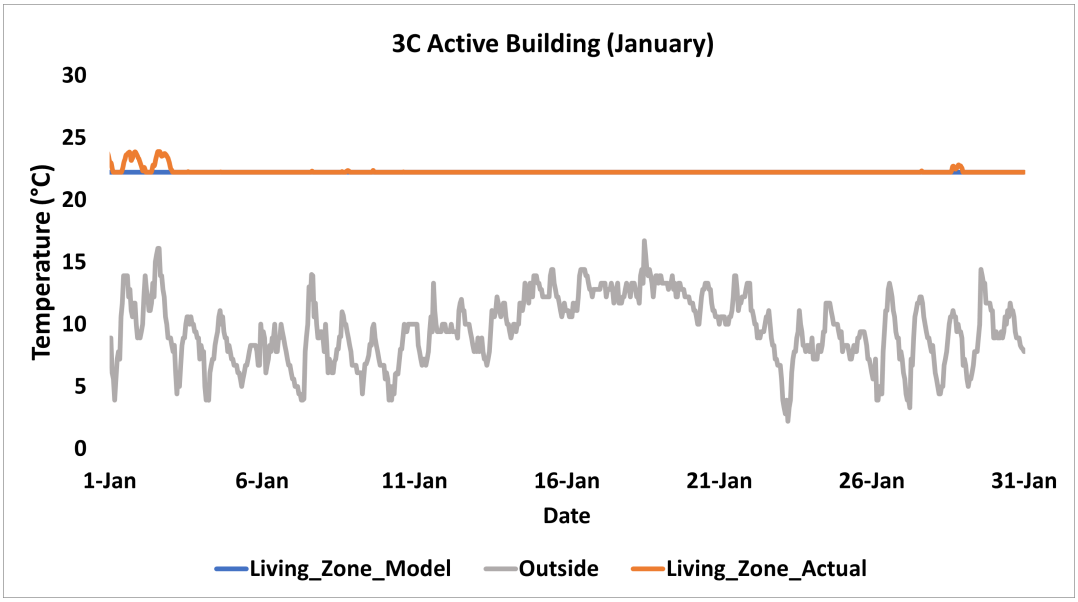

Fig. 3.15: Proposed Model vs. EnergyPlus™(Actual) for 3C Active (January)

the passive strategy and the controlled-passive strategy look almost similar for January. This is expected as the outside temperature condition is not harsh to trigger the ventilation control modules to open the windows and doors. Also, for the active buildings during the July period, the interior temperature of the integrated hybrid

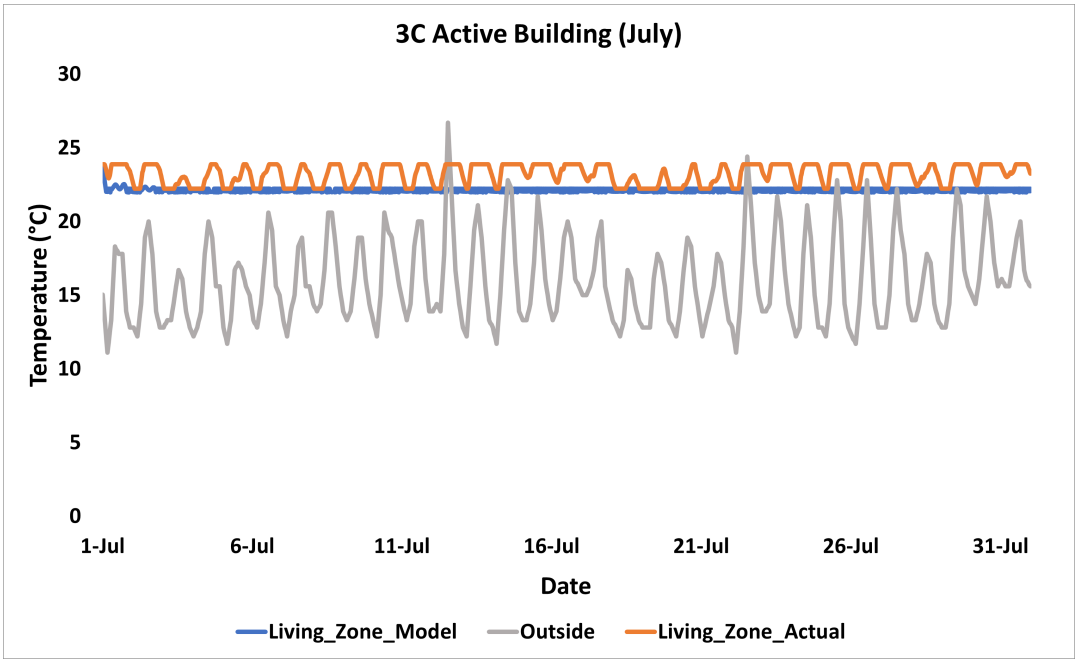

Fig. 3.16: Proposed Model vs. EnergyPlus^{TM}(Actual) for 3C Active (July)

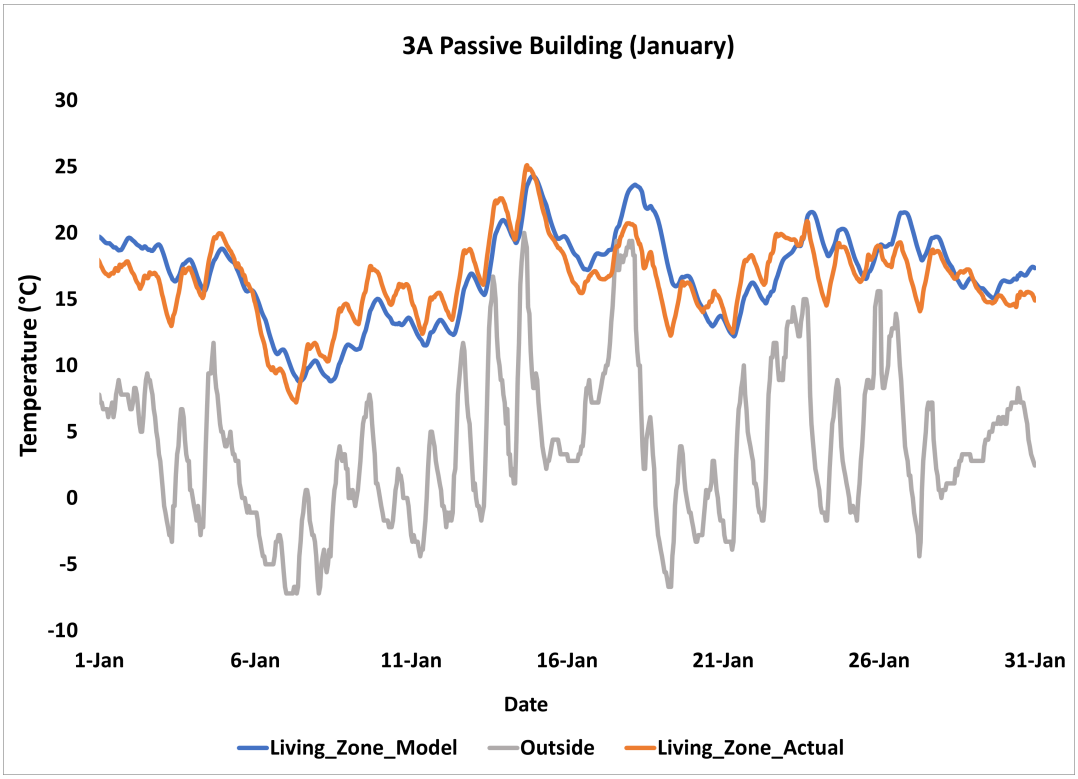

Fig. 3.17: Proposed Model vs. EnergyPlus^{TM}(Actual) for 3A Passive (January)

model is not stable compare to energy plus. This could be because the results being compared were generated directly from EnergyPlus simulations and not from actual

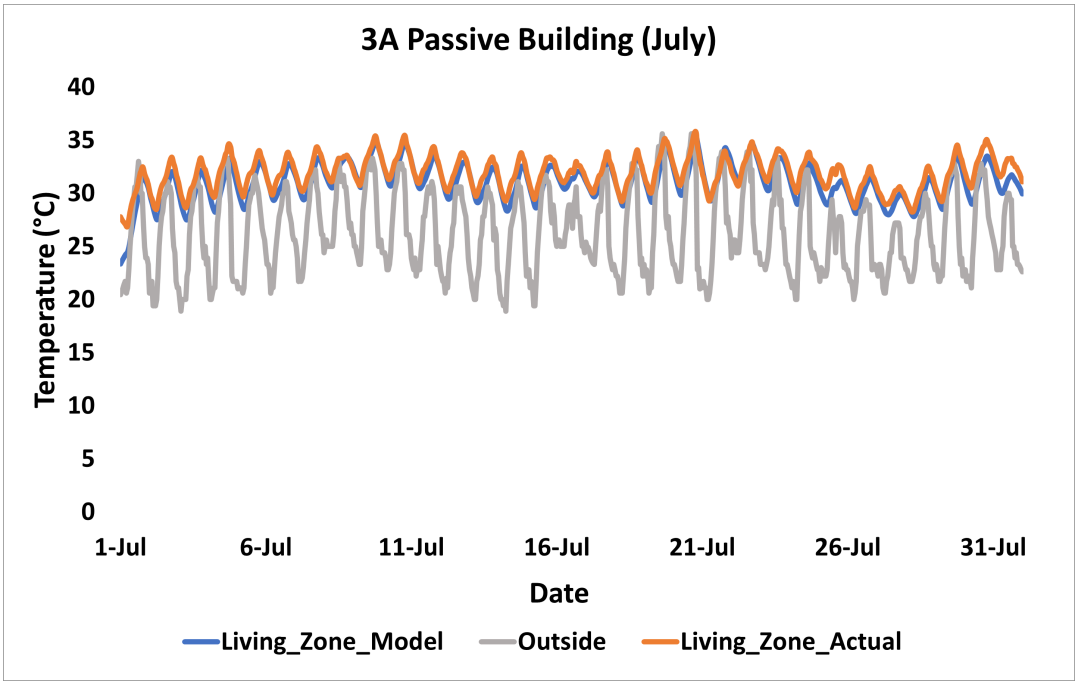

Fig. 3.18: Proposed Model vs. EnergyPlus™(Actual) for 3A Passive (July)

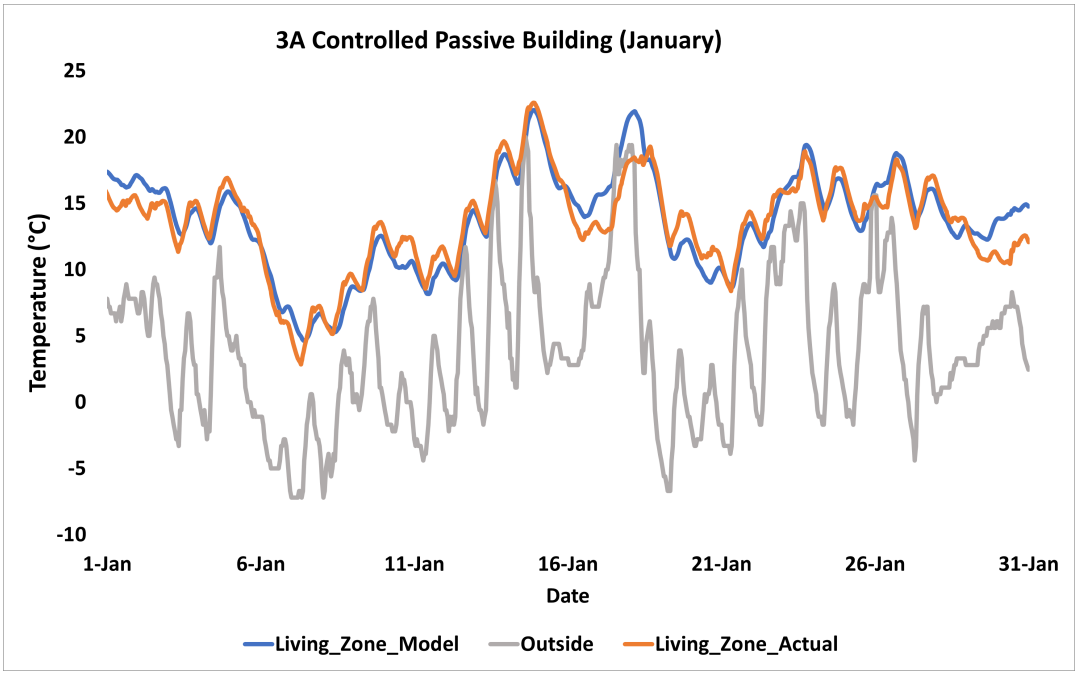

Fig. 3.19: Proposed Model vs. EnergyPlus™ for 3A Controlled Passive (January)

physical measurements from a real building. This project assumes that the typical HVAC systems found in residential buildings are constant air volume and only the temperature modulates to provide comfort. However, the mass flow rate of the energy

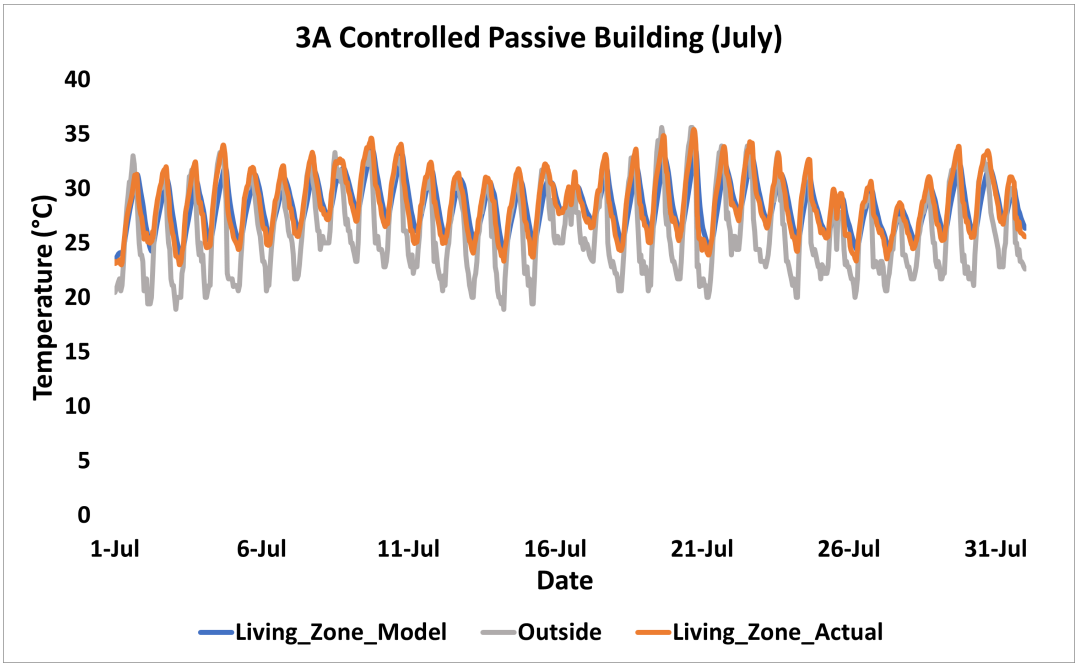

Fig. 3.20: Proposed Model vs. EnergyPlus™ for 3A Controlled Passive (July)

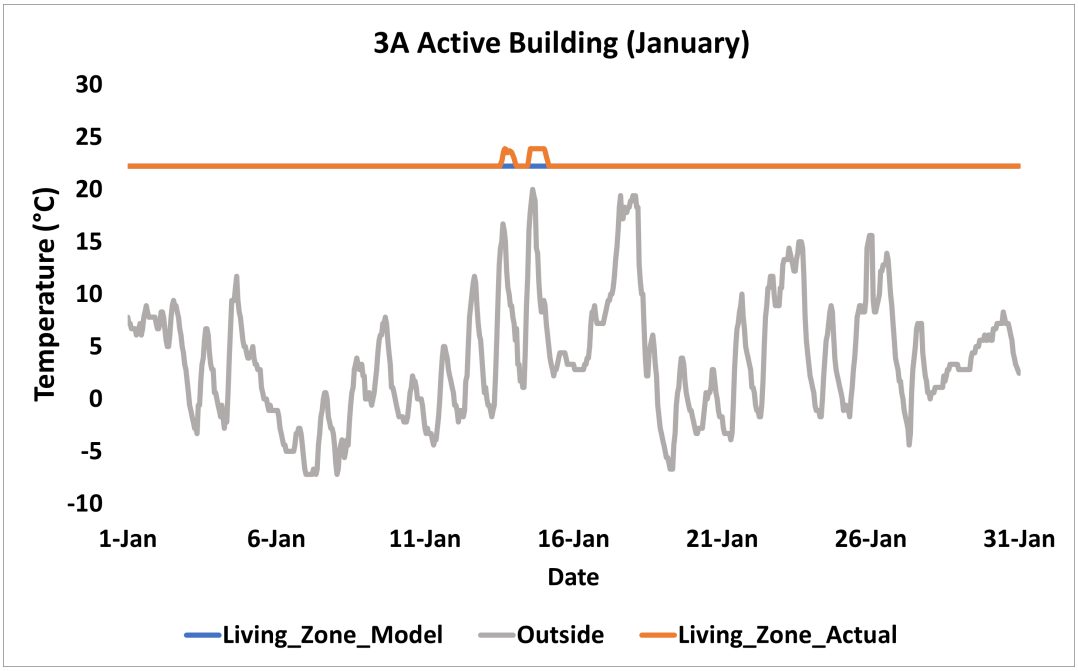

Fig. 3.21: Proposed Model vs. EnergyPlus™(Actual) for 3A Active (January)

plus model slightly vary at every timestep to maintain temperature stability. As a result, temperature data from actual buildings might provide more accurate results for comparison.

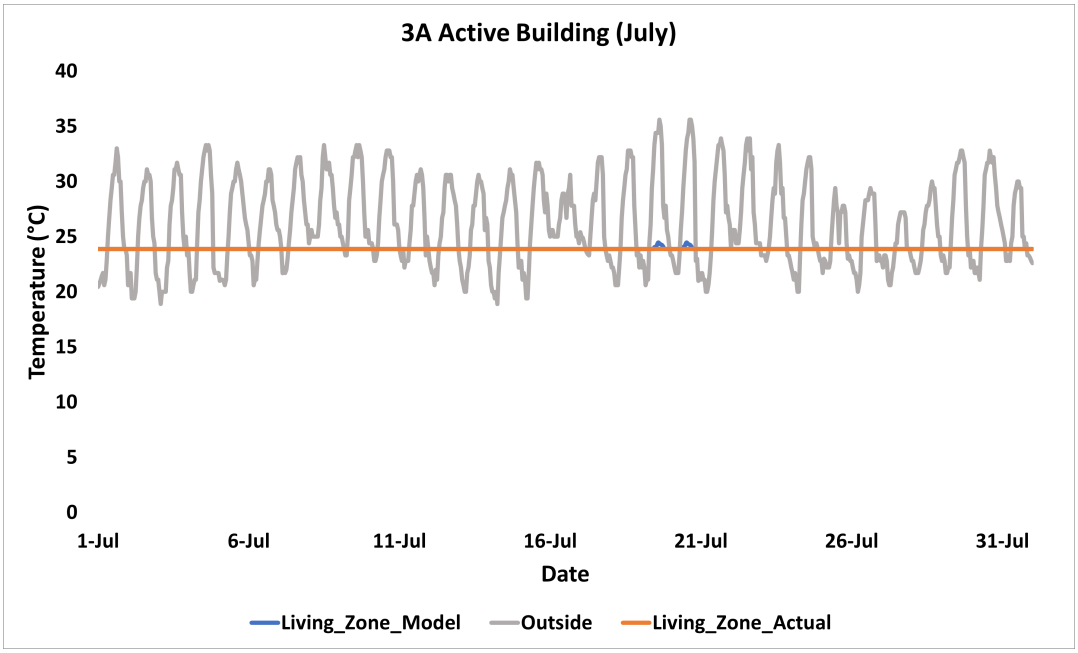

Fig. 3.22: Proposed Model vs. EnergyPlus^{TM}(Actual) for 3A Active (July)

Table 3.5: Simulation Result and Error Metrics for Zone 5B

ASHRAE Zone	Mode	Simulation Period	% CVRMSE
5B	Passive	January	7.2
5B	Passive	July	5.42
5B	Controlled Passive	January	7.01
5B	Controlled Passive	July	5.37
5B	Active	January	0.65
5B	Active	July	3.84

3.9 Summary

In this chapter, passive building designs for three different climate zones were simulated in EnergyPlus to get zone temperature information using the natural ventilation principle. The Passive strategy was needed to establish the annual periods that cooling or heating would be needed to supplement natural ventilation. Such action would minimize or replace energy related to a conventional HVAC system. Next, a hybrid model with a 1R-1C parameters network was formed for the passive buildings to establish parameters that would accurately replicate energy plus simulated results.

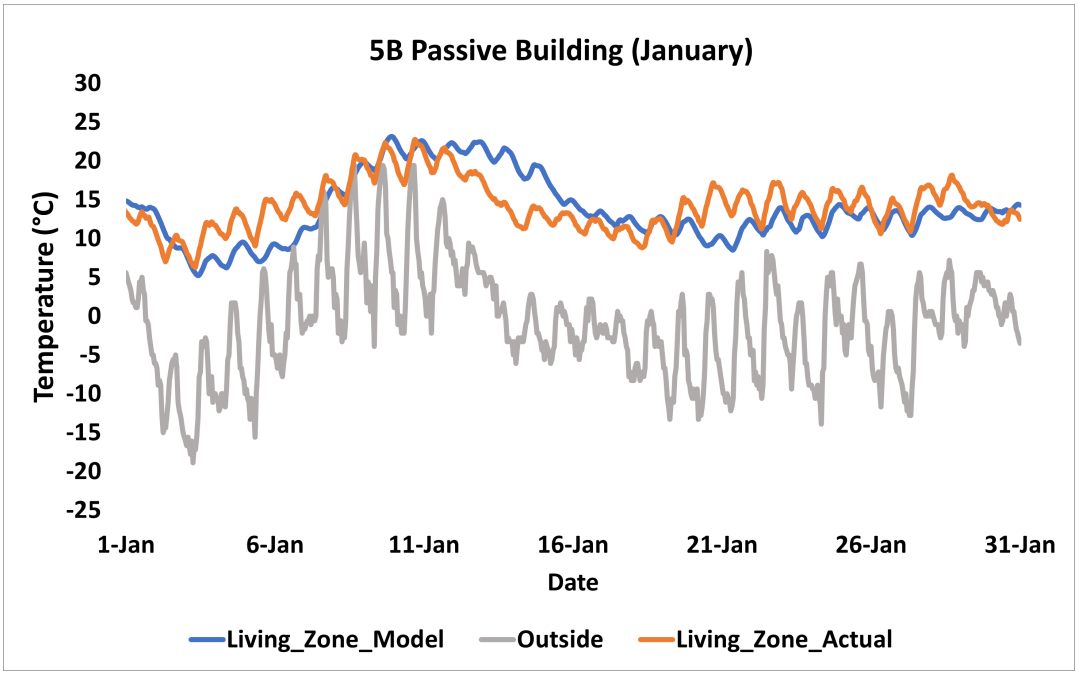

Fig. 3.23: Proposed Model vs. EnergyPlus^{TM}(Actual) for 5B Passive (January)

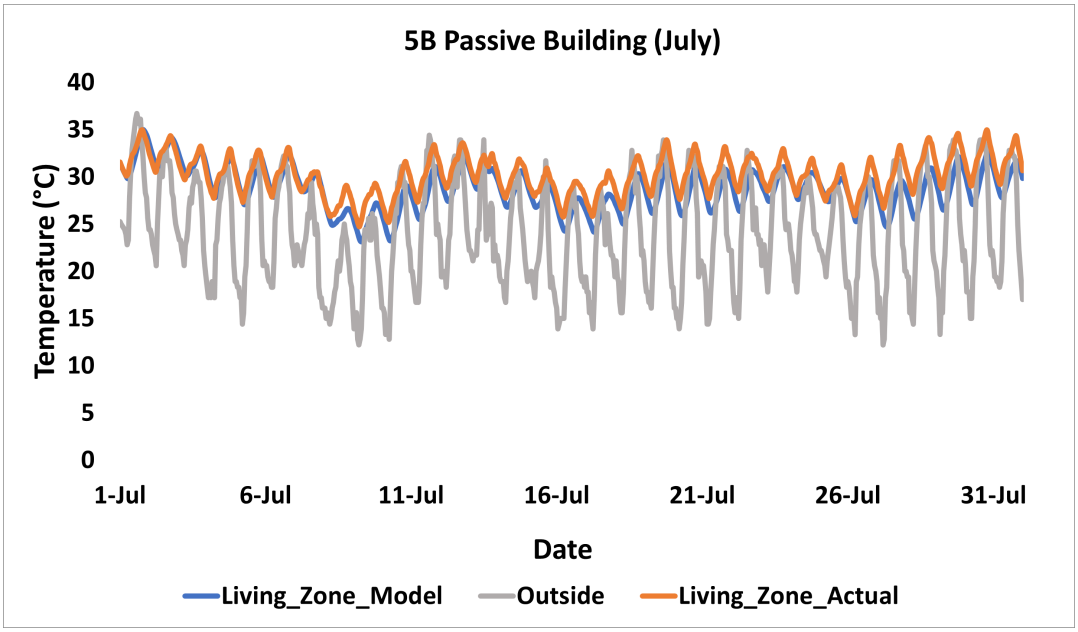

Fig. 3.24: Proposed Model vs. EnergyPlus^{TM}(Actual) for 5B Passive (July)

Parameter estimation was established through Levenberg Marquardt Algorithm due to nonlinear inputs from the weather parameters needed for the estimations. LM was used in this work because of its flexibility in reaching fast, stable, and guaranteed convergence considering the wide variations of nonlinear inputs needed for the R and

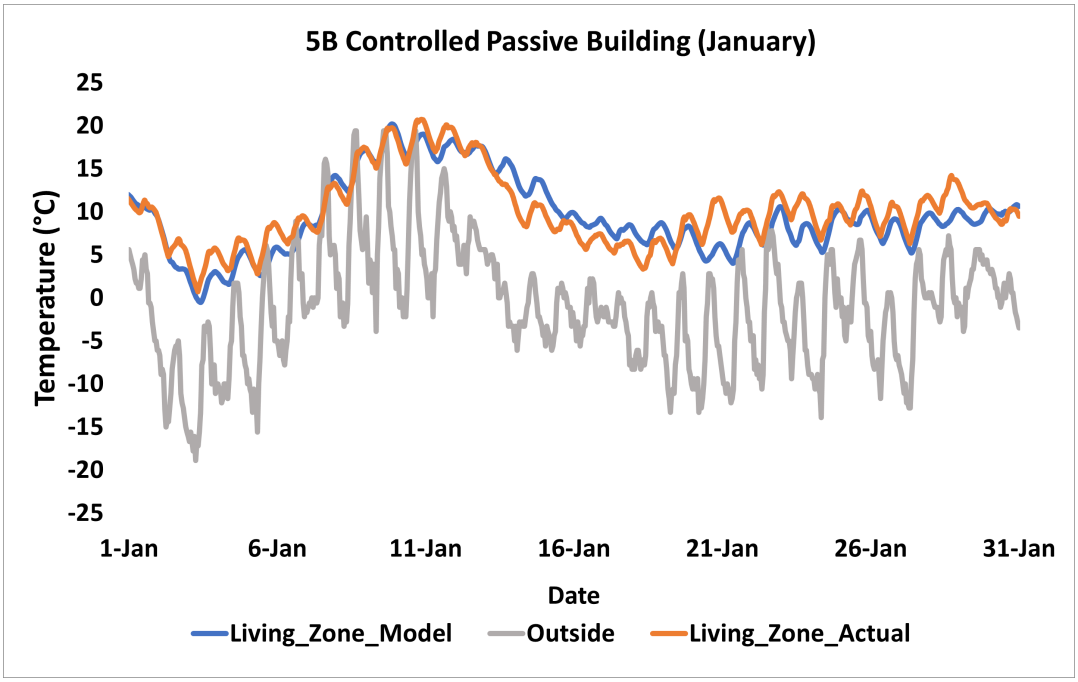

Fig. 3.25: Proposed Model vs. EnergyPlus^{TM} for 5B Controlled Passive (January)

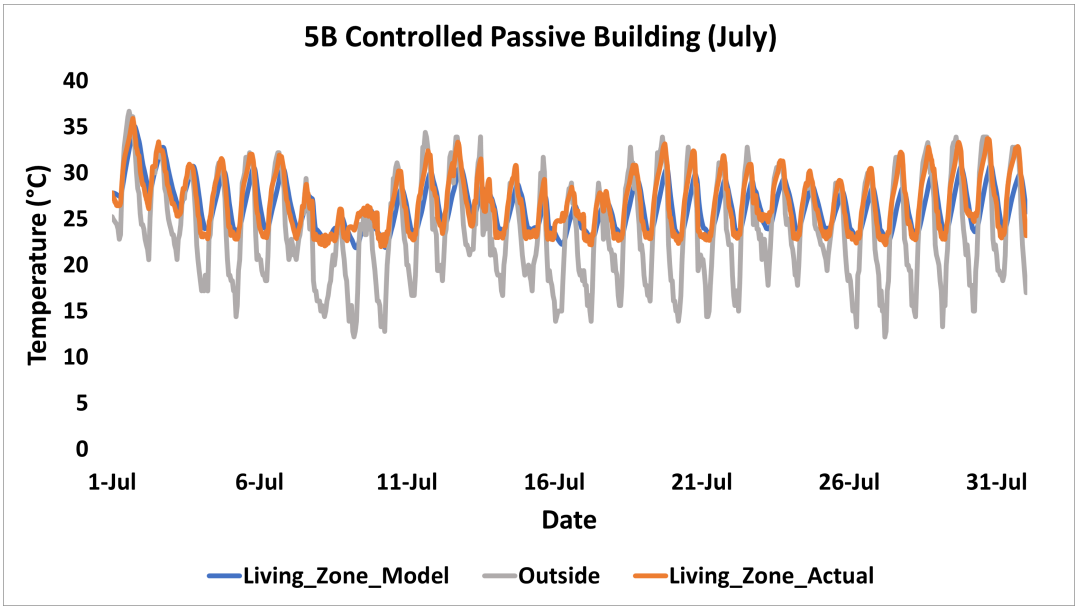

Fig. 3.26: Proposed Model vs. EnergyPlus^{TM} for 5B Controlled Passive (July)

C parameter estimations. The fully passive mode is the base model of the hybrid model and it was on this mode that parameters were generated. Then, the zone ventilation system which is temperature-controlled and executed through openable doors and windows is integrated into the base model for additional comfort.

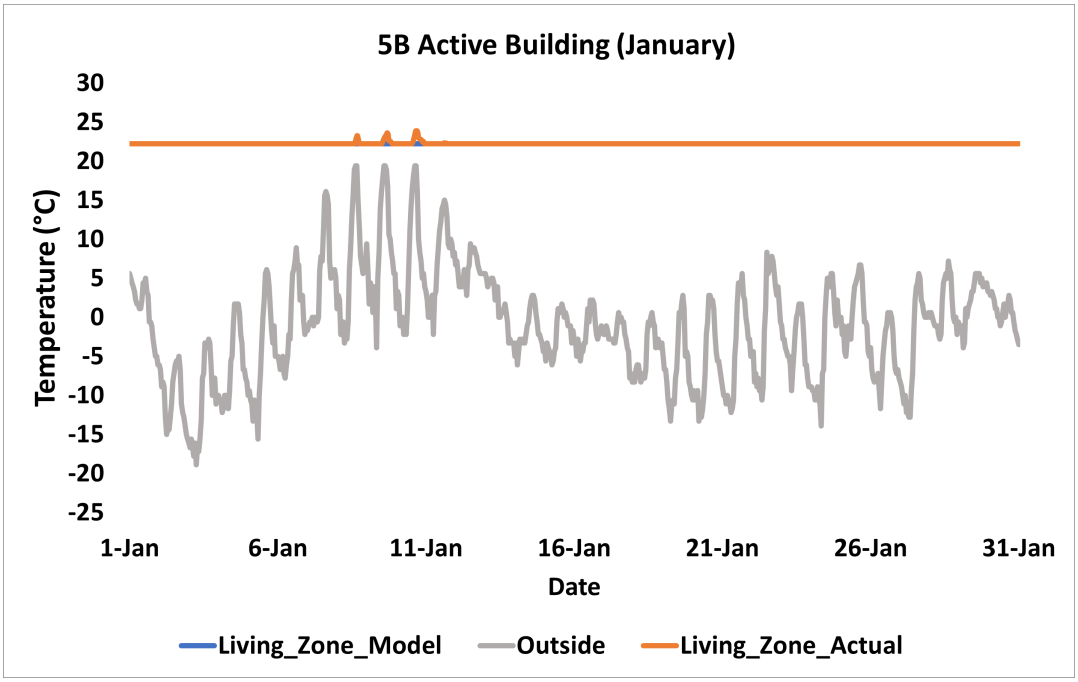

Fig. 3.27: Proposed Model vs. EnergyPlus^{TM}(Actual) for 5B Active (January)

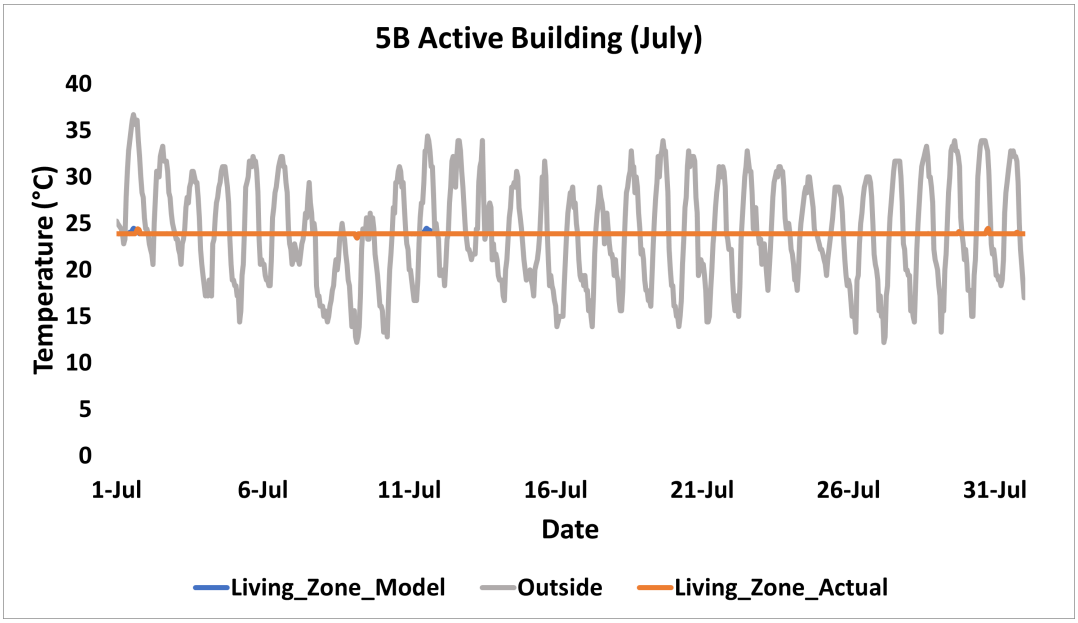

Fig. 3.28: Proposed Model vs. EnergyPlus^{TM}(Actual) for 5B Active (July)

Finally, the HVAC input was added in the active mode to let the building operates comfortably in extreme climate conditions. Results were presented for the two extreme climate periods of the year (January for the wintertime, and July for the summertime). Results showed that the fully passive buildings performed better

in the mild climate regions, Zone 3C. However, in other climates, buildings' active heating and cooling may be required for some periods annually to keep the comfort temperature of occupants within the ASHRAE acceptable limits. The developed hybrid models are good tools for future works in optimal control implementation and advanced control strategies that anticipate accurate thermal building behavior predictions considering expected energy gains in naturally ventilated buildings.

The temperature profiles of the simulated models reveal that the proposed architecture shows accuracies with EnergyPlus^{TM} at an average error of 4%. The next chapter reveals how the three operation modes identified in this chapter are integrated to deliver energy management benefits to hybrid residential buildings.

CHAPTER 4: PROPOSED FUNCTIONAL HYBRID CONTROLLER AND OPERATIONS

It is important to simulate and verify the functionality of the three hybrid building operation modes from the previous chapter when integrated together for load reduction. The methodology for such integration and its load reduction benefits associated are discussed in the next sections.

4.1 Introduction

Space heating and cooling remain the top end-use energy categories within the residential buildings sector. As such, any opportunity to reduce the operation of HVAC systems is always significant. The use of hybrid ventilation is one such strategy meant to reduce building operational demands and simultaneously satisfy occupants' comfort. As a means of realizing the benefits of the strategy, different operation modes, and control algorithms are developed and tested on three different ASHRAE climate zones to demonstrate the effectiveness of the functionality of hybrid ventilation for energy reduction. A significant part of the functional hybrid operation modes development methodology in this chapter matches a previous publication described in [120].

4.2 Main Contributions

The major goal of this chapter is to develop functional Hybrid modes of operation for Residential Buildings. This is essential to achieve energy efficiency and cost savings by prioritizing natural solutions while simultaneously meeting heating and cooling requirements considering a larger array of conditions. As such, the following contributions are achieved

- Developed three distinct functional operational modes of passively designed buildings that have not been designed in the state-of-the-art.

- Developed a simplified functional hybrid ventilation controller using a logic-based algorithm to prioritize the use of natural ventilation for comfort in residential buildings.

- Developed a complete framework for implementing mixed mode operation of hybrid ventilated buildings, including load reduction potential such that zone internal temperatures are maintained within occupants' desired range.

- Analytically established percentage energy reduction attributable to the operation of naturally ventilated residential buildings in three different ASHRAE-specified climate regions.

4.3 Functional Hybrid Operation Mode

A detailed and updated framework of the base modeling architecture of 3.2 is illustrated in 4.1 to include how the model connects with each other and controllers that allow them for functional hybrid (mix of all control modes) operation for occupants' comfort. Also, the results of the independent operation of the three basic operation modes have been discussed in Chapter 1. The next process here discusses the model and controllers' interdependency that allow them for functional hybrid (mix of all control modes) operation. This mixed operation mode is necessary as the passive buildings can flexibly leverage the significant advantages of both mechanical and natural ventilation operation, to reduce energy costs and robustly meet high Indoor Air Quality in a larger range of conditions. The controller selection of any of the three basic modes is illustrated in Fig. 4.2.

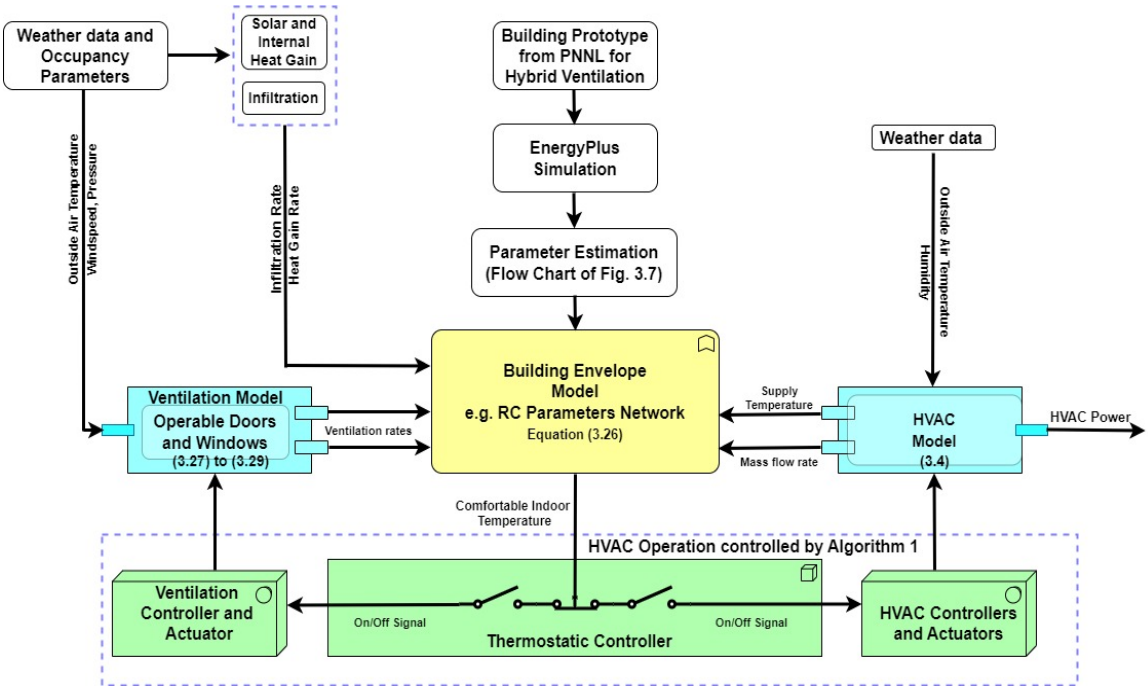

Fig. 4.1: Updated methodological framework of the study to capture interconnection of the models and their corresponding controllers

4.3.1 Mixed Operation Mode

In the mixed mode of operation, the building automatically switches its operation at any time between the fully passive mode, controlled-passive mode, and active mode to better manage the building's energy and improve indoor air quality. Comfortable temperature or any user-defined setpoints can be used as an input to control the mixed operation mode, but the control system must ensure that the HVAC system and the natural ventilation are not working simultaneously. Extensive details about the non-simultaneous working operation of both mechanical and natural ventilation systems are described in Algorithm 2.

In the mixed mode of this project, a comfortable temperature range between (19.5°C to 24°C) was used as an input, which falls between ASHRAE standard [108]. The comfortable indoor adaptive temperature range for natural ventilation as published by ASHRAE is presented in Fig. 4.3. The building operates in sequence. First, the building operates in the fully passive mode, and if comfortable indoor temper-

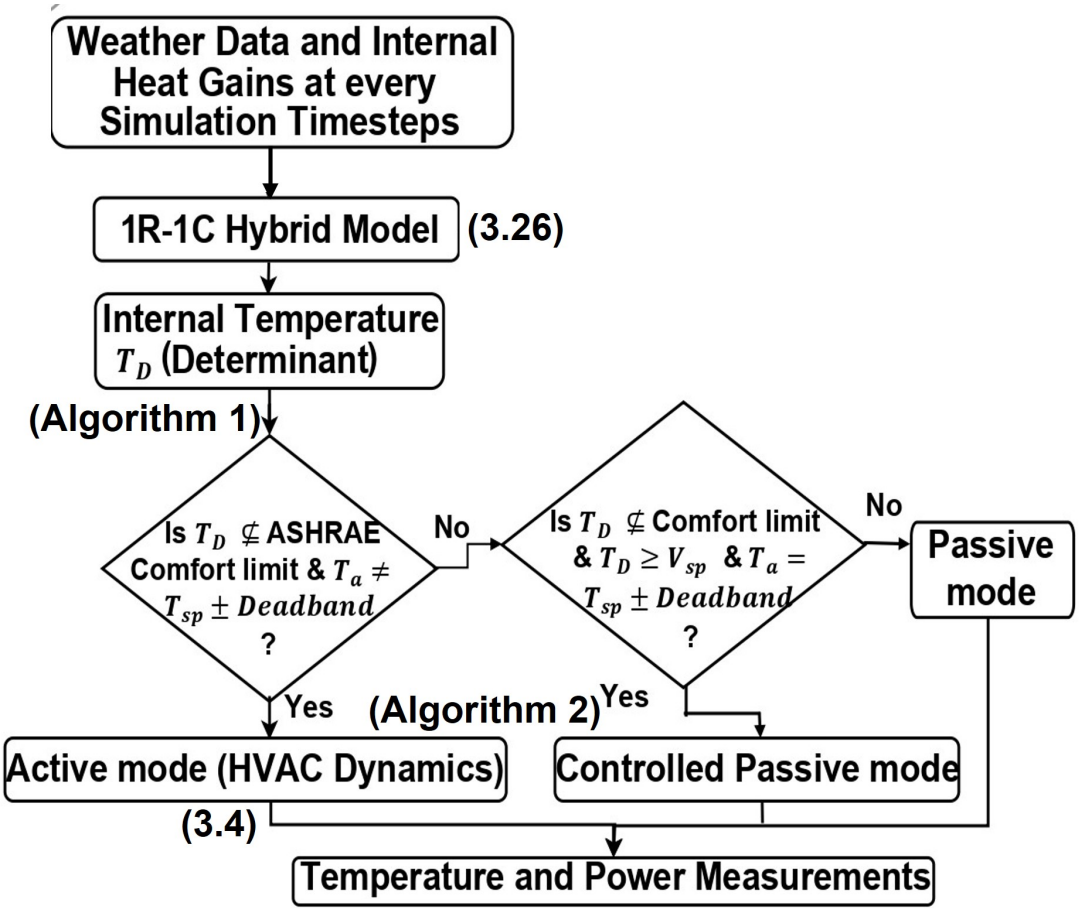

Fig. 4.2: Functional hybrid controller selection flow chart

atures are unsatisfied, it switches to the controlled-passive mode, and finally to the active mode. For best performances, the mixed-mode can be achieved and managed with other building resources using optimization algorithms as explained in the next chapter.

4.3.2 Controller Design

A simplified functional hybrid ventilation controller using a logic-based algorithm to prioritize the use of natural ventilation for comfort in residential buildings is designed according to Algorithm 2. The idea of a hybrid ventilation control system is the ability to automatically switch between the mechanical ventilation controller of the active mode, the natural ventilation controller of the controlled passive mode, and no control action of the fully passive mode. A general strategy for integrating these sets

Algorithm 2: Hybrid Ventilation Controller

Initialize or get $T_{i,z}(t-1)$ where, t = 1,2, ..., T. and T is the last simulation timestep
Get $m_{inf,z}$, $Q_{total,z}$, and other parameters in (3.26)
Get the ventilation setpoints (V_{sp}), thermostat setpoints (T_{sp}) and the deadbands
for *t = 1, 2, ..., T* **do**
    Find $T_{i,z}(t)$ without heating or cooling **end**
    if $T_{i,z}(t)$ *and* $T_a(t) \not\subseteq T_{sp} \pm deadband$ **then**
        $0 \leq P_{HVAC} \leq \infty, \quad A_{\text{open=0}}$
        compute the supply temperature T_s by using (3.4) and Algorithm 1
    end
    $T_{i,z}(t) \not\subseteq \mathrm{T}_{sp} \pm deadband$,
    and $T_{i,z}(t) > V_{sp}$
    and $T_a(t) \subseteq \mathrm{T}_{sp} \pm deadband$,
    $0 \leq A_{open} \leq 1, \quad P_{HVAC} = 0, in(3.27), (3.28), (3.4)$
    Building is operating using natural ventilation **else**
        $\mathrm{A}_{open} = 0, \quad P_{HVAC} = 0$
        Building internal temperature is acceptable
    end
return A_{open}, T_s, P_{HVAC}

of controllers which is a continuous type for the HVAC system and a discrete type for the window operation is to first design them separately, and then integrate them via a hierarchical logic control architecture that uses outside air temperature values as a priority in switching actions. As illustrated in Fig. 4.1 the controllers act to create decisions for the ventilation model by activating an open or shut position for the windows and doors, or turning on/off the HVAC system. The independent control action of the HVAC system without the natural ventilation piece has been discussed in Algorithm 1. The switching action within a ten-minute simulations timesteps used in this research allows for cycling of the HVAC system in a way that achieves building ventilation that promotes indoor air quality and improves HVAC equipment reliability.

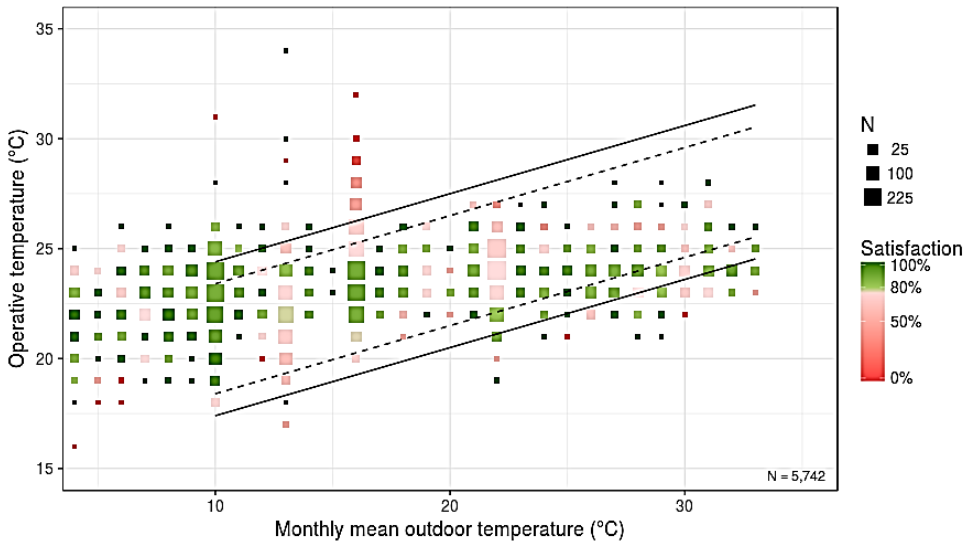

Fig. 4.3: ASHRAE Adaptive Thermal Comfort Range for Natural Ventilation [121]

4.4 Results and Discussions

The operation of the hybrid ventilation controller of Algorithm 2 is logic-based and the results of mixing the HVAC operations with natural ventilation are presented in this section. Fig. 4.4 illustrates the monthly indoor air temperature profile with the mixed-mode operations in comparison to when the HVAC only is in operation. Fig. 4.5 shows the corresponding HVAC power comparison between the mixed-mode operation and the action-only mode. The difference between the areas under the curves of Fig. 4.5 shows a significant power reduction of approximately 90% that can be attributed to the mixed-mode operation.

For all the three ASHRAE climate zones considered, the result established a significant reduction in HVAC energy consumption. Little requirement for HVAC operation in the summertime and wintertime of the mild climate region depicted as zone 3C made the region a potential territory for passive buildings. Results of the other two zones established HVAC is needed at most times to maintain comfortable indoor temperatures during the summertime.

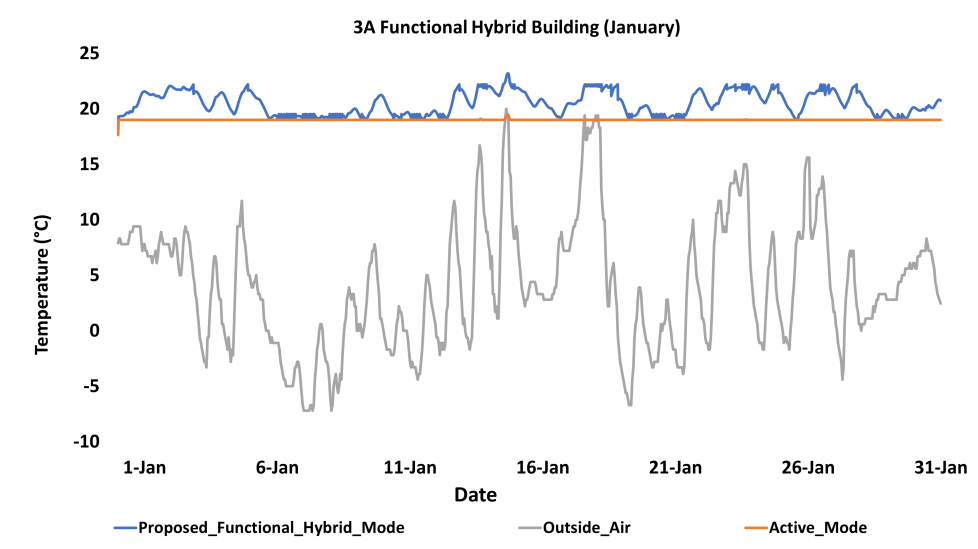

Fig. 4.4: Building 3A Functional Hybrid Operation (Winter)

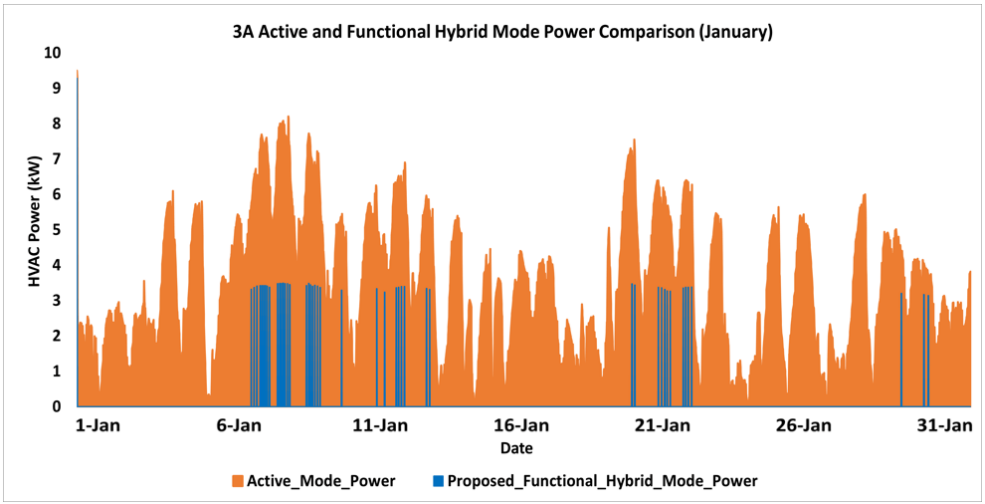

Fig. 4.5: Building 3A Active and Functional Hybrid Mode Power (Winter)

Generally, the functional hybrid (mixed) operation mode results are satisfactory in reducing building operational demands by switching between passive, controlled-passive, and active modes of operation. However, the building zones' interior temperature is not stable compared with the results obtained when the HVAC is the only mode of building operation. The simulated temperature results show that dynamics with smaller time constants are also well represented as their operating modes are able to switch based on their defined logics and setpoints during the mixed operation

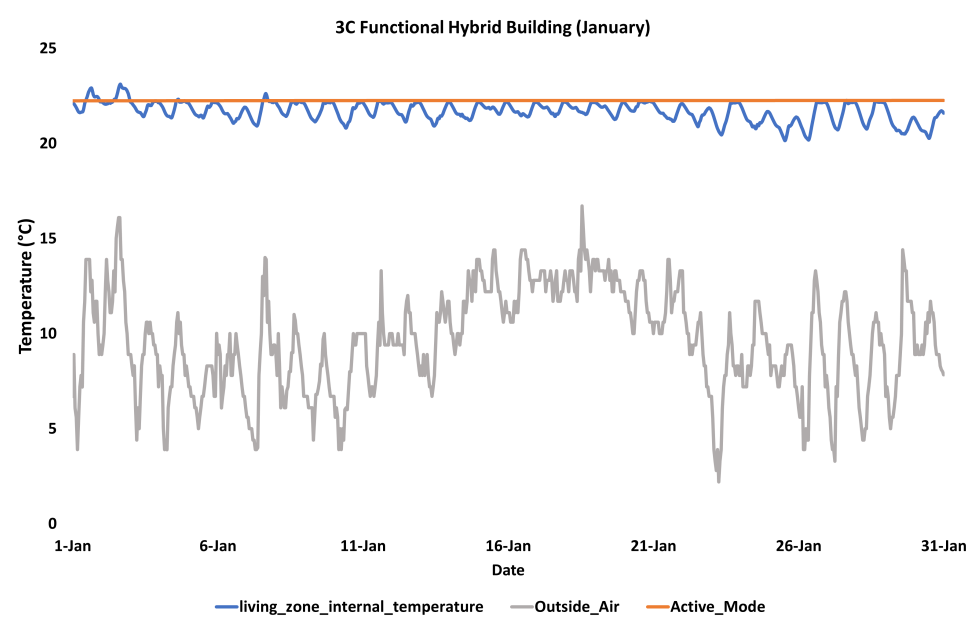

Fig. 4.6: Building 3C Functional Hybrid Operation (Winter)

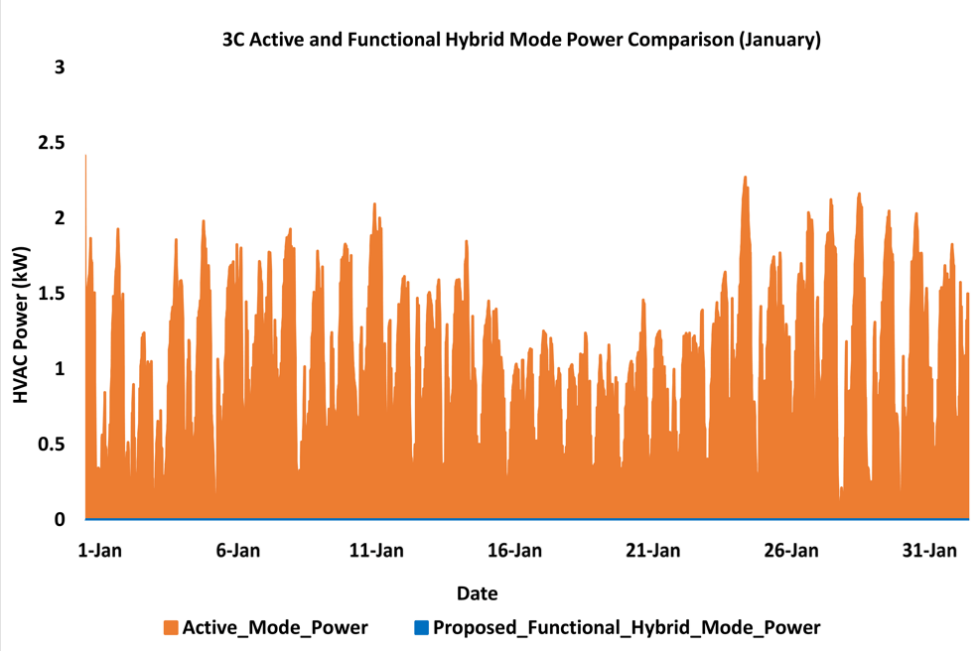

Fig. 4.7: Building 3C Active and Functional Hybrid Mode Power (Winter)

mode.

January and July simulation data for ASHRAE zone 3C revealed no HVAC demand is necessary for the mild climate region. These results also reinforced the effectiveness and viability of this ASHRAE zone to accommodate passive buildings with hybrid

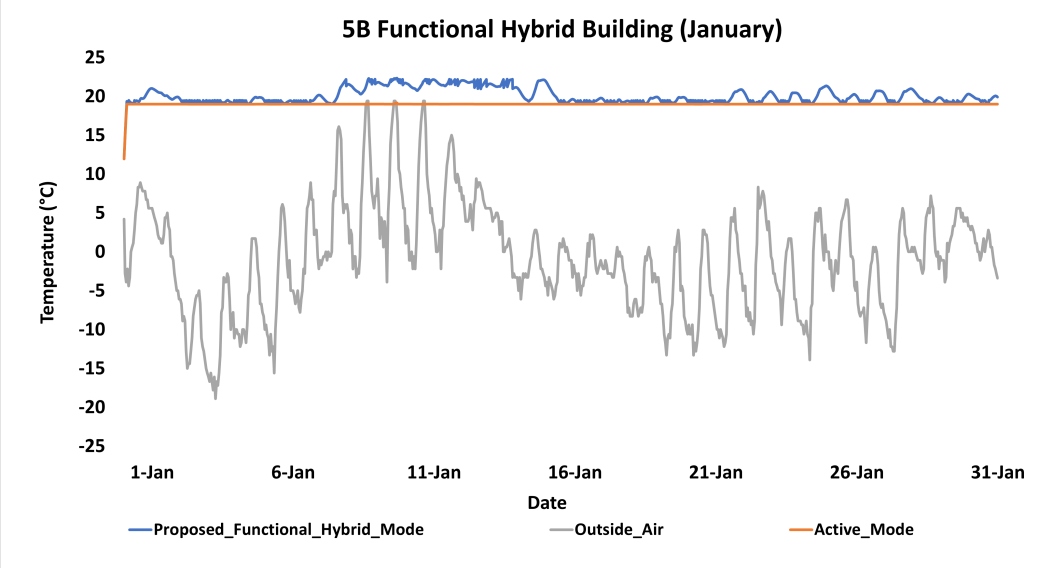

Fig. 4.8: Building 5B Functional Hybrid Operation (Winter)

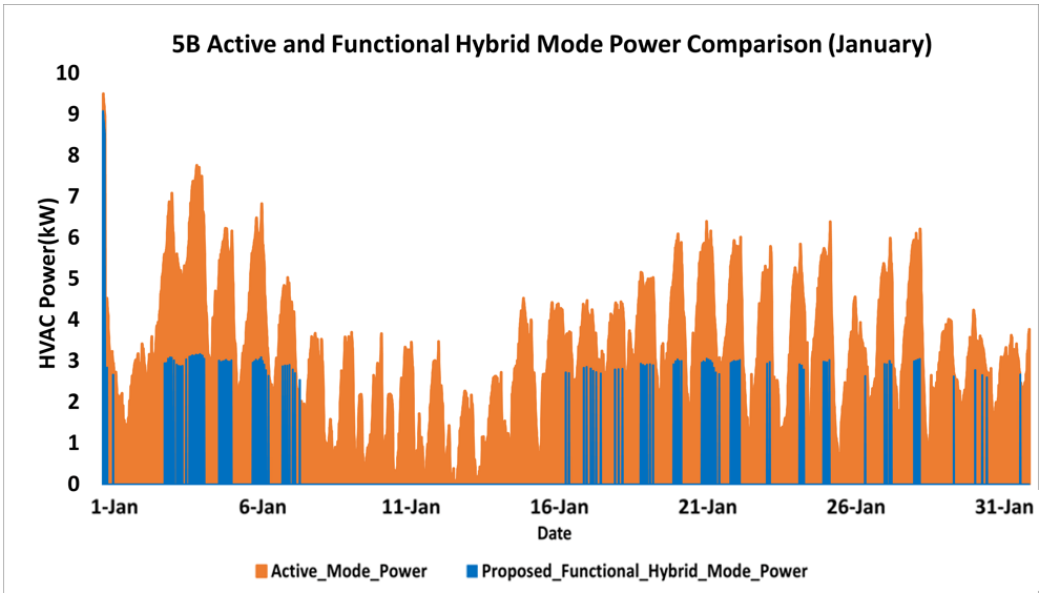

Fig. 4.9: Building 5B Active and Functional Hybrid Mode Power (Winter)

ventilation technology. The least HVAC demand reduction occurred in the Charlotte region with a power decrease of only 5%. This is due to the significant operation of the HVAC system in the ASHRAE 3A zone as hot summer weather (observed from the outdoor temperature values) is not conducive enough to trigger the passive and controlled passive mode more often except during a few night ventilation. Comprehensive optimal ventilation strategies are discussed in the next chapter and are

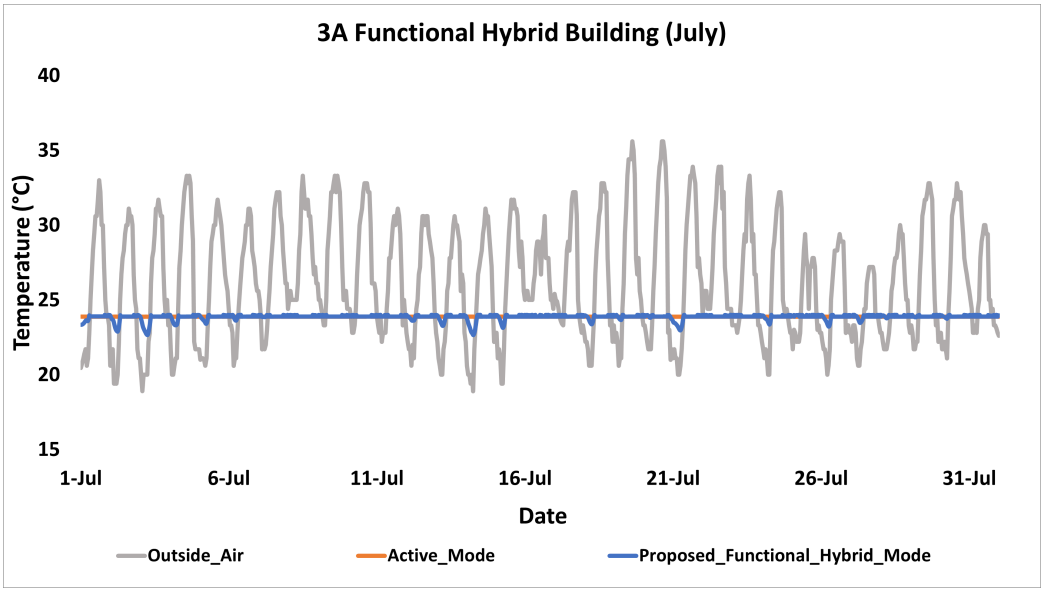

Fig. 4.10: Building 3A Functional Hybrid Operation (Summer)

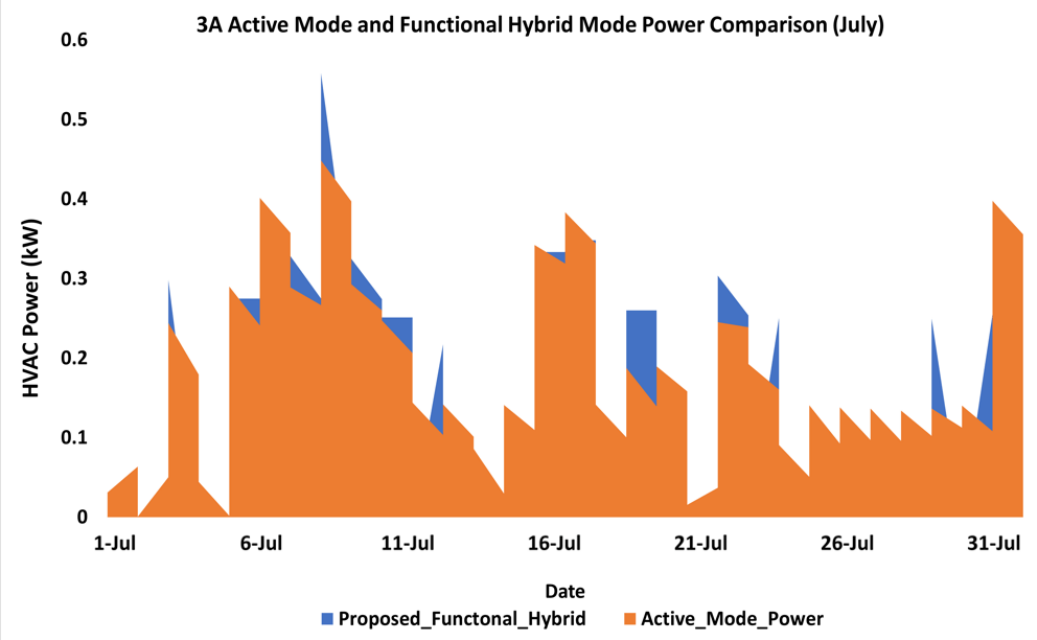

Fig. 4.11: Building 3A Active and Functional Hybrid Mode Power (Summer)

fundamental to achieving additional energy savings for the hot and humid ASHRAE zones such as the one seen in Charlotte. The optimal framework for the mechanical and natural ventilation systems aims to exploit precise cooling from the mixing of the ambient air with the indoor counterpart as frequently as possible while eliminating overcooling and overheating perods

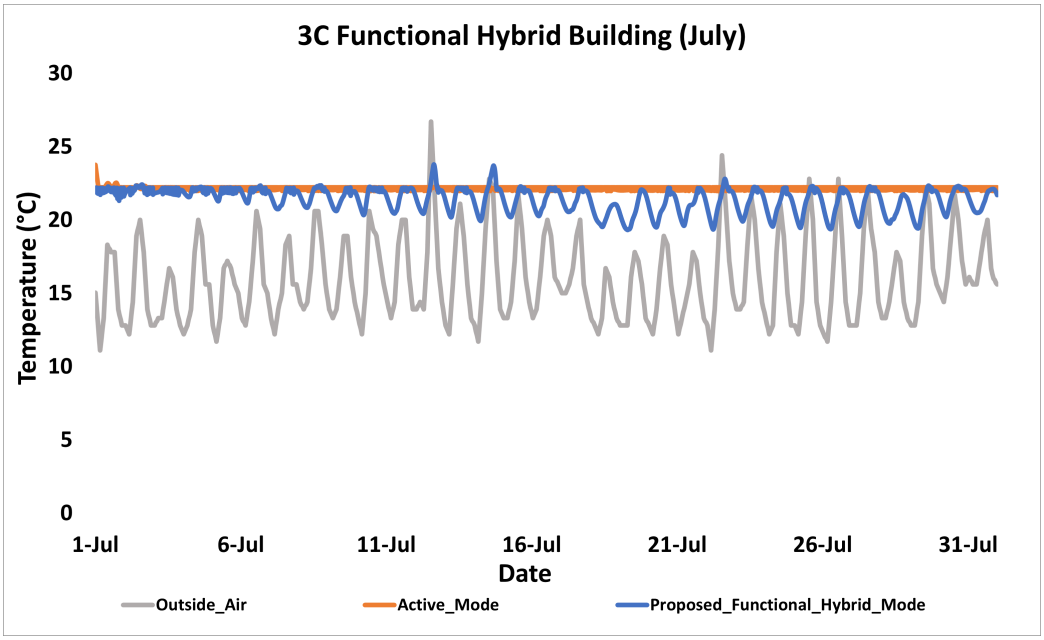

Fig. 4.12: Building 3C Functional Hybrid Operation (Summer)

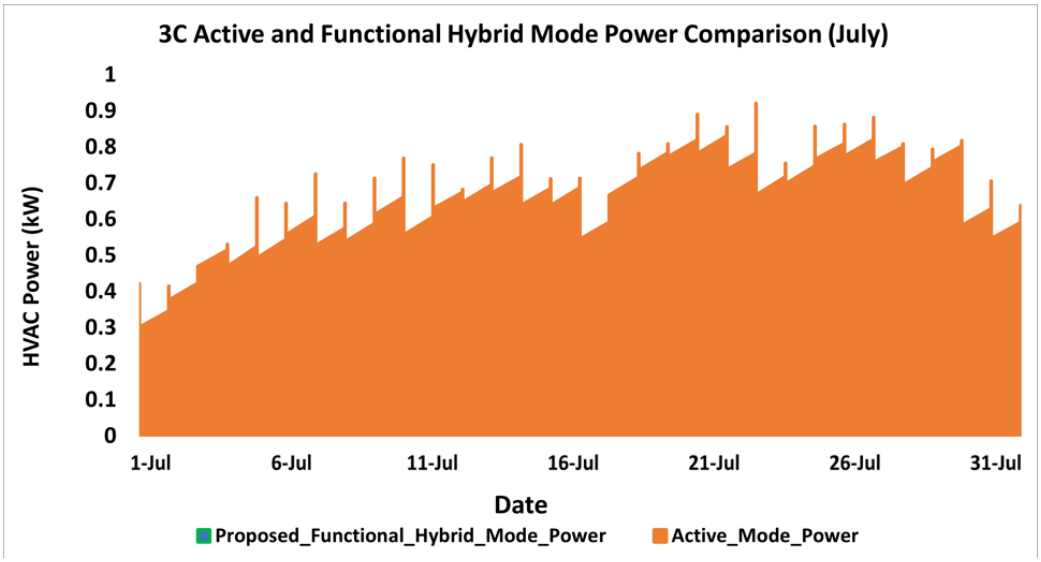

Fig. 4.13: Building 3C Active and Functional Hybrid Mode Power (Summer)

For all three simulated zones, the fully passive building mode of operation occurs more often during the winter times. This is expected because the outdoor temperature values are not high to trigger the controlled-passive mode of the functional hybrid controller to open the windows and doors often. The tolerable internal temperature results obtained in the wintertime are due to the effects of using a passive Trombe

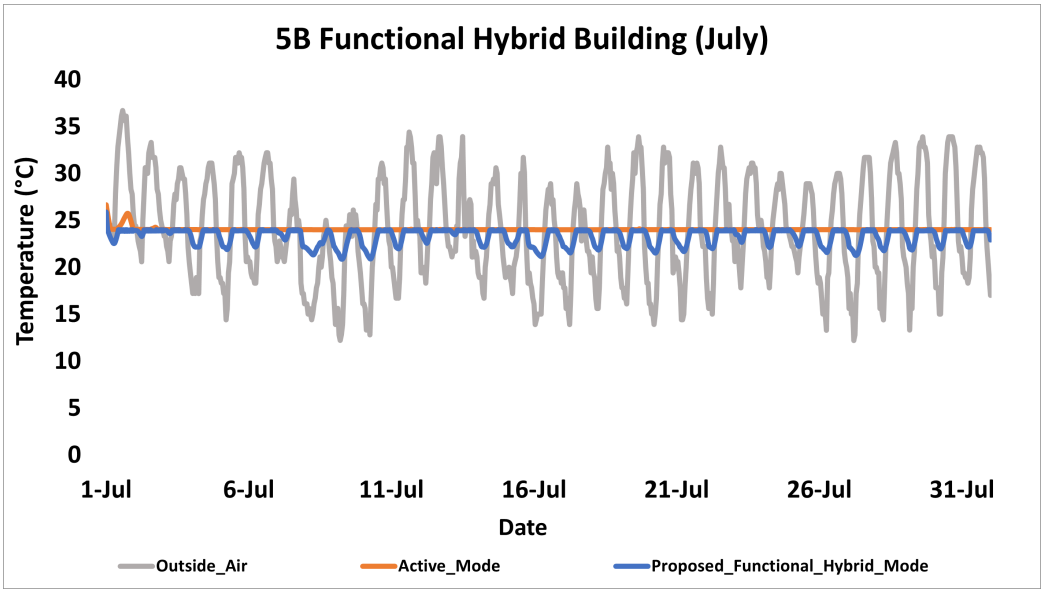

Fig. 4.14: Building 5B Functional Hybrid Operation (Summer)

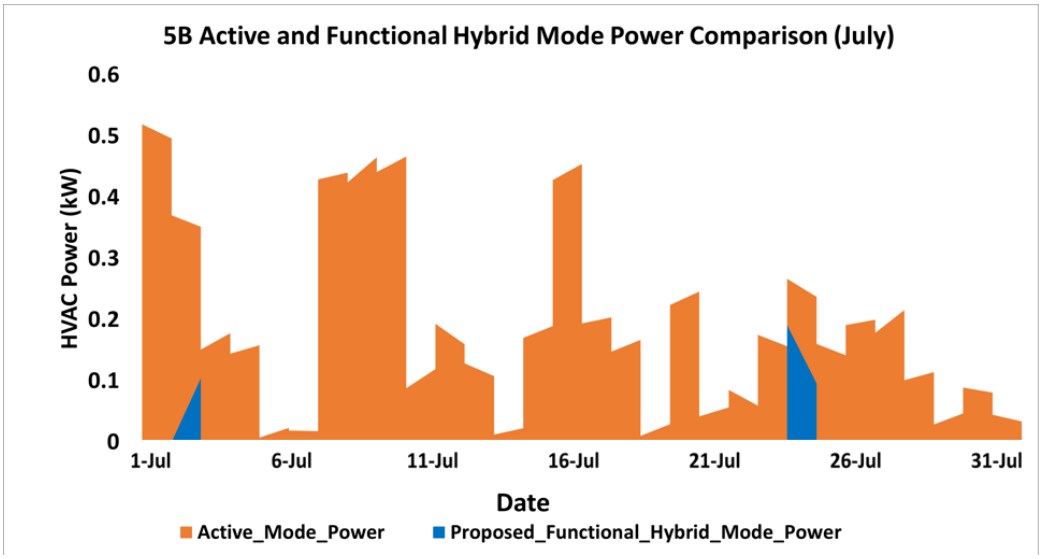

Fig. 4.15: Building 5B Active and Functional Hybrid Mode Power (Summer)

wall within the building's initial designs.

4.5 Summary

Natural ventilation is the key technology in new residential buildings for substantial energy reductions. In this chapter, a simplified functional hybrid model for residential buildings using natural ventilation is presented to provide thermal comfort with a reduced building operational demand. Passive residential building models for three

Table 4.1: Power comparison between the Active Mode and the Proposed Functional Hybrid Mode

ASHRAE Zone (Month)	HVAC Consumption (kWh)		% Difference in area under the power curve
	Active	Proposed Hybrid	
3A (January)	2545	81	96
3A (July)	464	437	5
3C (January)	762	0	100
3C (July)	284	0	100
5B (January)	2384	183	92
5B (July)	435	270	38

different ASHRAE climate zones were used to demonstrate the effectiveness of the functional hybrid mode. Like the previous chapter, Simulations were carried out for two extreme months of the annual climate periods (January for winter and July for summertime). Differences in the area under the power curves showed a significant demand reduction in the mild climate region and a less reduction in the summer of other climate regions. The results showed the capability of this framework to be deployed for extensive applications which are discussed in the next chapter.

Also, three distinct functional hybrid operation modes of the developed model for energy management not present in the state-of-the-art were presented in this chapter and results revealed an average of 70% energy costs reduction impacts on consumers in the evaluated ASHRAE climate zones.

Although the mixed operation mode proves effective in reducing the building operational demands of the simulated cases in this chapter, however for additional efficient operation, it was observed that conventional HVAC control is not adequate enough to control the thermal comfort level in the passive buildings. There is a need to anticipate the heating and cooling effects and provide less temperature dynamics of ventilation as passive buildings have a slow response to additional energy inputs, e.g. passive solar gains, which increases the risk of overcooling and overheating periods. Such circumstances raise the need for advanced control strategies that anticipates the

thermal building behavior and the expected energy gains. Deploying an optimization framework rather than logic based as discussed in the next chapter is meant to solve the controlling problems while simultaneously providing better energy efficiency.

CHAPTER 5: MODEL PREDICTIVE CONTROL ALGORITHM

Formal problem definitions and how the hybrid building framework interacts with the smart grid are presented in this section. First, the optimization framework for maximum load control is presented, followed by the topology of how hybrid building responds to different signals from the grid.

5.1 Introduction

Passive Building Energy Management Systems (PBEMS) can control, coordinate, and schedule energy resource equipment based on certain functions and operations as discussed in Chapter IV. However, these systems can provide improved efficiency, better economic returns, and higher reliability services to smart grids if embedded within optimization frameworks. To explore these benefits, a comprehensive methodological framework that applies model predictive control (MPC) is deployed for three use cases of demand management and is evaluated in the future sections. A significant part of the optimization methodology framework in this chapter matches a previous publication described in [122].

5.2 Main Contributions

The goal of this chapter is to develop an Optimization Framework that also makes the building energy aware - enabling the buildings to forecast, react, and adjust to utility signals to address major challenges facing the evolving smart grid, all while providing optimal cost savings, efficiency improvements, and comfort to consumers. Here are the contributions:

- Developed a scalable and extensible framework for implementing model predictive strategy operation of hybrid ventilated buildings for real-time control of

the intermittent operation of their active systems.

- Used three distinct test cases of demand side management to gain insight into the efficacy of the model predictive optimization framework in supporting grid services and optimally providing reliability.

- Compared the effectiveness of using an optimization framework for better comfortable temperature stability in relative to the functional hybrid operation modes discussed in the last chapter.

- The proposed optimization framework is validated for the correctness of operation through power balance analysis.

- Analytically established benefits such as incentives gain or percentage energy reduction attributable to the participation of the hybrid buildings on three test cases.

5.3 Model Predictive Optimization Strategy

The optimization problem is the core of the building operational modes to reduce building energy demand while putting other loads into consideration. In simplified terms, we want to minimize the use of HVAC systems in passive buildings, which are needed in extreme weather conditions. If the building operating condition warrants the HVAC system to be used, then we find the temperature setpoint predictions and corresponding equipment operation that gives us the lowest cost when local energy generations and storage have been exhausted. The objective function is formulated as follows.

$$J\left(\mathbf{x}_0, \mathbf{u}\right) = \sum_{t=0}^{H-1} (J_{grid}(t)) \tag{5.1}$$

where H is the horizon, J_{grid} is the cost of electricity consumption at every timestep (t) determined by the power from the grid expressed as

$$J_{grid} = \pi_{grid} P_{grid} \tag{5.2}$$

where π_{grid} is the unit price of electricity Similarly,

$$J_{as,t} = \pi_{as} P_{as,t} \tag{5.3}$$

where $J_{as,t}$ is the ancillary service payment received for building demand reduction, π_{as} is the unit price of ancillary service, and $P_{as,t}$ is the power capacity that qualifies for the ancillary payment. $\mathbf{x}_0$, represents various state variables of interests. and u represents the matrix of core decision variables as expressed in (5.4)

$$u = [T_{set}, T_{sp}, U]^T \tag{5.4}$$

The updated model that integrates the MPC optimization framework with other model that have been discussed in the previous section is provided in Fig. 5.1

The discretization process through the Euler solution method for the building thermal dynamics, water heater, and HVAC equipment model is explained in parametric identification methodology section. Other building energy resource constraints have been given earlier in this section. The problems are formulated and a Mixed Integer Quadratic Programming and the optimization is carried out according to Fig. 5.2 using Gurobi as solver [123].

5.4 Validation of MPC Control Actions

While the mixed-mode can combine the functions of the fully passive, controlled-passive, and active mode to save a significant amount of energy with reduced HVAC system operations, there are other schedulable and thermostatically controlled loads

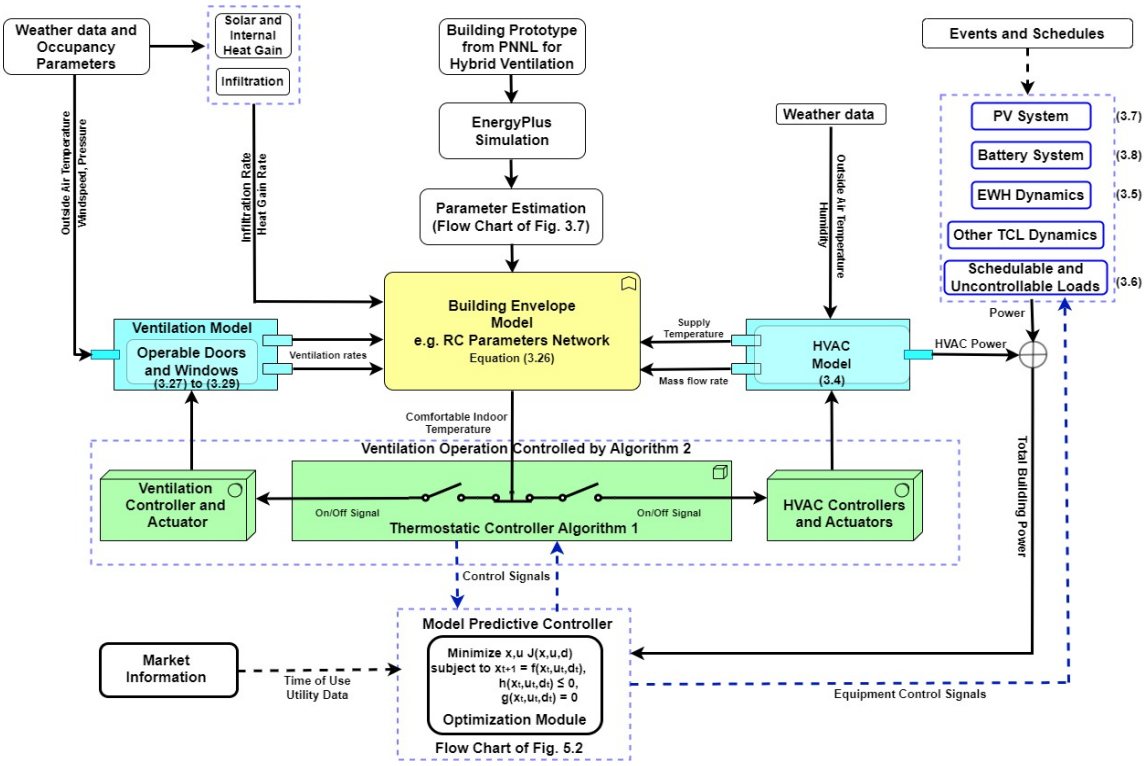

Fig. 5.1: A comprehensive methodological framework of the study

consuming a considerable amount of energy in the building. This consumption can suppress the successful impacts of the mixed-mode building if they are not operated efficiently. The water heater is a perfect example of such an energy-consuming appliance. Therefore, proper coordination is essential. Unfortunately, it is difficult for consumers to find out exactly how to adjust their energy usage under economic signals, especially when using a complicated Time-of-Use (TOU) rate. Applying MPC control would integrate the mixed operational mode with forecasts and other equipment constraints to give a result that helps decide on optimal building loads operation setpoints for energy cost reduction. The results for the basic control modes of the San-Francisco location (climate zone 3C) have been presented previously in this work, the same building and location were used to demonstrate the MPC control applications. The TOU electricity rate used is available from PGE residential customers in the area [124]. First, validation of the expected control signals of the building

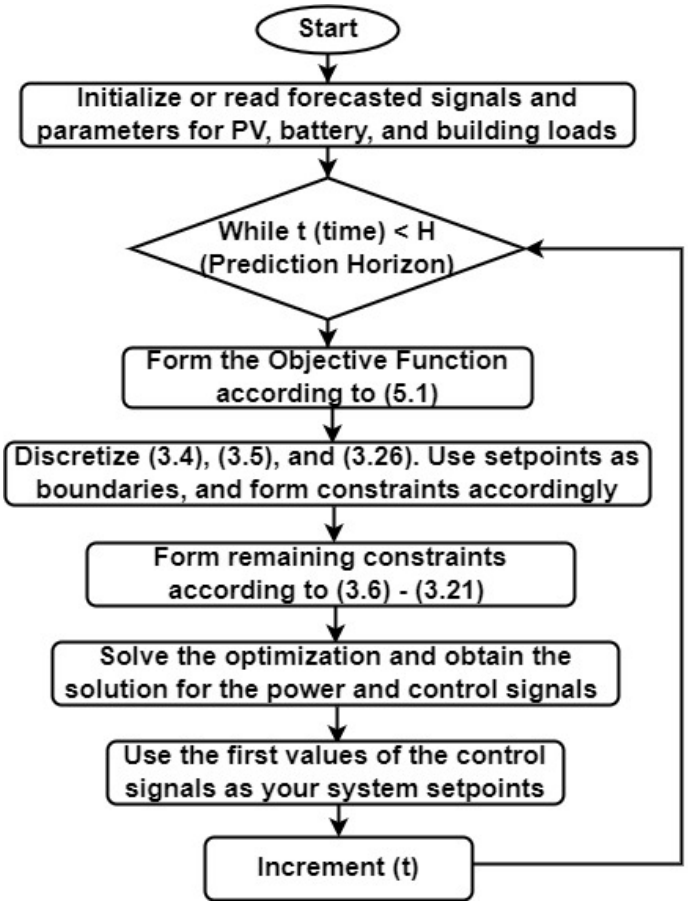

Fig. 5.2: Predictive Optimization Process

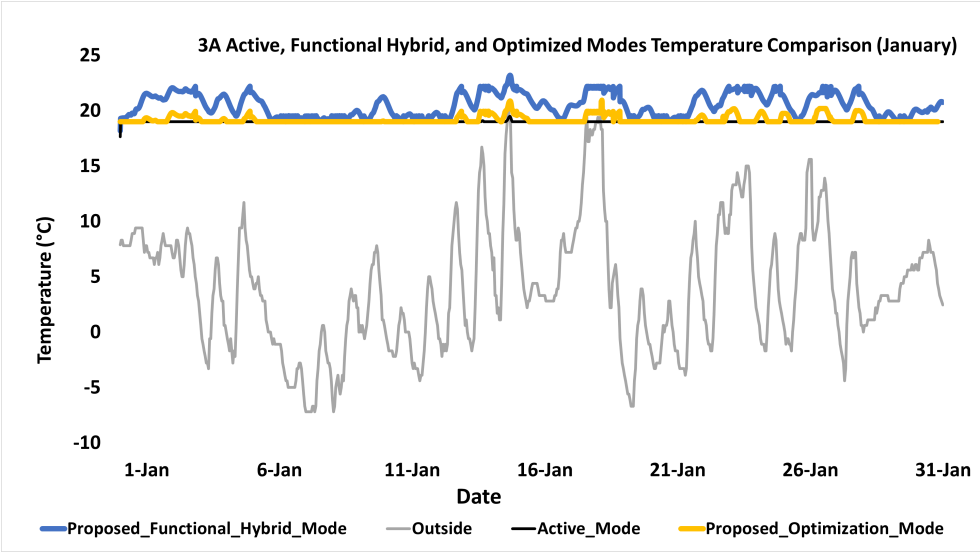

Fig. 5.3: Building 3A Active, Functional Hybrid, and Optimized Modes Temperature Comparison (Winter)

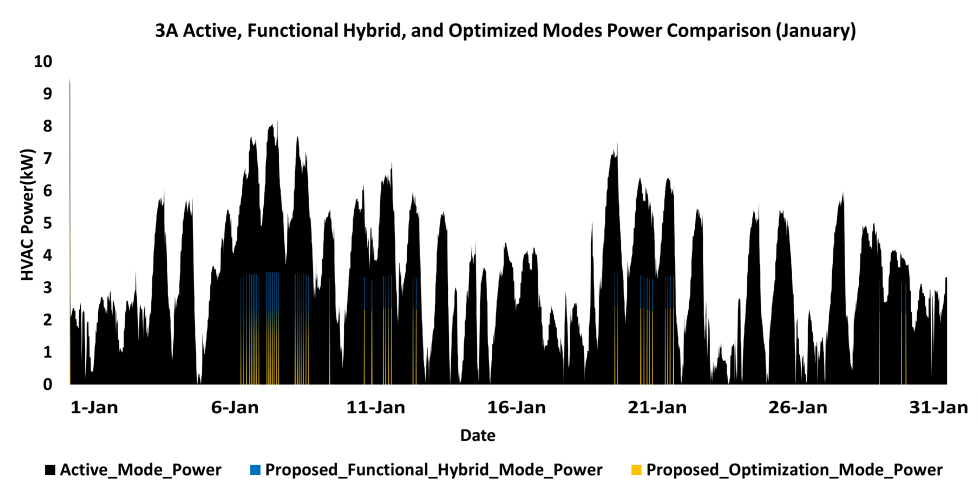

Fig. 5.4: Building 3A Active, Functional Hybrid, and Optimized Modes Power Comparison (Winter)

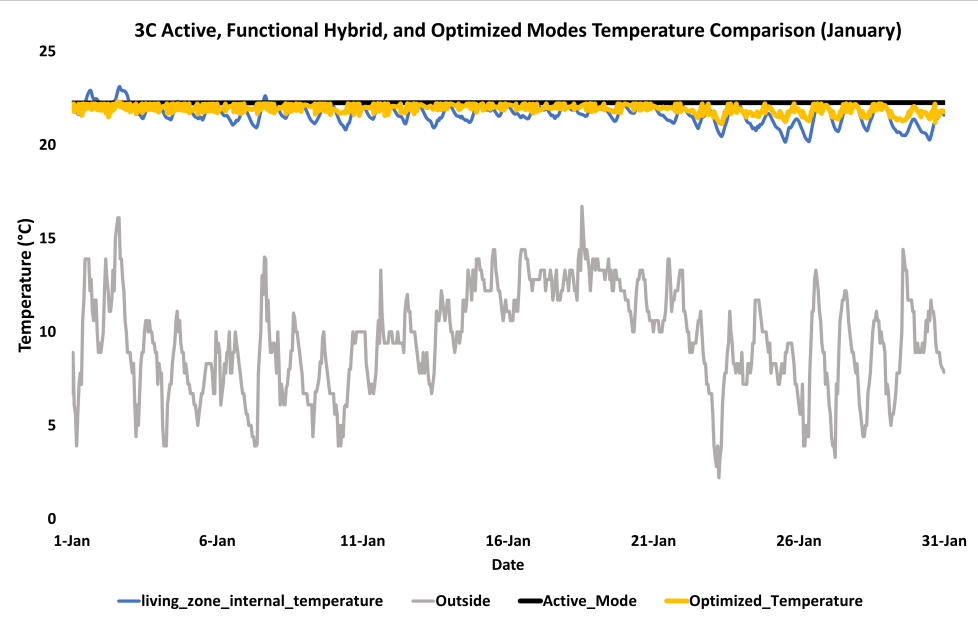

Fig. 5.5: Building 3C Active, Functional Hybrid, and Optimized Modes Temperature Comparison (Winter)

resource models was carried out to confirm the passive building, with the associated HVAC model, electric water heater model, PV model, and battery model functioning as expected. The baseline control for the HVAC is given in Fig. 5.4 for the whole month and operates as expected. The temperature profiles using the baseline MPC control (optimized mixed-mode), normal mixed-mode, and active mode operations were compared and results are illustrated in Fig. 5.4 to Fig. 5.14. It can be observed

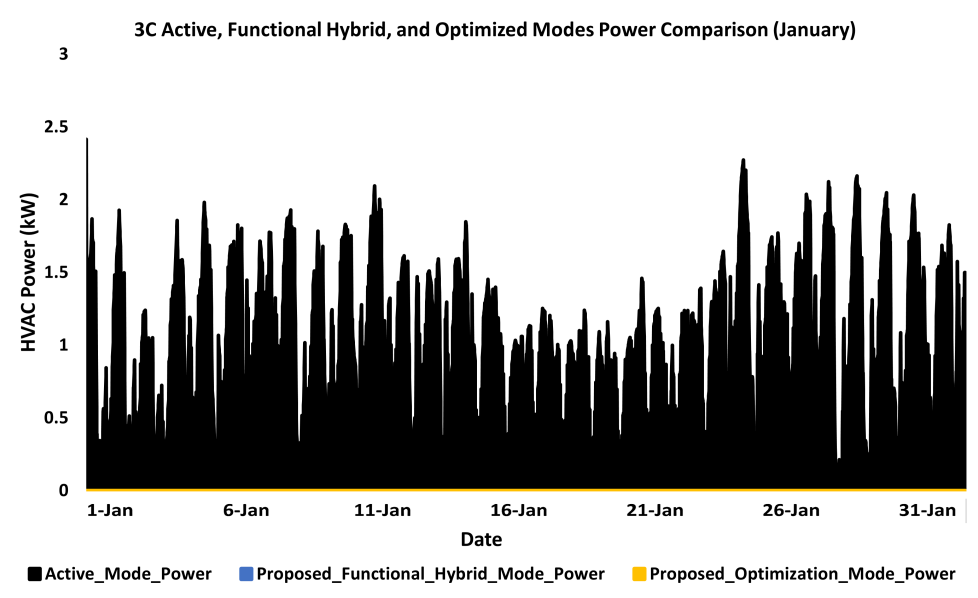

Fig. 5.6: Building 3C Active, Functional Hybrid, and Optimized Modes Power Comparison (Winter)

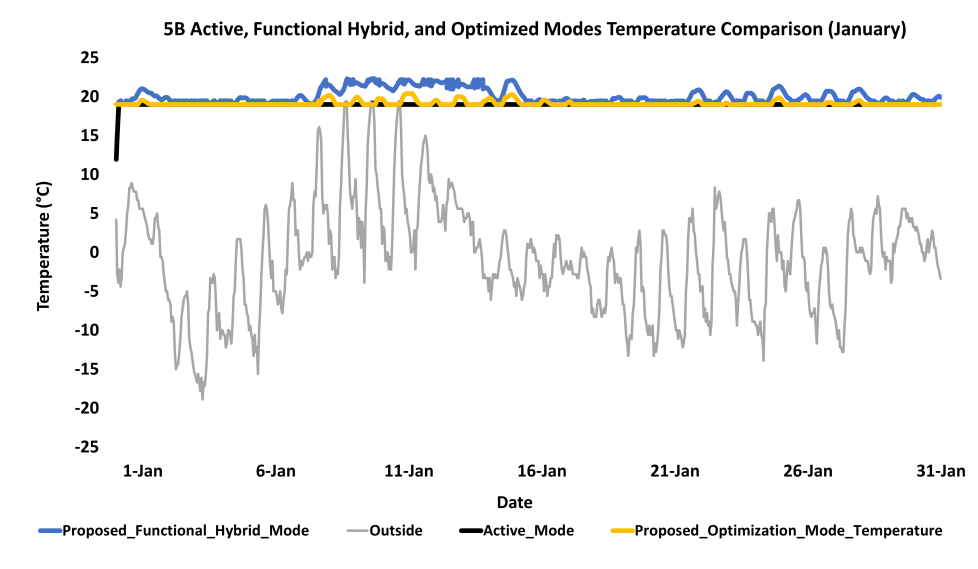

Fig. 5.7: Building 5B Active, Functional Hybrid, and Optimized Modes Temperature Comparison (Winter)

that without the use of the HVAC power for the entire month, the temperature results of the baseline MPC control are better than the normal mixed-mode operation and almost similar to the active mode operation. Similarly, the ON/OFF control signal for the electric water heater was validated visually for the building using a 24 hours prediction horizon as shown in Fig. 5.15, which also operates as expected. Finally,

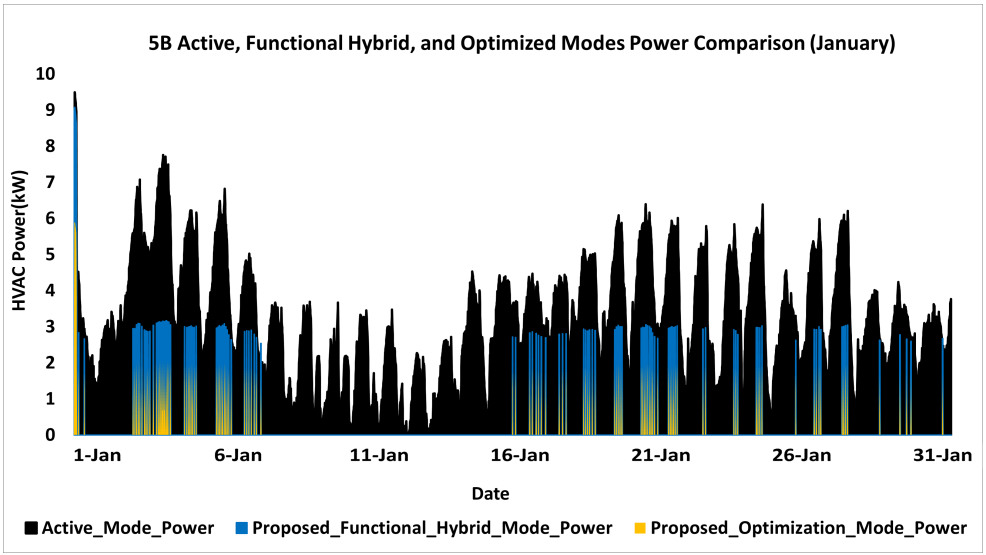

Fig. 5.8: Building 5B Active, Functional Hybrid, and Optimized Modes Power Comparison (Winter)

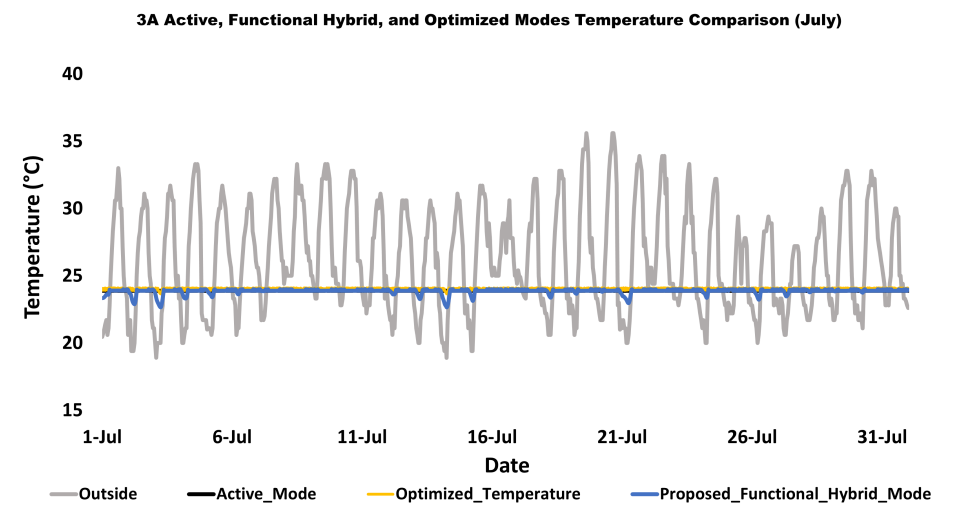

Fig. 5.9: Building 3A Active, Functional Hybrid, and Optimized Modes Temperature Comparison (Summer)

other building resource model validation is represented in Fig. 5.15 and Fig. 5.16 with a 24-hour prediction horizon. It can be observed that the battery energy state never exceeds the specified limits; the battery charging and discharging power never exceeds 5kW, and simultaneously charging and discharging never occurred. Also, the battery did not have to be fully discharged before charging could occur. The onsite power generation from PV is curtailed to 5kW (maximum) and is being used when available. Finally, the total building load and the rest of the power needed from the

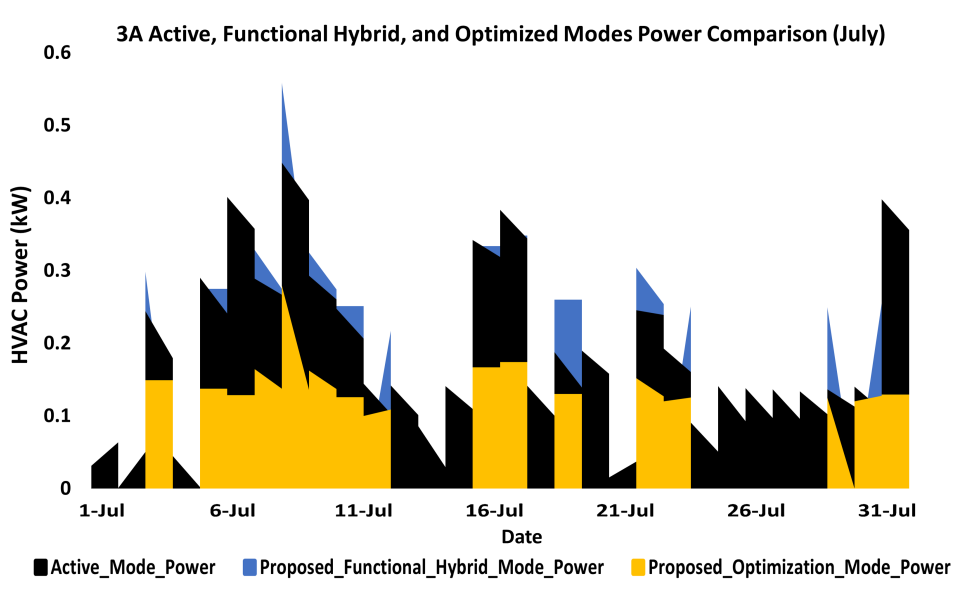

Fig. 5.10: Building 3A Active, Functional Hybrid, and Optimized Modes Power Comparison (Summer)

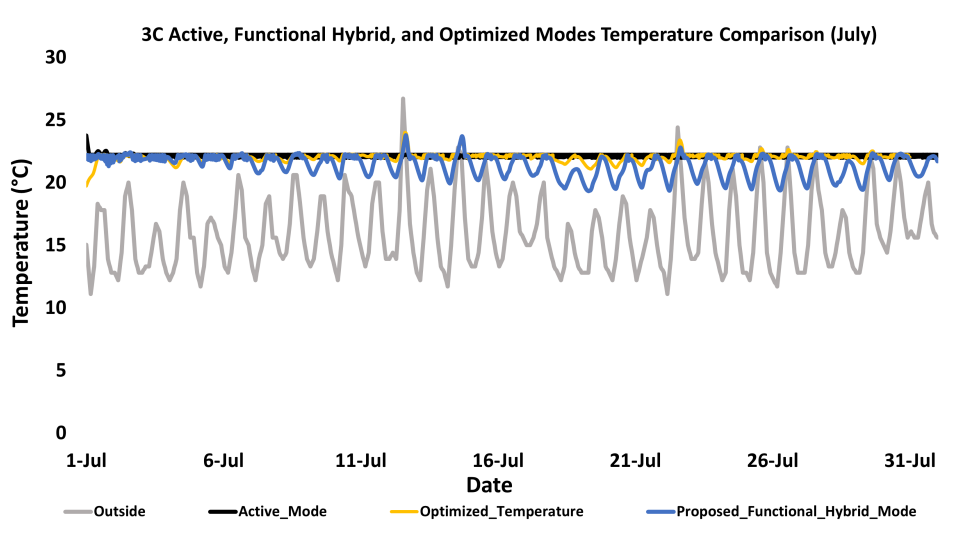

Fig. 5.11: Building 3C Active, Functional Hybrid, and Optimized Modes Temperature Comparison (Summer)

grid demand are consistent with constraints specified in Chapter 3. As observed in Fig. 5.16 and Fig 5.17, since this building has limited use of the HVAC system due to the optimized mixed-mode operation, the major load which is operated and optimized in the building according to Fig. 5.17a is the electric water heater.

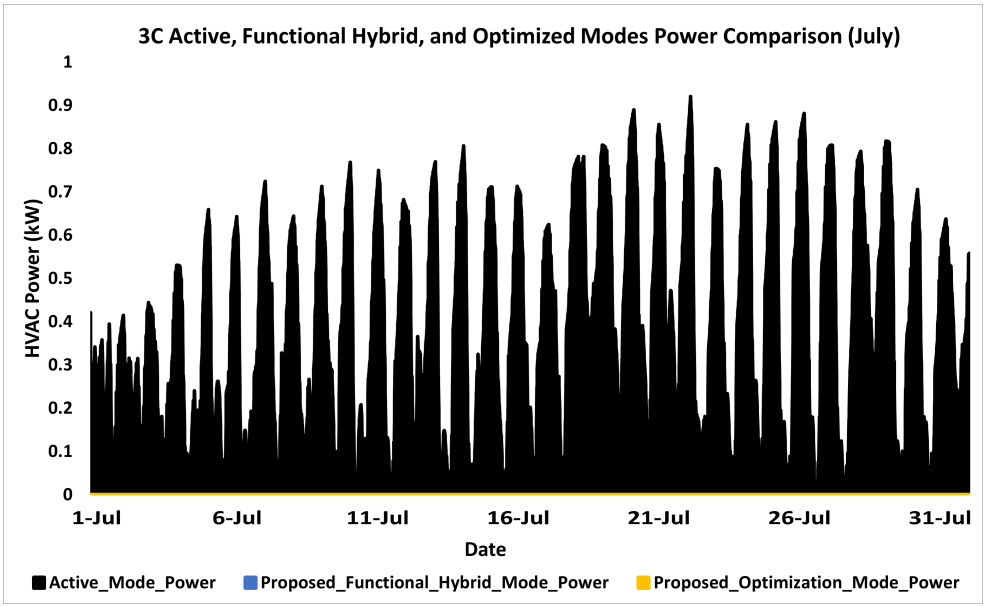

Fig. 5.12: Building 3C Active, Functional Hybrid, and Optimized Modes Power Comparison (Summer)

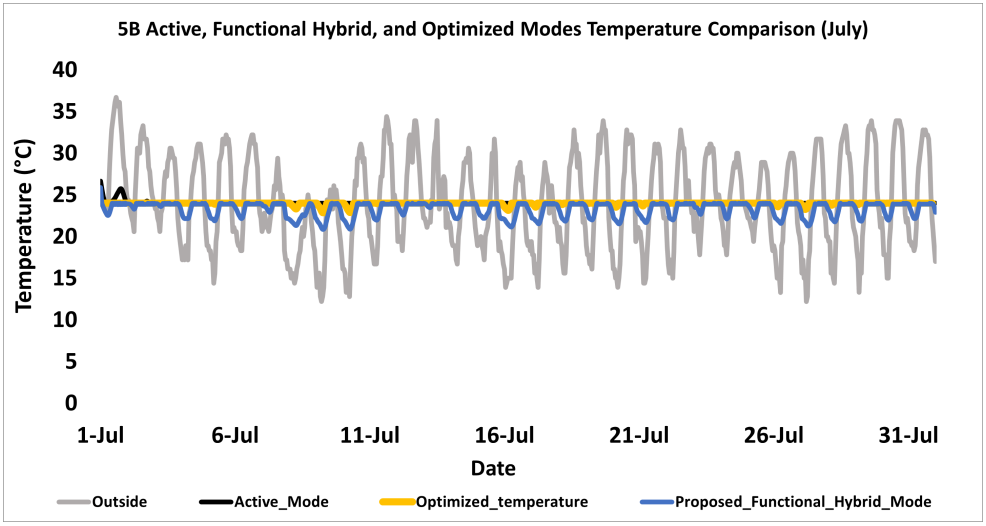

Fig. 5.13: Building 5B Active, Functional Hybrid, and Optimized Modes Temperature Comparison (Summer)

5.5 Results and Discussions

Different applications were developed to demonstrate the efficacy of the hybrid building thermal dynamic models and their control architecture. For this, first, a comparative evaluation between the controller operating to perform the Energy Management function and the baseline case where the building is allowed to operate tra-

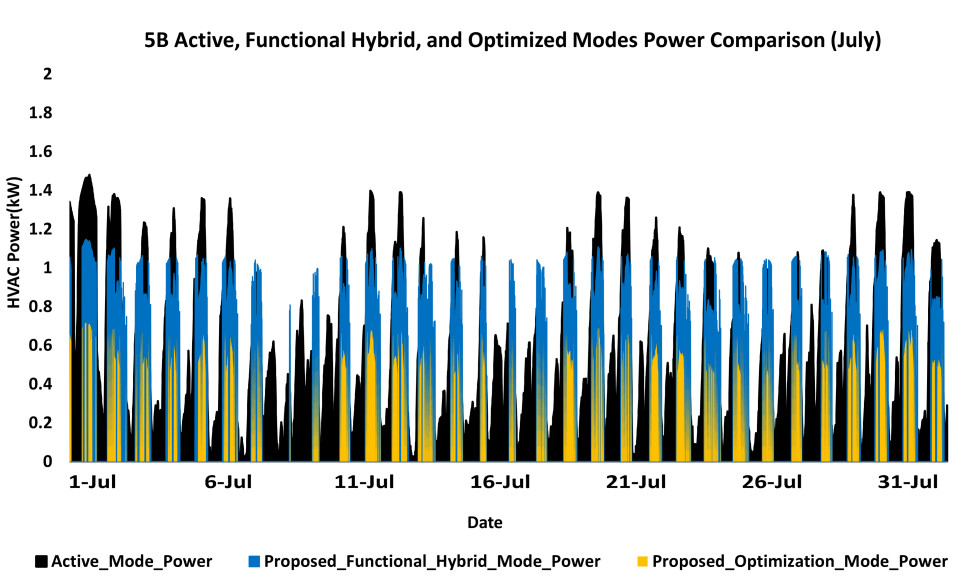

Fig. 5.14: Building 5B Active, Functional Hybrid, and Optimized Modes Power Comparison (Summer)

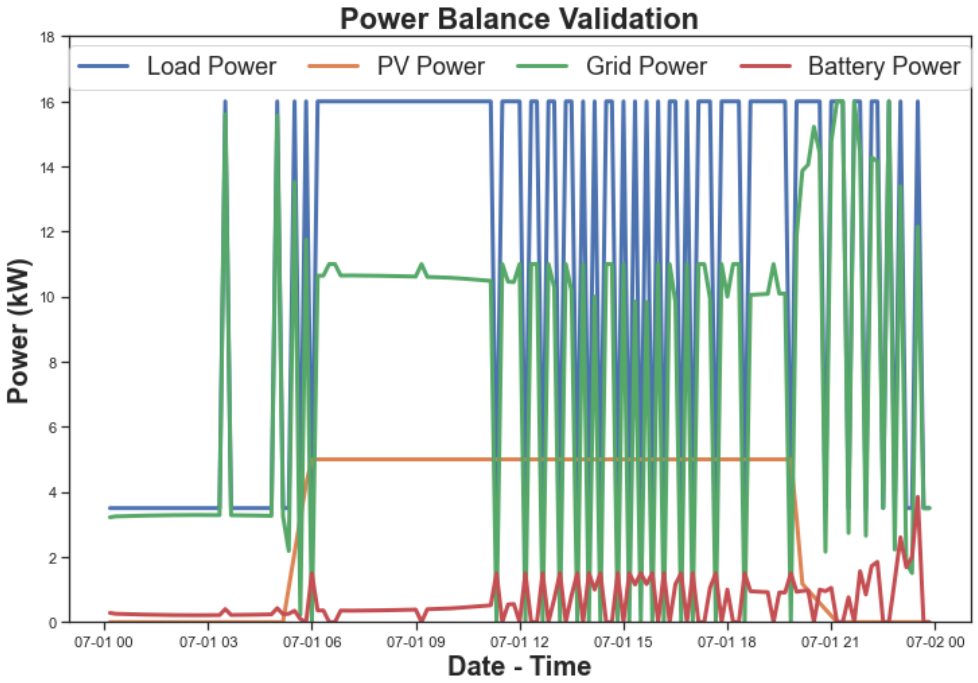

Fig. 5.15: Power Balance Validation for the MPC

ditionally (using only deadband) controllers is presented. Then, another application where the building is allowed to respond to certain signals (power-reference tracking) was examined. Finally, two demand response applications where the building is

Table 5.1: Power comparison between the Active, Proposed Functional Hybrid, and Optimized Modes

ASHRAE Zone (Month)	HVAC Consumption (kWh)			% Difference in power curve area	
	Active	Hybrid	Optimized	Hybrid	Optimized
3A (January)	2545	81	43	96	98.3
3A (July)	464	437	358	5	22.8
3C (January)	762	0	0	100	100
3C (July)	284	0	0	100	100
5B (January)	2384	183	102	92	95.7
5B (July)	435	270	128	38	70.5

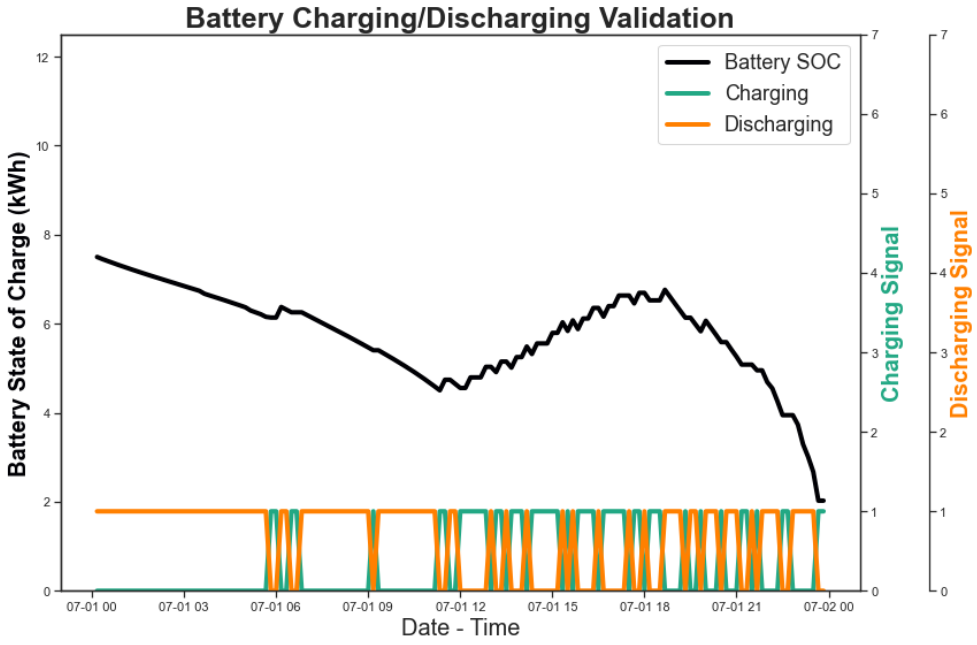

Fig. 5.16: Battery Energy Capacity Status for the MPC

allowed to respond to load shed events or increase its loads use were analyzed and compared against the traditional control performance and the Energy Management mode. This work assumes that demand response events for load sheds typically occur on cold winter days for the heating periods and hot summer afternoons for cooling periods. On the contrary, the rare occasions of load increase would typically occur during mild weather conditions and due to over-generation. As such, sets of full-day simulations were implemented for the hybrid building to estimate the significance of

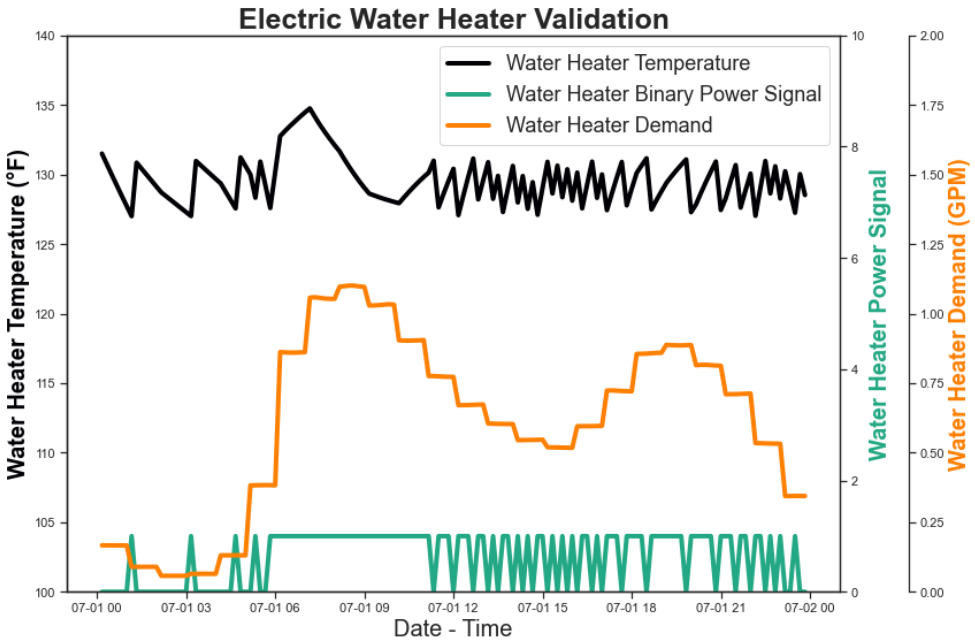

Fig. 5.17: Controls Validation for the Electric Water Heater

the model to respond accurately to the load shifts.

5.5.1 Case 1: Energy Management Application

The energy management-based application of the controller advance towards finding the most efficient and economical strategy for the reduction of the power consumption from the building loads. In most cases, it involves prioritizing the reduction at costly periods, such as certain peak hours. Controllable loads around peak hours would have flexible consumption patterns. The Time-Of-Use (TOU) Rates are what the utility providers set as opposed to a wholesale market to differentiate the peak periods (evenings) and the off-peak hours. The unit cost of energy is higher during peaks. These of rate structure is common with utilities, although prevalent for commercial consumers rather than residential. Pacific Gas and Electric utility in California is a utility provider that uses the time-of-use residential rates schedule, and customers can choose between a peak time of 4 pm to 9 pm or 3 pm to 8 pm on weekdays except for holidays.

Therefore, proper coordination is essential. Unfortunately, it is difficult for con-

sumers to find out exactly how to adjust their energy usage under economic signals, especially when using a complicated Time-of-Use (TOU) rate. Applying MPC control would integrate the mixed operational mode with forecasts and other equipment constraints to give a result that helps decide on optimal building loads operation setpoints for energy cost reduction. Due to data availability from PGE [124], for the Energy management application, this work prioritized residential customers in the area. The TOU rate for Cedar City is obtained from [125] while for Duke Energy Carolinas, residential time of use is not available for the Charlotte area [126]. However, answers to inquiry from the Duke Energy representative on the history of when demand response was deployed into residential buildings allowed this work to utilize 6:00 am to 10:00 am for the peak residential period. Also, electric vehicle was used as a distributed energy resource in Building 3A to show the variability of operation, extensibility, and additional functionality of the optimization framework. The results highlight the controller's percentage energy and cost savings during both the peak period and the entire day. It also presents the amount of reduction in carbon footprint as compared to the baseline.

5.5.1.1 Results for Energy Management Application with Time-Of-Use Test Case

An MPC control was implemented in the whole building using the TOU utility rate as the control signal, for a 24-hours prediction horizon; according to Fig. 5.21, significant peaking was observed in the building loads before 4 pm, and after 9 pm. The early peaking allowed for additional energy storage and provided an avenue for the building to consume 65% less electricity from the grid during the peak pricing period (4 pm - 9 pm) compared to the system operation in Fig. 3.7. Finally, in comparison to studies from [127] and [102] where the MPC controls resulted in 22.2% and 32.7% daily building energy savings respectively, the profile of Fig. 5.20 translated to the consumption of 141 kWh/day from the grid which is 41% less than the total estimated active consumption in building in 3C without MPC operation. Similarly,

the results for building 3A and 5B are presented in Table 5.2 and Table 5.4.

Table 5.2: Building 3A Energy Usage Comparison for MPC Control Utilization during TOU rate Event

Period	Without MPC	With MPC	% Reduction
Peak (6 am - 10 am)	59.6 kWh	23.3 kWh	60.9
Day	268.7 kWh	154.2 kWh	42.6

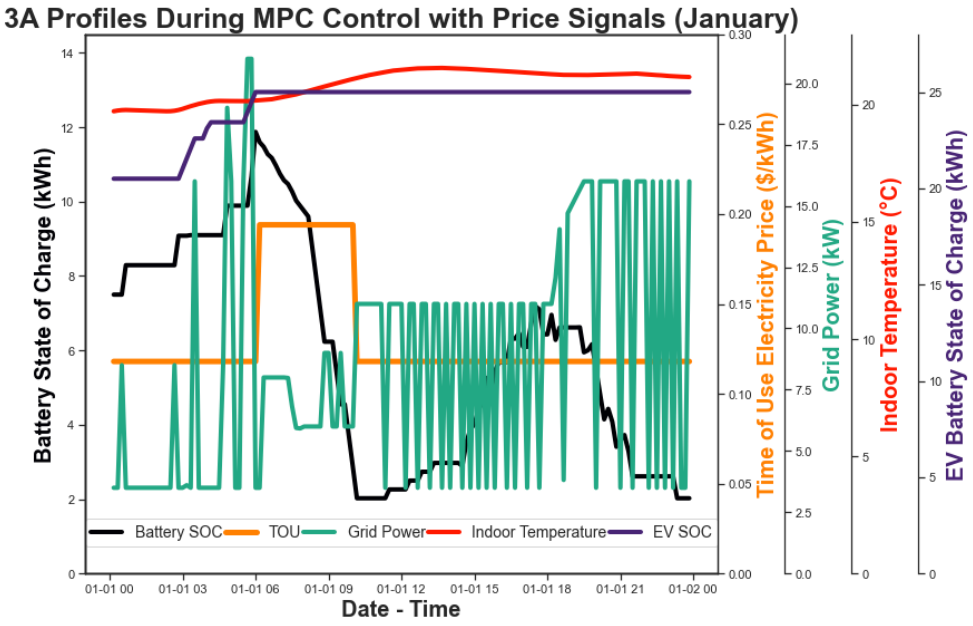

Fig. 5.18: 3A Battery and Zone Temperature Response Profile to the TOU rate

Table 5.3: Building 3C Energy Usage Comparison for MPC Control Utilization during TOU rate Event

Period	Without MPC	With MPC	% Reduction
Peak (4 pm - 9 pm)	61.4 kWh	21.6 kWh	65
Day	237.6 kWh	141.2 kWh	40.6

Table 5.4: Building 5B Energy Usage Comparison for MPC Control Utilization during TOU rate Event

Period	Without MPC	With MPC	% Reduction
Peak (1 pm - 8 pm)	79.8 kWh	28.5 kWh	64.2
Day	259.5 kWh	138.6 kWh	46.6

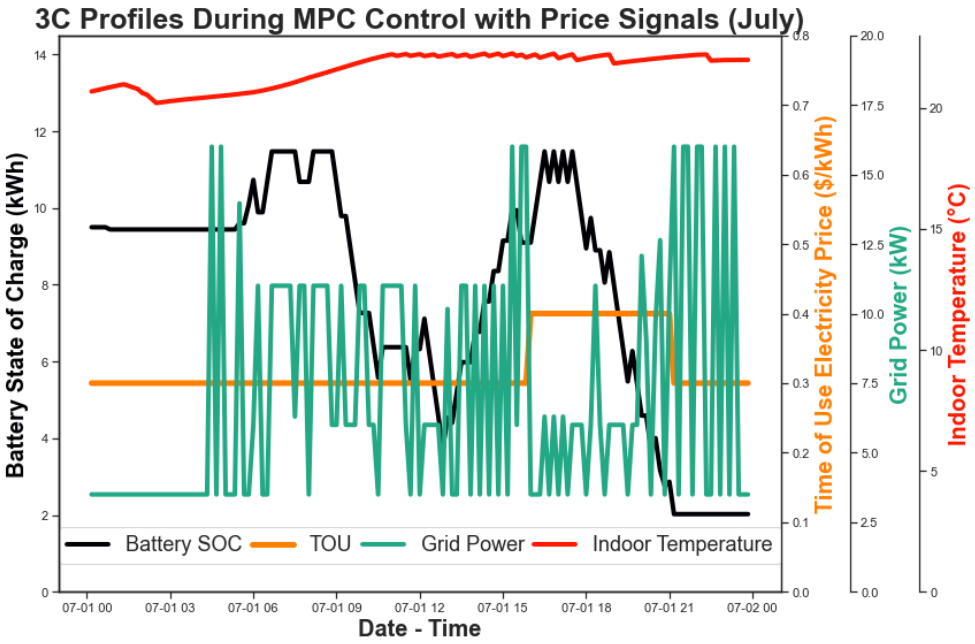

Fig. 5.19: 3C Battery and Zone Temperature Response Profile to the TOU rate

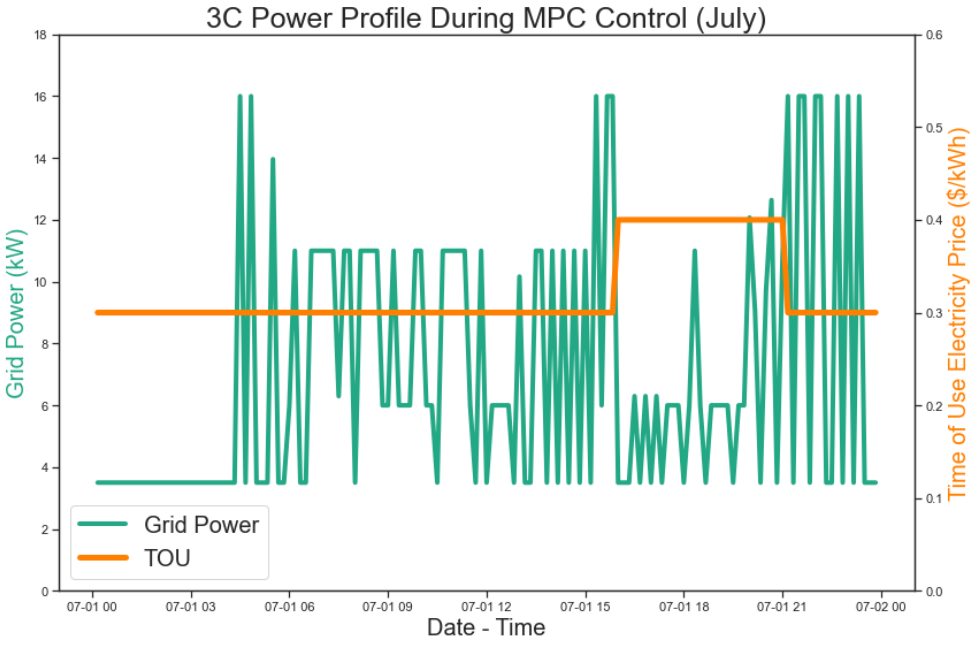

Fig. 5.20: Grid Profile During MPC Control

5.5.2 Case 2: Power Reference Tracking

The necessity for the controller to track a given power reference signal comes as utility deemed to balance the small real-time imbalances in generation with the load

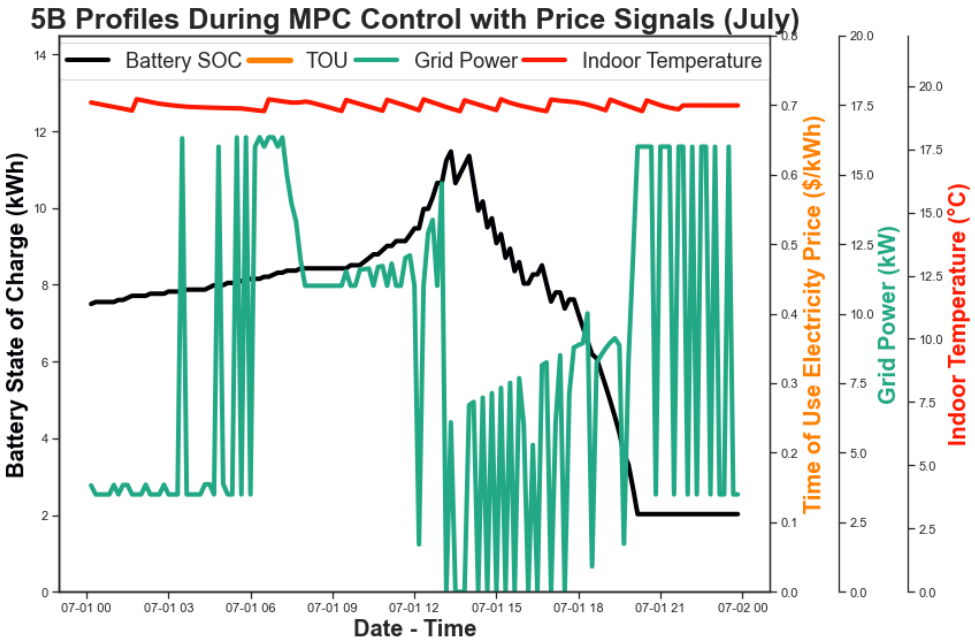

Fig. 5.21: 5B Battery and Zone Temperature Response Profile to the TOU rate

being delivered to the consumer. For this, the objective of the hybrid building and its end-use loads is to follow the power reference. The new objective is given in equation 5.5.

$$minimize \sum_{t=1}^{T} (P_{grid} - P_{ref})^2 \tag{5.5}$$

In this work, the demand-side controller allows the building to follow a given power reference signal during a real-time operation at a resource level through a fast time-scale control. In the presence of an aggregator that combines the operation of the building in a supervisory level, individual end-use loads are managed by the same load aggregator. The introduced power reference in this work is randomly selected; it is expected that the controller will provide a tracking accuracy in results without significant violation of the building comfort limits.

5.5.2.1 Results for Power Reference Tracking Test Case

The power-constrained tracking of the model produced an interesting results as revealed by the metrics in Table 5.7. Also, Fig. 5.28 graphically illustrates the results. According to Fig. 5.28, the graph shows that the hybrid building model has little discrepancies in perfectly tracking the power reference, especially in the very early morning periods. This is expected because the power reference signals were randomly generated, and significant violations of the comfortable temperature limits are not entertained. As such, the controller prioritized comforts over tracking accuracy.

Table 5.5: Differential and Power Reference Tracking Metrics for Building 3A

RMSE (kW)	% RMSE Using Max Power Ref as Base	% Energy Difference for the Event Day
0.933	4.1	1.1

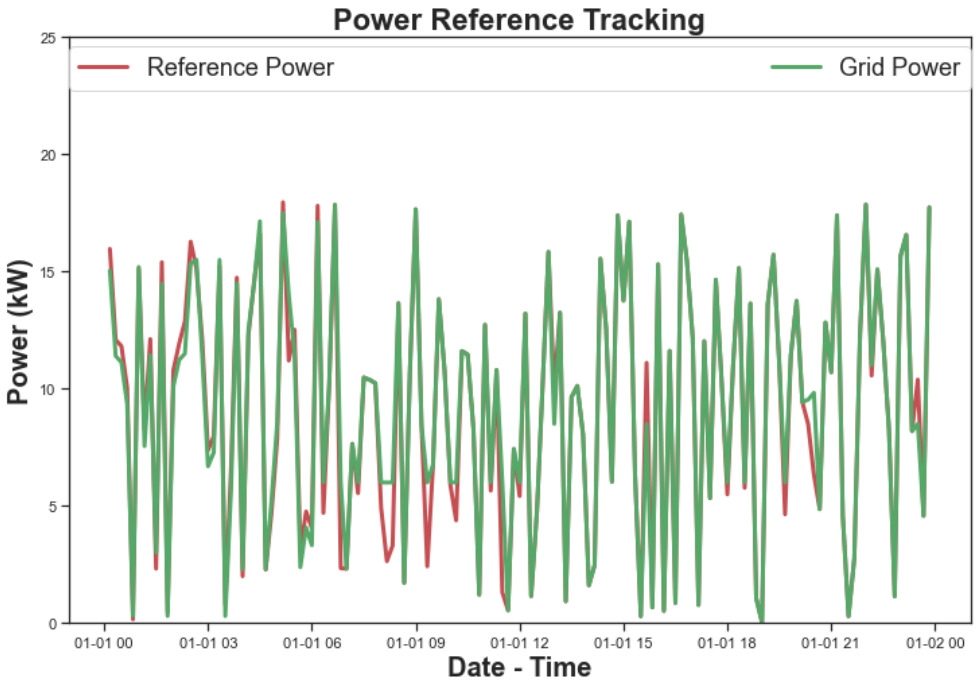

Fig. 5.22: Building 3A Power Reference Tracking Test Case

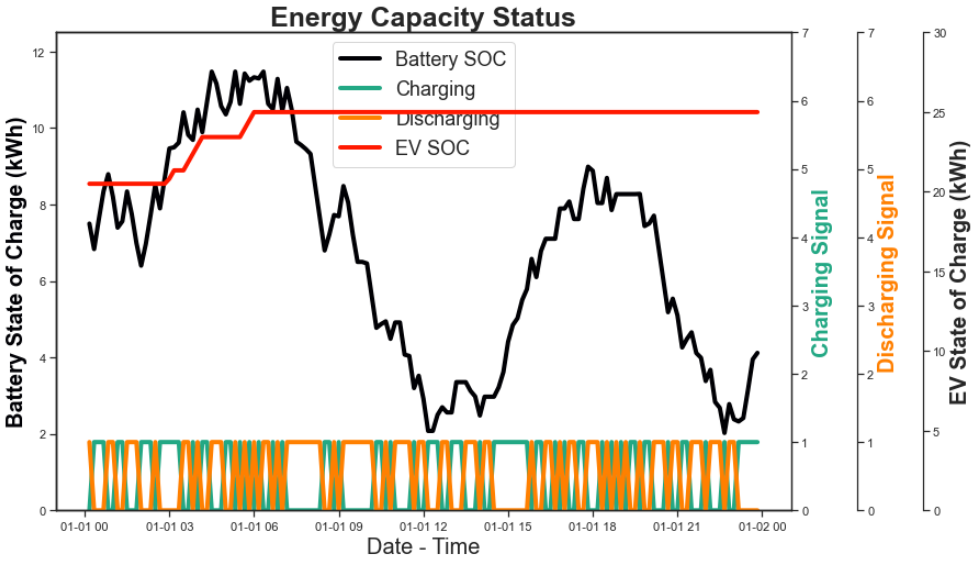

Fig. 5.23: Building 3A Response of the Battery to the Power Reference Signal

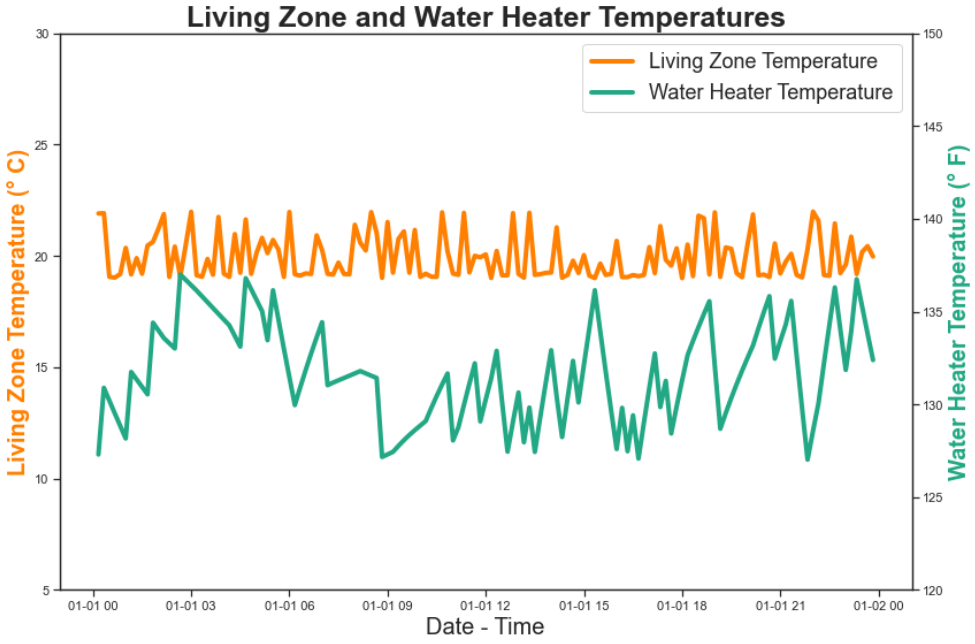

Fig. 5.24: Response of Building 3A Thermostatic Control Loads to the Power Reference Signal

Table 5.6: Differential and Power Reference Tracking Metrics for Building 3C

RMSE (kW)	% RMSE Using Max Power Ref as Base	% Energy Difference for the Event Day
0.759	3.5	1.1

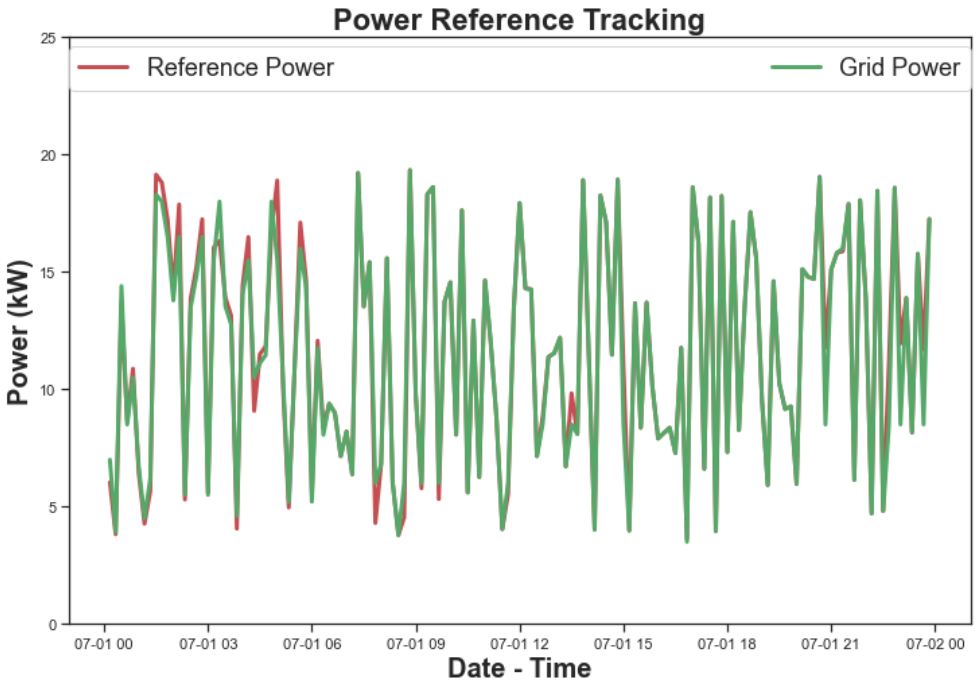

Fig. 5.25: Building 3C Power Reference Tracking Test Case

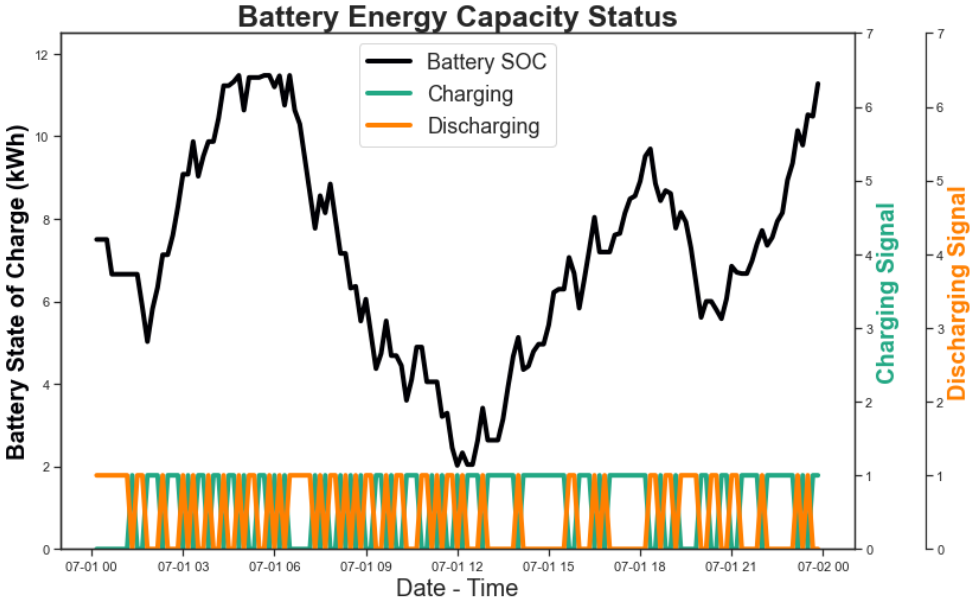

Fig. 5.26: Building 3C Response of the Battery to the Power Reference Signal

Fig.5.29 and 5.30 further show the behavior of the other distributed energy resources as random power signals arrive from the grid. The interesting profiles reveal that the hybrid building model can confidently respond to any power control reference assigned to it by the grid comfortably.

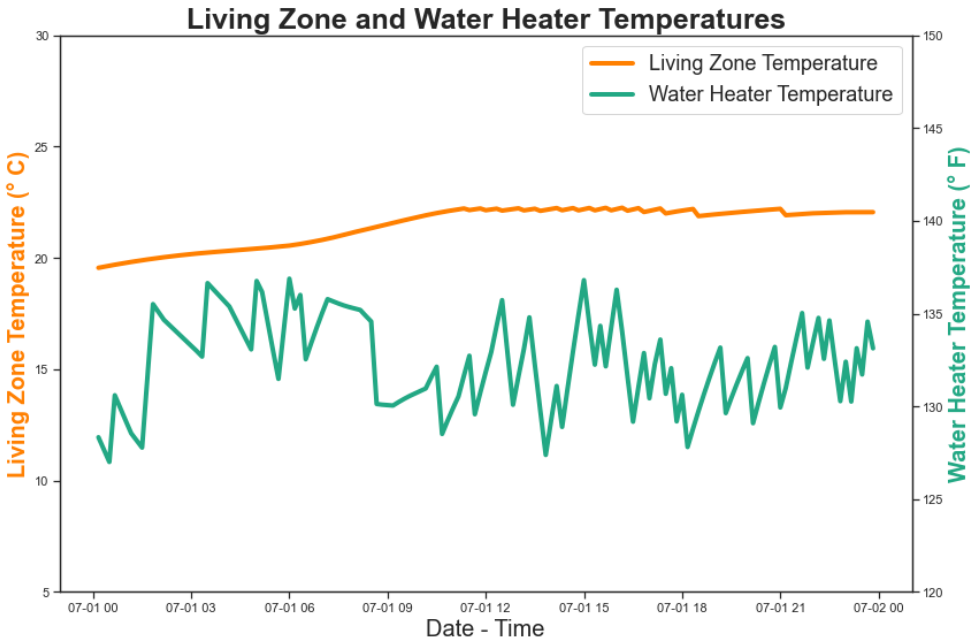

Fig. 5.27: Response of Building 3C Thermostatic Control Loads to the Power Reference Signal

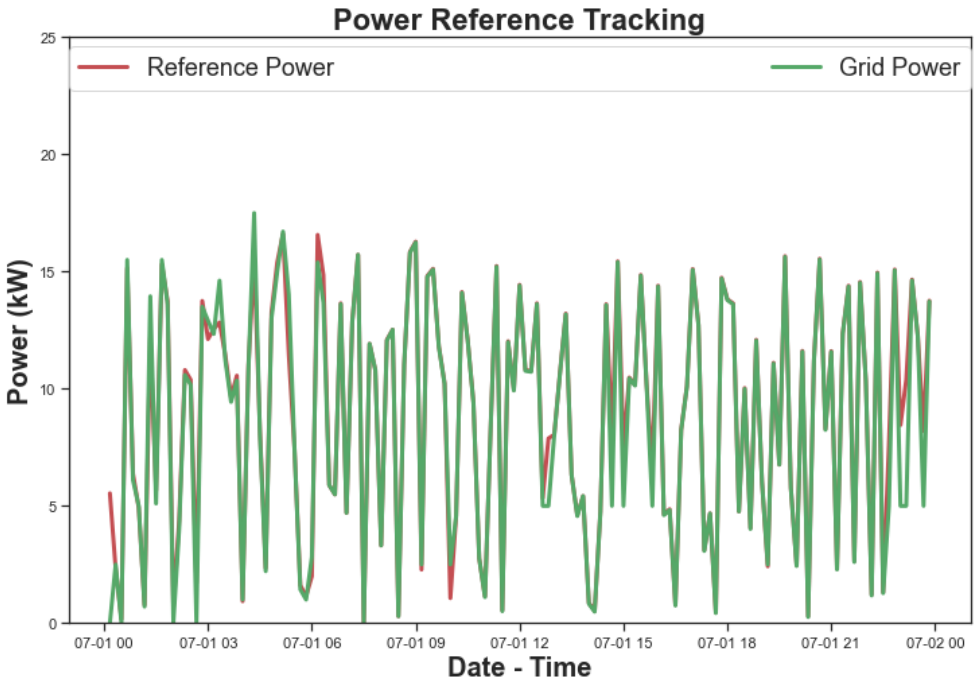

Fig. 5.28: Building 5B Power Reference Tracking Test Case

5.5.3 Case 3: Demand Response

Under this application, the hybrid building is being evaluated to accurately predict the operation of the distributed energy resources to reliably deliver any expected load

Table 5.7: Differential and Power Reference Tracking Metrics for Building 5B

RMSE (kW)	% RMSE Using Max Power Ref as Base	% Energy Difference for the Event Day
0.9283	3.9	1.5

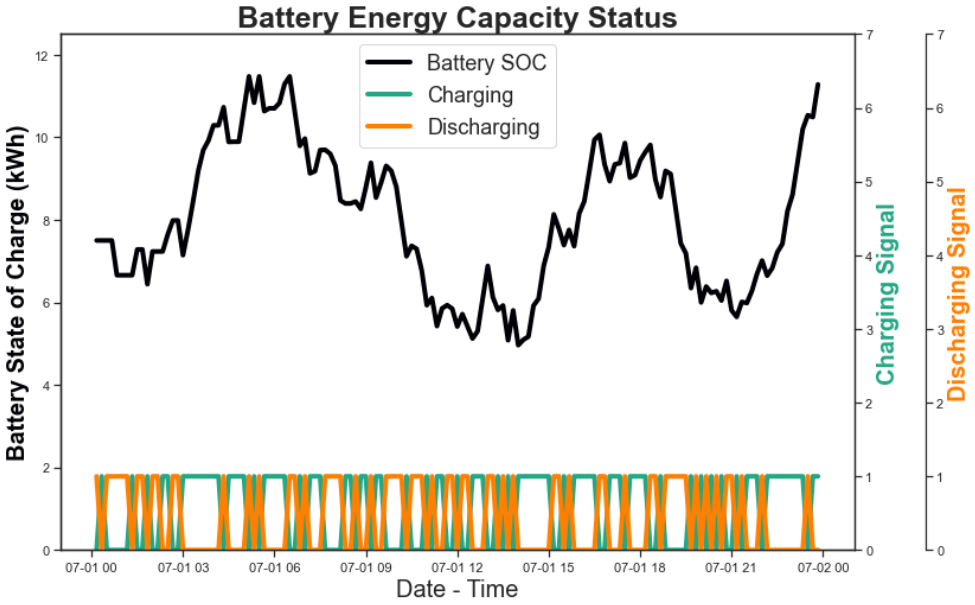

Fig. 5.29: Building 5B Response of the Battery to the Power Reference Signal

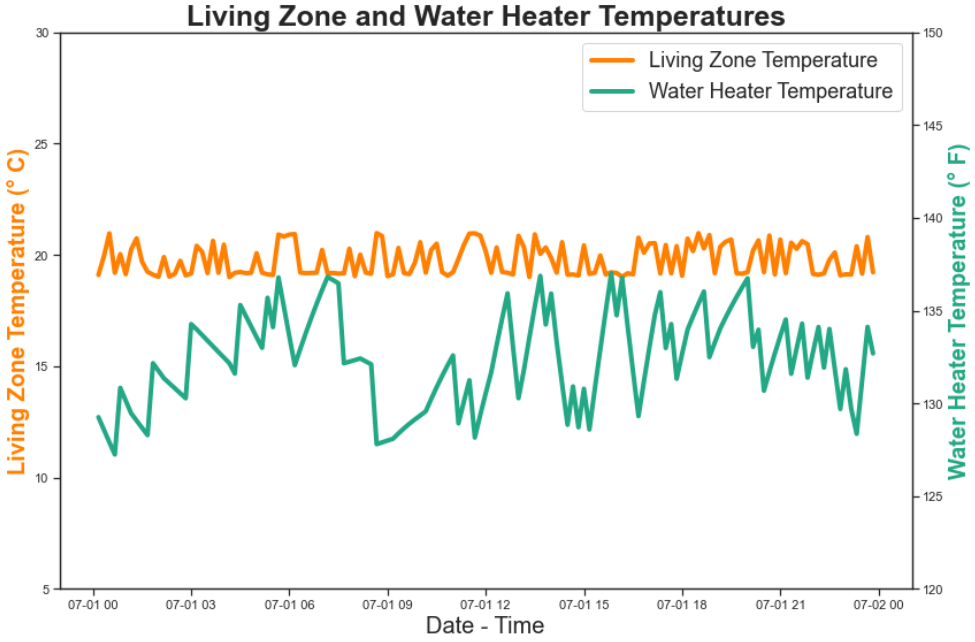

Fig. 5.30: Response of Building 5B Thermostatic Control Loads to the Power Reference Signal

shedding or load scheduling services upon the receipt of such action as a request from the grid during any DR events. This approach helps utilities to create an avenue to enable reliable and resilient distribution grids. The load shedding is somewhat similar to demand shifts during Time of Use rates as discussed in the Energy Management Application section. As such more attention is directed to other Load scheduling events that may warrant the customer to increase their load use at certain times of the day while receiving incentives for such actions.

In the load scheduling application, the controller in the hybrid building is expected to coordinate the energy resources to use the maximum amount of energy upon receipt of a such signal from the utility. This seems to be a rare case of application to maintain reliable and resilient power grids. However, the events sometimes occur in mild geographical locations and when generation exceeds consumption. As an example, the load increase event occurrence was witnessed by the Bonneville Power Administration in the first two weeks of June 2010, where the company was compelled to market over 50,000MWh at \$0/kWh to consumers [128]. The most common area for the Load increase application is Pacific Northwest; as such, in this study, the hybrid building of zone 3C (San Francisco is in close proximity to the pacific, and it is deployed to analyze load increase DR events upon requests from the utility. Similar to the load shed events with the TOU case, a 24-hour advance notification of potential load increase is received by the controller to modulate and accommodate excessive generation coming from the grid.

5.5.3.1 Results for Demand Response Application with Load Scheduling Test Case

The results of the load scheduling event are simulated for a 24-hour time period. Events for load increase were scheduled for midnight and morning hours, 12:00 am - 5:00 am and 9:00 pm and 12:00 am. During the course of these events, the MPC controller provided the resource forecast for the increase in load the utility needs for the building.

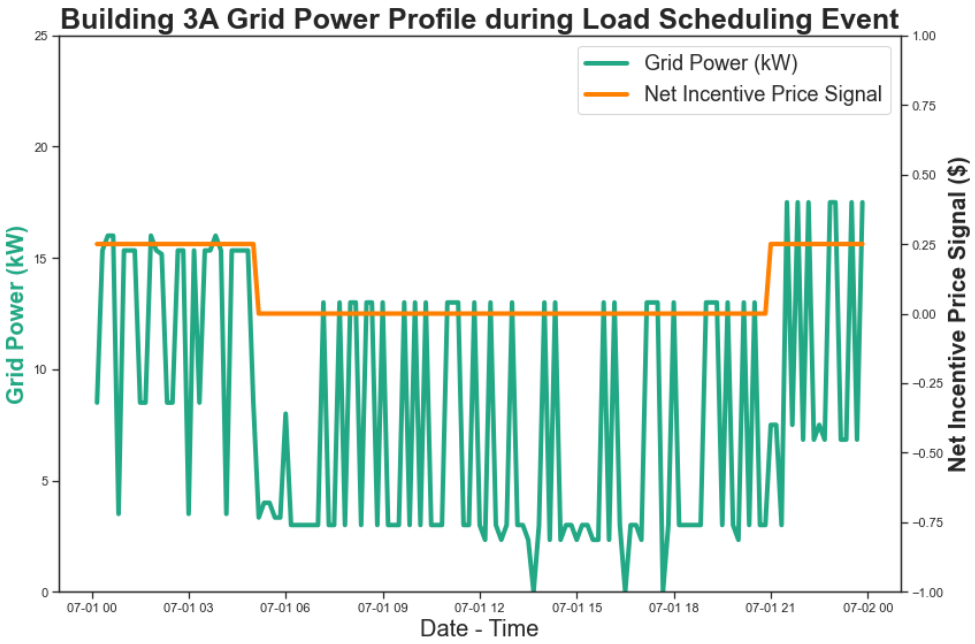

Fig. 5.31: Building 3A Power Profiles During Load Scheduling Test Case

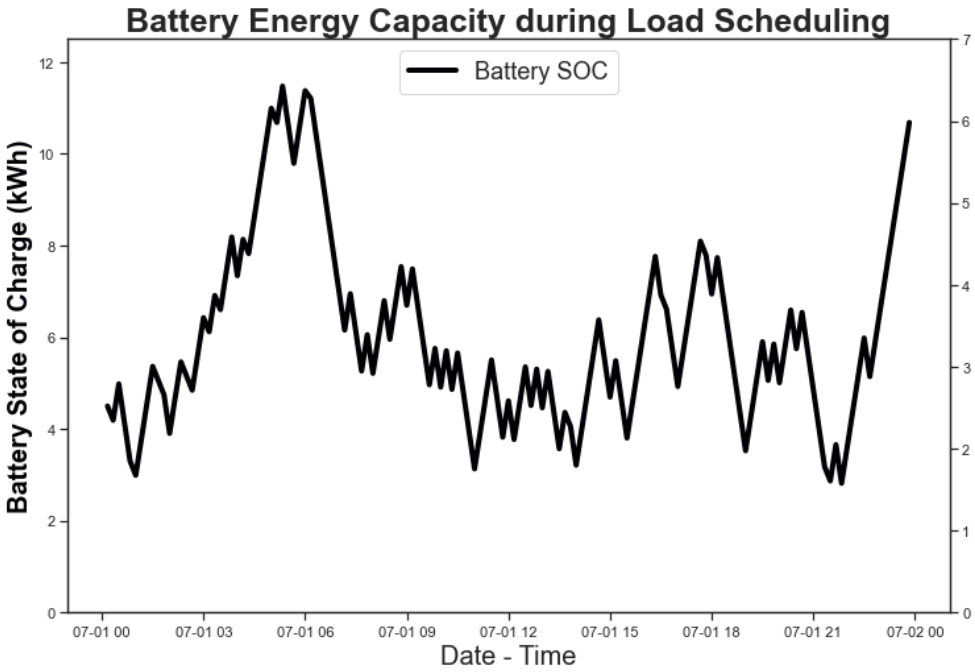

Fig. 5.32: Building 3A Response of the Battery to the Load Scheduling Event

As compared to the base case, load increases were recorded during the event time, especially with the HVAC system as illustrated in Fig. 5.39, which typically would

[1]Includes 96.54 Customer does not have to pay for

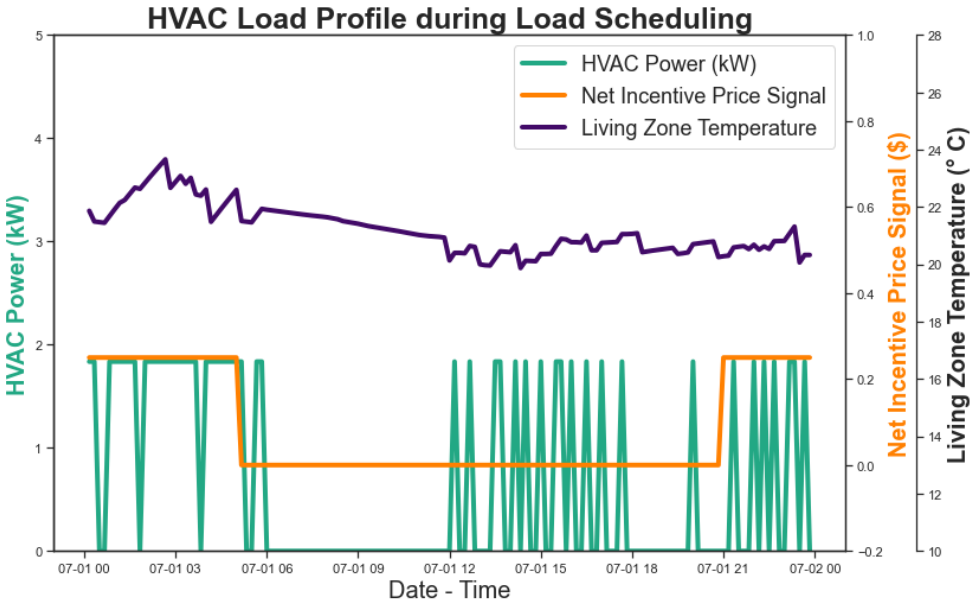

Fig. 5.33: Building 3A HVAC Power Profile During the Load Scheduling Event

Table 5.8: Building 3A Energy Usage Comparison for MPC Control Utilization during Load Scheduling Event

Period	Base Case	With MPC	% Gain on Incentives
Event hours	49.23 kWh	96.54 kWh	49
Day	268.65 kWh	302.89[1] kWh	23.2

not turn on due to the mild ambient condition. A similar profile was noticed with the HVAC system, with most temperatures kept at the upper bands, while maintaining all building thermal comfort conditions and meeting other preferences. The response of the Battery Energy Storage System is also illustrated in Fig. 5.38 An interesting observation is that the battery is able to maintain the charging operation using the grid power during these events while still running normally at other times

Table 5.9: Building 3C Energy Usage Comparison for MPC Control Utilization during Load Scheduling Event

Period	Base Case	With MPC	% Gain on Incentives
Event hours	50.61 kWh	103.13 kWh	52.5
Day	237.6 kWh	280.9[2] kWh	25.2

[2]Includes 103.13 Customer does not have to pay for

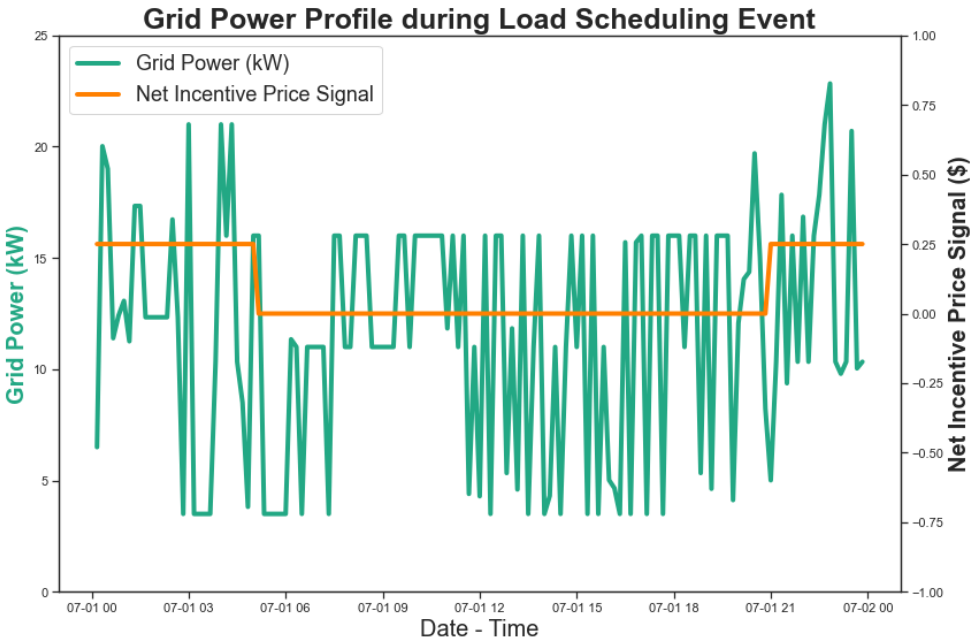

Fig. 5.34: Power Profiles During Load Scheduling Test Case

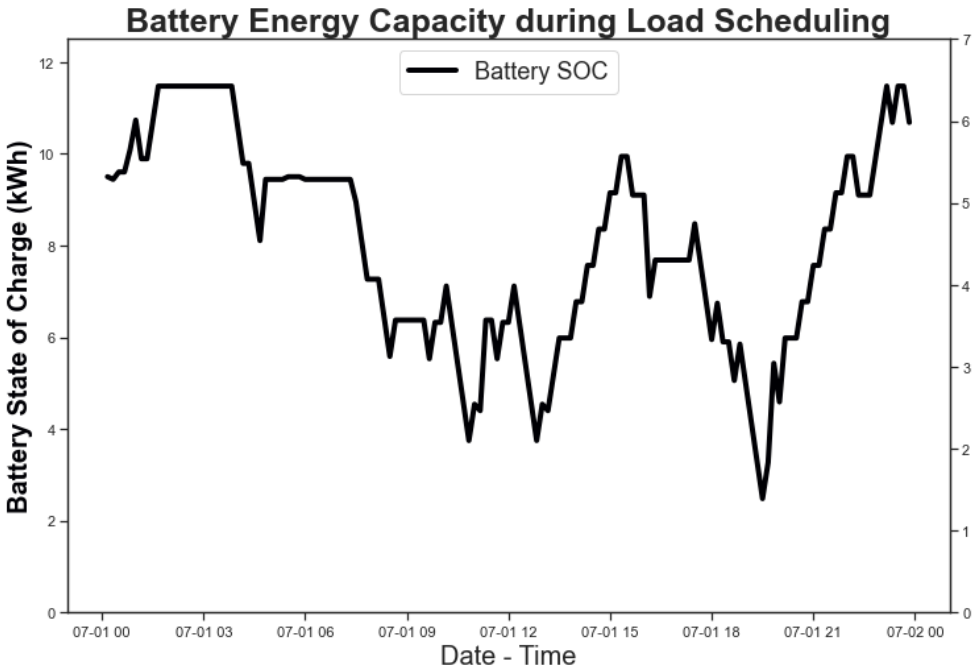

Fig. 5.35: Response of the Battery to the Load Scheduling Event

[3]Includes 112.56 Customer does not have to pay for

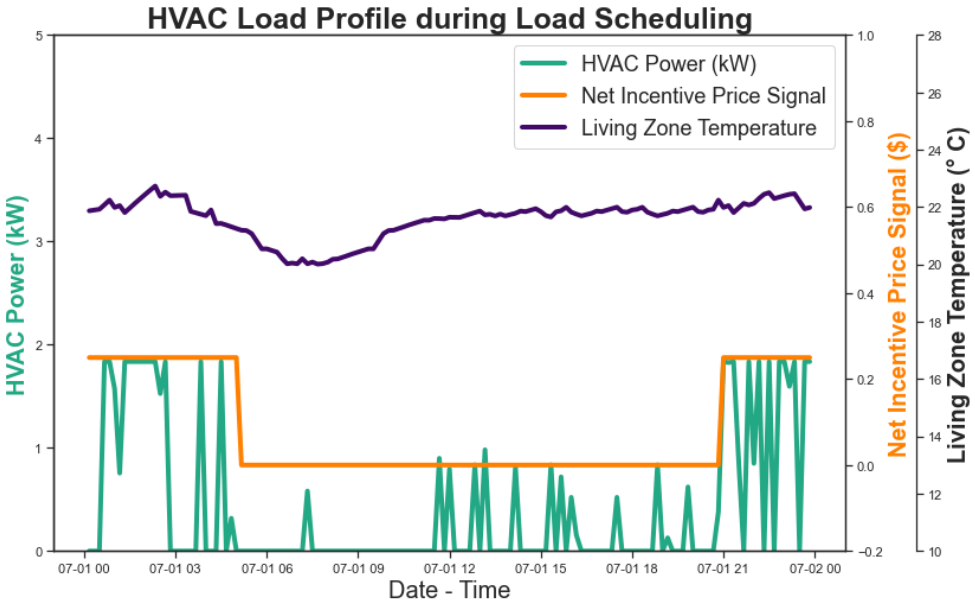

Fig. 5.36: HVAC Power Profile During the Load Scheduling Event

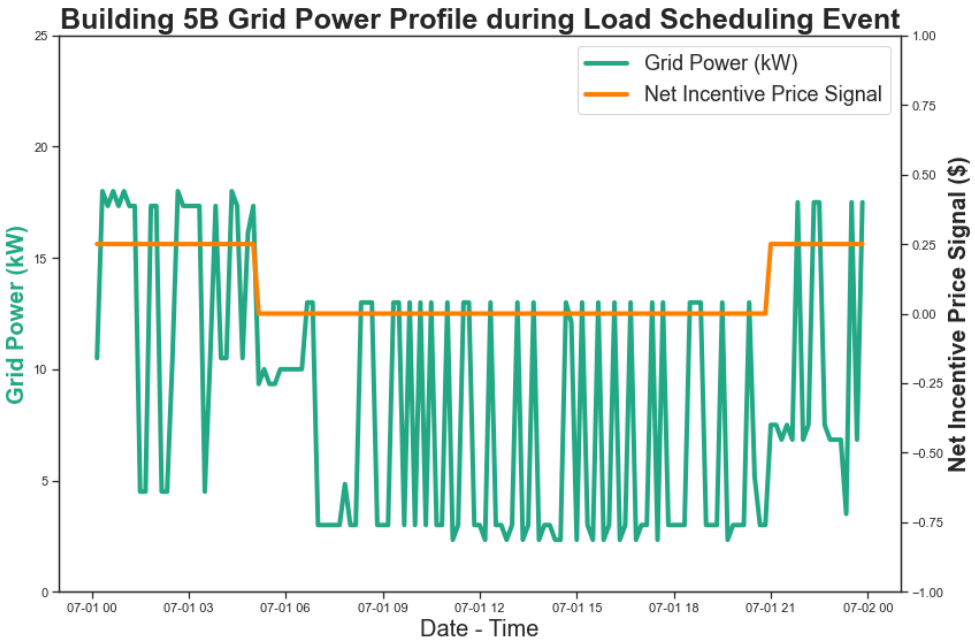

Fig. 5.37: Building 5B Power Profiles During Load Scheduling Test Case

5.6 Summary

The proposed model and the control modes were suitable and validated for use within an optimization framework for MPC control applications in grid energy management. The optimization was used to validate the mixed-mode operation of the

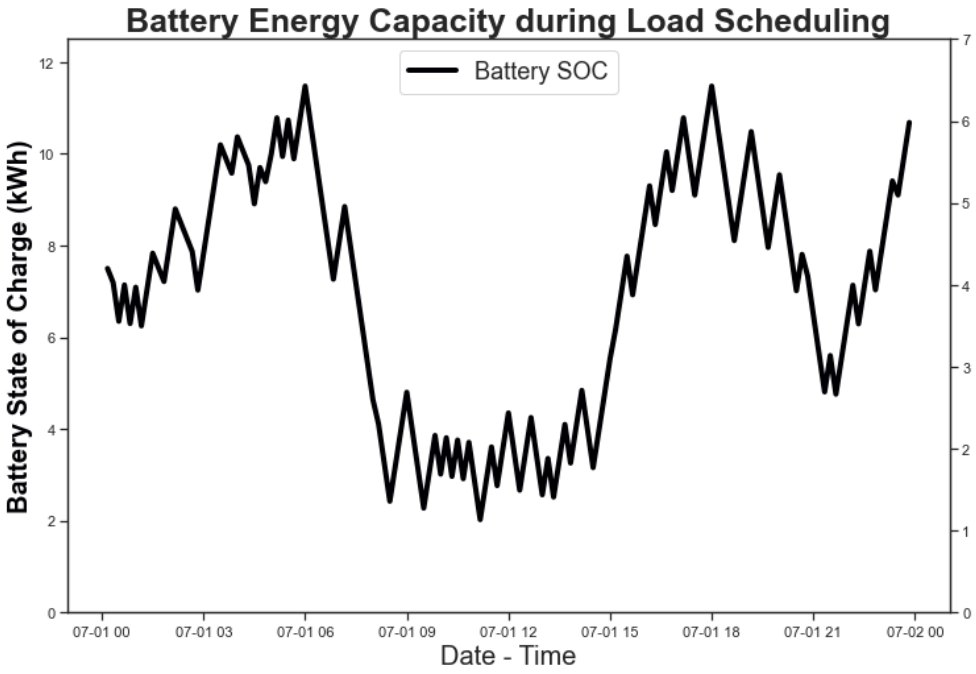

Fig. 5.38: Building 5B Response of the Battery to the Load Scheduling Event

Table 5.10: Building 5B Energy Usage Comparison for MPC Control Utilization during Load Scheduling Event

Period	Base Case	With MPC	% Gain on Incentives
Event hours	49.12 kWh	112.56 kWh	56.3
Day	260 kWh	329.78[3] kWh	16.4

passive building in conjunction with the onsite generation, storage system, and other populations of building loads. The novel framework for the advanced load control for the building DERs performed much better than the legacy setpoint change-based method described in Chapter 4 in improving temperature stability and reducing the peak energy during a DR event. For the Time-of-Use application, It was observed that the proposed controller successfully avoids excess consumption at peak demand hours by providing a 60% to 65 % reduction in electricity consumption in the evaluated zone when compared with traditional un-optimized operational methods. The MPC control also resulted in an average of 1.2% error in power reference tracking, and 49% to 56% gain on incentives during a daily load scheduling strategy in the

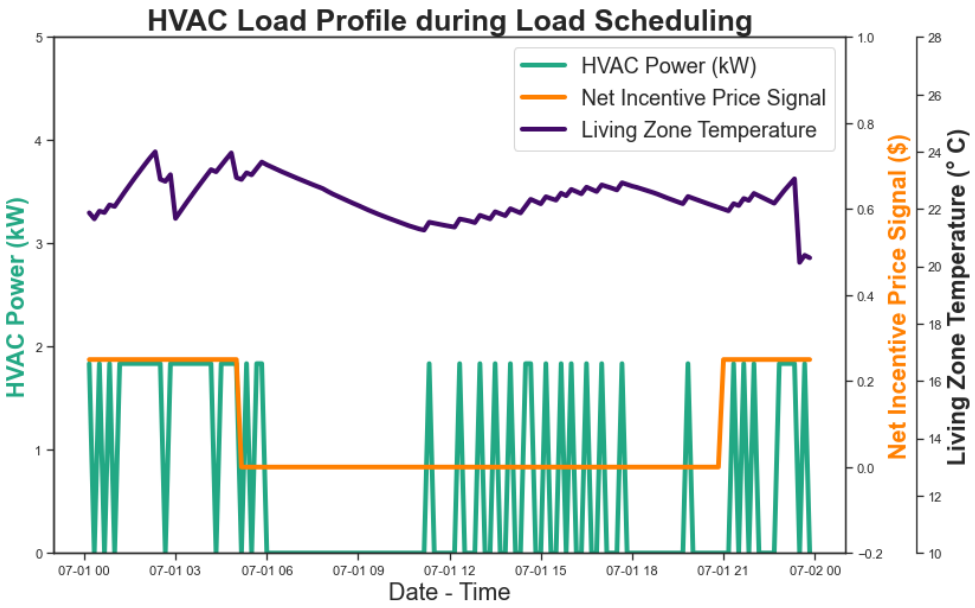

Fig. 5.39: Building 5B HVAC Power Profile During the Load Scheduling Event

evaluated zones.

CHAPTER 6: AGGREGATOR FORMULATION

The framework of how the comprehensive hybrid building optimization framework presented in the last chapter interacts with the smart grid through an aggregator is formulated in this section. First, the aggregator takes direct implemention of the market information, then, characterizes the flexibility limits of the distributed energy resources in its network, then through optimization, implements control strategies to coordinate how the hybrid ventilated buildings respond to requirements from the grid.

6.1 Introduction

The MPC formulation in the last chapter has objective functions formulated to reduce energy costs and improve thermal comfort for hybrid ventilated buildings at each building level. Typically, each building is unable to communicate directly with the operators, as such, a centralized aggregator with the sole responsibility of maintaining demand compliance imposed by the regional operators across multiple homes at a feeder level is required. This is especially important to allow the homes that a geographically co-located to collectively bid on markets and allow any non-conforming effects with the grid to average out after providing their flexibility limits. As such a use case that allows building owners to reduce energy costs and be subjected to TOU pricing while ensuring aggregate demand requirement is maintained is evaluated in the future sections.

6.2 Main Contributions

Bearing in mind the intermittent power operations of hybrid ventilated buildings, the goal of this chapter is to develop a model of the building loads in virtual bat-

teries and characterize their flexibility for resource unification and efficient control realization. As such, the following contributions are achieved

- Proposed a simultaneous optimization-based flexibility characterization strategy and aggregator oversight for a large population of passive buildings designed for special applications such as hybrid ventilation.
- Developed an MPC-based dispatched algorithm for passive building energy resources and a hierarchical coordination framework that allows aggregators to manage effective grid compliance.
- Analytically quantified the benefit assessments of coordinating aggregated distributed loads for grid services rather than independently.

The simulation model consists of a flexibility aggregator model and the comprehensive

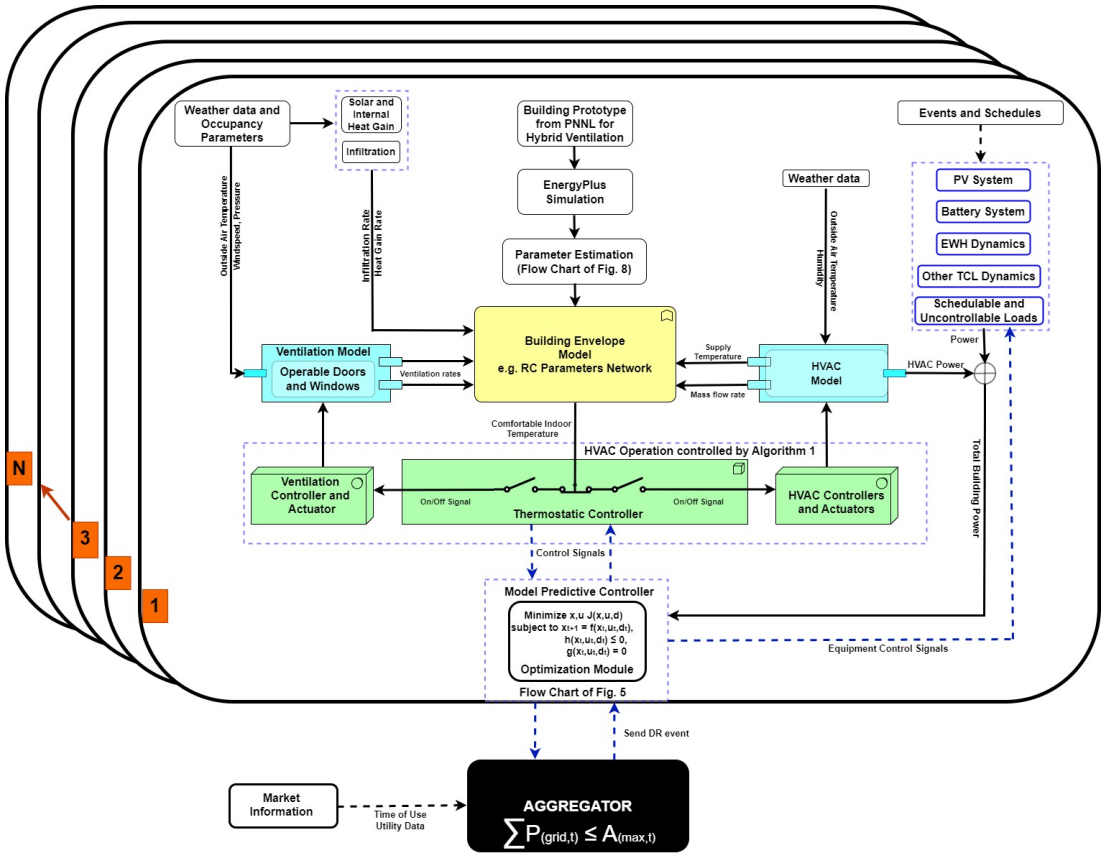

Fig. 6.1: Aggregator integration with the comprehensive hybrid building methodological framework

hybrid modeling framework that house the passive building model, the controller model and their operation modes, and each of the other distributed energy resource in the building. This architecture is represented in Fig. 6.1.

The schematic of how the aggregator receives requirement from the grid is represented in Fig. 6.3 and the functional interaction between the aggregator and the building controllers. The framework also shows the virtual model of resources and their interaction, as well as output at each state variable that impacts the building energy use.

6.3 Flexibility Aggregation Methodology

Different flexible energy resources are essential to be coordinated uniformly for efficient power grid operation. Such resources are often thermostatically controlled including HVAC systems and electric water heaters which have the capacity to store thermal energy and can be conceptualized as the state-of-charge, as power usage coincides directly with the level of their thermal energy. In the subsequent subsections, two examples of virtual battery formulations were presented for the HVAC system and the electric water heater.

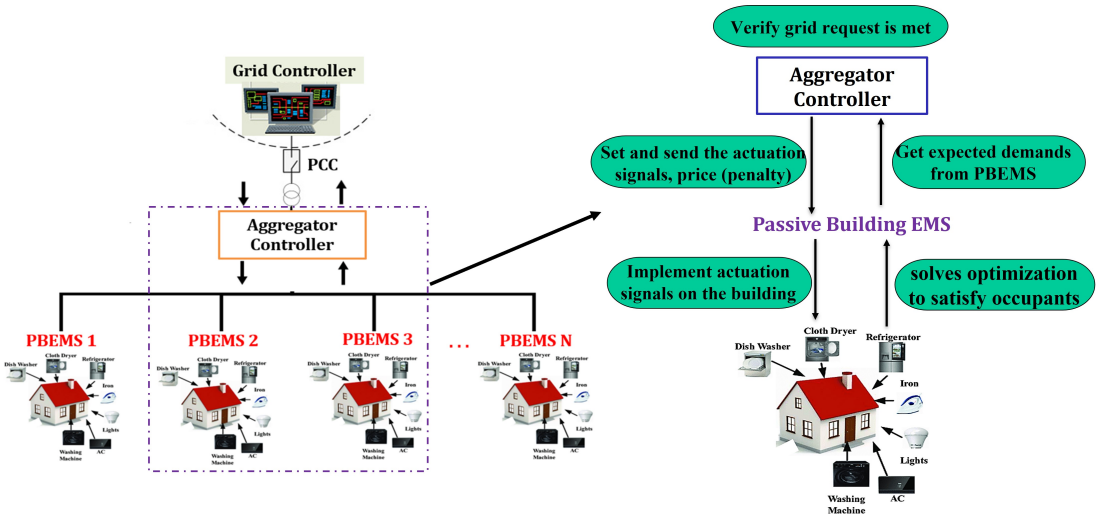

Fig. 6.2: Defined loop interactions between the aggregator and building controllers

The virtual battery model is represented in equation 6.1

$$\dot{X}_t = -\alpha X_t + \Delta P_t \tag{6.1}$$

where α is the self-discharge rate, Δ the size of the discrete time-steps, X_t is the energy state, and P_t is the power input referencing additional power consumed over some base profiles

6.3.1 Virtual Battery Formulation for the HVAC

Considering the large population of passive residential buildings with N number of HVAC equipment, such that $N \gg 1$, the virtual battery representation for the building's HVAC system is represented in equation 6.2. The occupants' comfort requirements are modeled as the virtual energy bounds (state-of-charge) of the battery.

$$\dot{X}_{HVAC,t} = -\alpha_{HVAC} X_{HVAC,t} + \Delta P_{HVAC,t} \tag{6.2}$$

Recall the building thermal dynamic model, the three operational modes (passive, controlled-passive, and active), the mixed operation mode, and the HVAC equipment model represented in Chapter 3.

$$\begin{aligned} C_z \frac{dT_z}{dt} &= \frac{1}{R}(T_a - T_z) + \sum_{adj=1}^{N_z} \frac{1}{R_{adj}}(T_{adj} - T_z) \\ &+ c_p m_{inf}(T_a - T_z) + c_p m_{vent}(T_a - T_z) + Q_{total} + Q_{HVAC} \end{aligned} \tag{6.3}$$

$$P_{base} = Q_{HVAC} \tag{6.4}$$

and Q_{HVAC} is electric power directly associated with the coils to provide sensible heating or cooling rates.

As such, passive building thermal dynamics of equation 6.3 with the integration of

our proposed operation modes in mind as discussed in Chapter 4 needs to be presented as equation 6.2. First, this begins by defining the virtual battery representation of the energy state variable during the HVAC operation, which is given in equation 6.5.

$$X_{HVAC,t} = \frac{C(T_{z,t} - T_{set})}{COP} \tag{6.5}$$

At steady state, it is assumed that $C_z \frac{dT_z}{dt} = 0$ in equation 6.3, as a result, $Q_{HVAC,t}$ represents the base power from the active system $P_{base,t}$, which is the nominal power to keep the indoor temperature at its setpoint, considering the whole thermal dynamics representation, this is given in equation 6.6. The fundamental idea about the formulation of equation 6.6 is presented in [129, 130].

$$\begin{aligned} P_{\text{base,t}} = \sum_{i=1}^{N} \frac{1}{COP^i} [\frac{1}{R^i} \left(T^i_{set} - T^i_{a,t}\right) + \sum_{adj=1}^{N_z} \frac{1}{R_{adj}} (T^i_{set,t} - T^i_{adj,t}) \\ + c_p \dot{m}^i_{inf} (T^i_{set,t} - T^i_{a,t}) + c_p \dot{m}^i_{vent} (T^i_{set,t} - T^i_{a,t}) - Q^i_{total,t})] \end{aligned} \tag{6.6}$$

The upper and lower bounds of the power are represented in equation 6.7 and equation 6.8 where both equations are minimized and maximized respectively

$$P^-_{HVAC,t} = -P_{\text{base,t}} \tag{6.7}$$

$$P^+_{HVAC,t} = \sum_{i=1}^{N} P^i_{HVAC} - P_{\text{base,t}} \tag{6.8}$$

Similarly, the upper and lower energy bounds of the HVAC system are given in equation 6.9 and equation 6.10

$$X^-_{HVAC,t} = \sum_{t=1}^{T} P^-_{HVAC,t} \tag{6.9}$$

$$X^{+}_{HVAC,t} = \sum_{t=1}^{T} P^{+}_{HVAC,t} \tag{6.10}$$

The self-discharge rate which depends on the building's thermal parameters is given in equation 6.11

$$\alpha = \frac{1}{N} \sum_{i=1}^{N} \frac{1}{C^i_z R^i} \tag{6.11}$$

6.3.2 Virtual Battery Formulation for the Electric Water Heater

The single-node Electric Water Heater model of equation 6.12, previously discussed in Chapter 3 is adopted for the virtual battery representation. Consider a large population of electric water heating loads N, such that $N \gg 1$

$$C_w \frac{dT_w}{dt} = \frac{1}{R_w} [T_a - T_w] - \dot{m}_{\mathrm{w}}\, C_p\, (T_w - T_{in}) + UQ_{wh} \tag{6.12}$$

The virtual battery representation of the energy variable of the water heater is given in equation 6.13,

$$X_{w,t} = C(T_{w,t} - T_{w,set}) \tag{6.13}$$

where $X_{w,t}$ represents the energy variable of the electric water heater at time t and $T_{w,set}$ represents the electric water heater temperature setpoint.

As stated earlier that power usage coincides directly with the level of their thermal energy. Thus, in representing the water heater model in form of a virtual battery, equation 6.14 is generated.

$$\dot{X}_{w,t} = -\alpha_w X_{w,t} + \Delta Q_{wh,t} \tag{6.14}$$

If $Q_{wh,t}$ represents the base power $P_{base,t}$. The baseline power and other representations of the virtual battery are given in equation 6.15. Recall U is the water heater

binary control signal for the heating element's on and off.

$$P_{\text{base,t}} = \sum_{i=1}^{N} \left[\frac{1}{R_w^i} \left(T_{w,set}^i - T_{a,t}^i \right) + \dot{m}_t^i C_p \left(T_{w,set}^i - T_{in,t}^i \right) \right] \tag{6.15}$$

The upper and lower bounds of the power are represented in equation 6.16 and equation 6.17.

$$P_{w,t}^- = -P_{\text{base,t}} \tag{6.16}$$

$$P_{w,t}^+ = \sum_{i=1}^{N} P_w^i - P_{\text{base,t}} \tag{6.17}$$

Similarly, the upper and lower energy bounds of the electric water heating system are given in equation 6.18 and equation 6.19.

$$X_{w,t}^- = \sum_{t=1}^{T} P_{w,t}^- \tag{6.18}$$

$$X_{w,t}^+ = \sum_{t=1}^{T} P_{w,t}^+ \tag{6.19}$$

The self-discharge rate which depends on the Water Heater's thermal parameters is given in equation 6.20.

$$\alpha = \frac{1}{N} \sum_{i=1}^{N} \frac{1}{C_w^i} \left(\dot{m}_{w,t}^i C_p^i + \frac{1}{R_w^i} \right) \tag{6.20}$$

6.4 Aggregator Implementation for End User Services

The primary objective of optimal aggregator coordination is to minimize utility cost at a certain time of the day using TOU energy rate. A resource allocation problem is solved to dispatch the virtual battery power to each building controller while the aggregator tracks the maximum power requirement from the grid and the building controllers maintain all comfort constraints and operation requirements are not being

violated. As such, the objective function of the optimization problem is represented in equation 6.21.

$$Minimize \sum_{t=1}^{T} \sum_{i=1}^{N} \left(\left(\pi_t P_t^i \Delta t \right) \right) \tag{6.21}$$

where π_t is the time-of-use (TOU) electricity price at timestep t.

Moreover, the objective function is subjected to the following additional constraints

- Real battery constraint and EV constraint (if applicable) represented in equation 3.8 to equation 3.17
- Aggregate power constraint at every timestep given in equation 6.22

$$\sum_{i=0}^{N} P_t^i \leq A_{\max,t} \tag{6.22}$$

  where $A_{\max,t}^i$ represents the maximum power the aggregator must comply with.

- deterministic flexibility limits results obtained by solving power and virtual energy maximization and minimization problems using the expected base profiles from equations 6.7 to 6.11 and equations 6.15 to 6.20.
- End-user comfort levels which are also virtual battery-related constraints as depicted in equation 6.23 and equation 6.24.

$$X_t^- \leq X_t \leq X_t^+ \tag{6.23}$$

$$P_t^-, \leq P_{\mathrm{t}} \leq P_t^+ \tag{6.24}$$

$$X_t = X_{HVAC} + X_{WH} + X_{\text{batt}} + X_{EV} + X_{\text{non-flex}} \tag{6.25}$$

$$P_t = P_{HVAC} - P_{HVAC_{\text{base}}} + P_{WH} - P_{WH_{\text{base}}} + P_{\text{Batt}} + P_{EV} - P_{EV_{\text{base}}} + P_{\text{non-flexible}} \tag{6.26}$$

Then, the characterized flexible loads results are added to other loads such as the uncontrollable load values of each building, and at every time step to obtain the total flexibility of the buildings.

The proposed flexibility aggregation methodology for the power grid and end-user resources is demonstrated in the framework and logic problem definitions of Fig. 6.3. This is represented using a REDIS client implementation platform with a population of 10 passive buildings, each having a real battery storage system, solar PV system, an electric water heater, an HVAC system, and uncontrollable electrical loads. The passive buildings' flexibilities are characterized by individual homes but implementation states are provided by the aggregator according to equations in 6.7to 6.20. Additionally, the TOU electricity price are from [131]. Additional information about the REDIS platform and how aggregator functions in the platform are explained in [132].

The detailed process for aggregator controller operation when the request is enforced by the system operator is explained in Algorithm 3. Optimize each site flexibility according to Output

To generate a large population of building resources, the passive building thermal parameters and other building energy resource parameters obtained for 10 houses in building zone 3C were randomized using a normal distribution with the mean value represented in Table 3.2 and the standard deviation of 20% of the mean value. Similarly, water heater profiles of the homes were randomly generated from a pool of profiles presented in [133].

6.5 Results and Discussions

For the ten passive buildings, the peak demand attained for the day using the MPC optimization framework of chapter 5 when all buildings were optimized independently was 160 kW. In comparison with an aggregator, the maximum demand achieved during the same period was 97.5 kW which is less than 100kW imposed by the grid controller on the aggregator. Similarly, the total daily energy reduction percentage

Algorithm 3: Aggregator Control Operation

Input $A_{\max,t}$, T_{set}, $T_{w,set}$, C_w
Input R, R_w, C_w, C_z in 6.11, 6.20
At t, compute baseline power $P_{base,t}$ for each resources as in 6.6, 6.15
Output: α, $P_{base,t}$
Aggregator receives baseline power and energy event notice
for *t = 1, 2, 3, ..., T* **do**
    if $\sum_{i=0}^{N} P^i_{grid,t} \leq A_{\max,t}$ **then**
        Minimize energy costs 6.21,
        Prioritize $A_{\max,t}$ 6.22
        Send states X^i_t to individual resources.
    end
    else if $\sum_{i=0}^{N} P^i_{grid,t} > A_{\max,t}$ **then**
        Modify operator's request or compute penalty
        recompute baseline power $P_{base,t}$ using 6.6, 6.15
        Minimize energy costs 6.21 with new price π_n
        Send states X^i_t to individual resources.
    end
    else
        Send states X^i_t to individual resources
    end
    Hold for next event
end
return P^i_t, X^i_t

and the total percentage demand reduction during the TOU event are summarized in 6.1.

Table 6.1: Building 3A Energy Usage Comparison for MPC Control Utilization during TOU rate Event

Period	No Aggregator	Aggregator	% Reduction
Partial Peak	106.57 kW	70.99 kW	33.3
Main Peak (12:00 pm - 6:00 pm)	65.05 kW	36.73 kW	43.5
Day	160 kW	97.5 kW	39
Day	1091.38 kWh	736.92 kWh	32.4

The aggregated power profile and individual building profile during the aggregator optimization are presented in Fig. 6.4. The total flexibility characterization of each building as determined by the aggregator is also depicted in Fig. 6.4. It is also

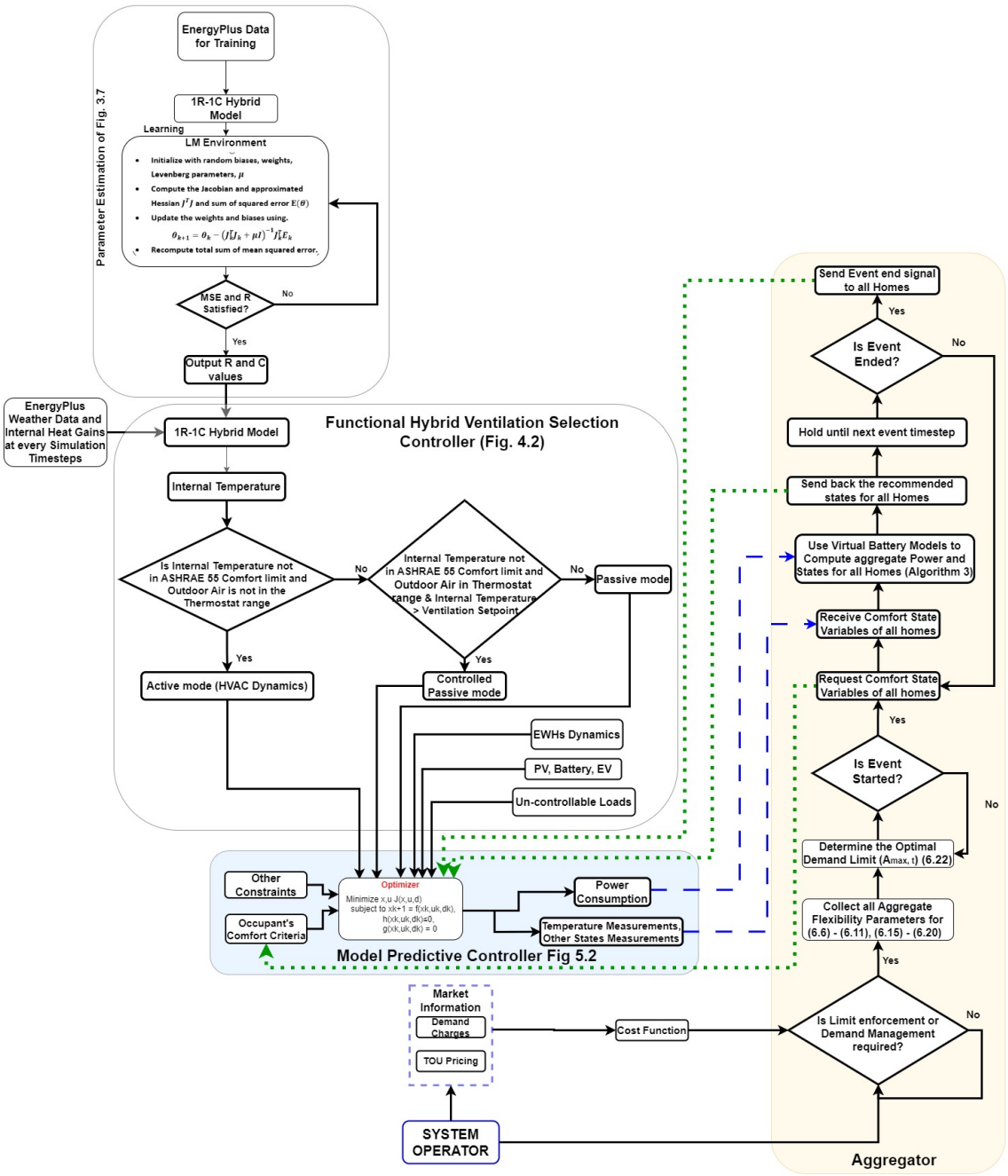

Fig. 6.3: Framework for Aggregator Interaction with all Buildings and Resources

observed that real battery storage significantly prioritizes limiting the average demand to ensure compliance by aggregator according to Fig. 6.8 while in contrast the virtual energy, majorly from the HVAC power profile helps provide both cost savings and demand through hybrid ventilation.

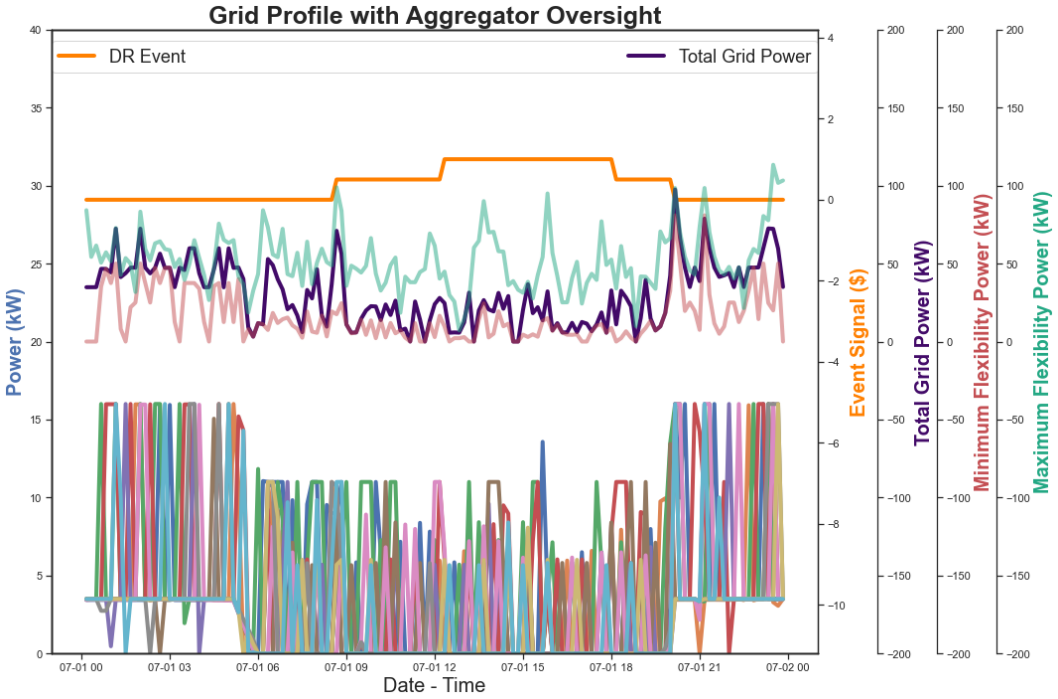

Fig. 6.4: Grid Profile with Aggregator Oversight

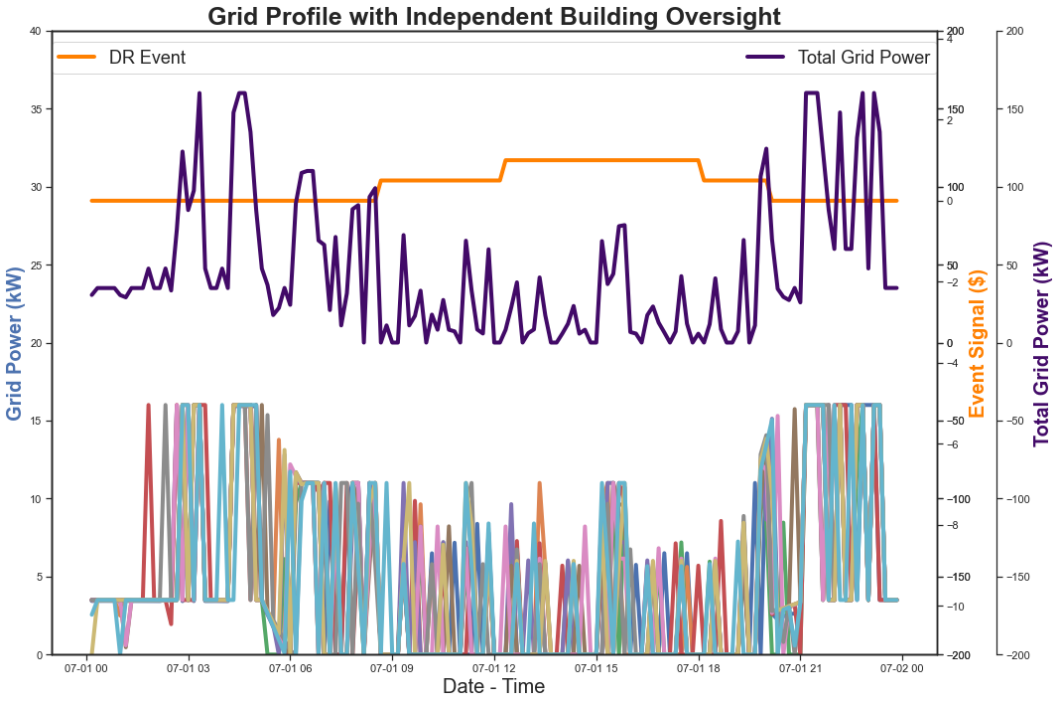

Fig. 6.5: Grid Profile without Aggregator Oversight

The aggregated charge/discharge operations through the average energy states of the battery is illustrated in Fig. 6.8 It can be observed that batteries charge to full

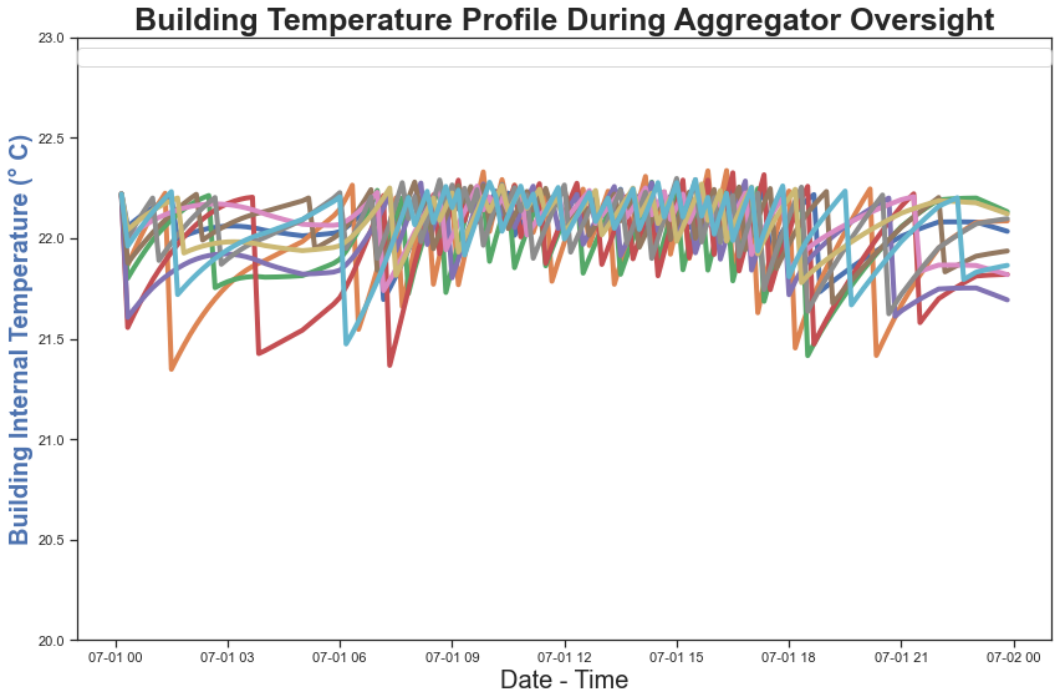

Fig. 6.6: Buildings' Internal Temperature Profile During Aggregator Oversight

capacity prior to the peak hours starting at 8:30 am to save energy and demand during peaks. As such, two periodical peaks were recorded, the first peak prior to the TOU pricing period and the second after the TOU event. Fig. 6.6 and Fig. 6.7 show the aggregated internal temperature profiles of the passive buildings and that of the electric water heater respectively. It is observed that both temperatures are still within the comfort limits, as such no temperature violations occurred as combined energy was significantly reduced.

While the aggregator is able to enforce the limit requirements, either to provide peak shaving or any reliability services that the grid needs, it is worth mentioning that the residential end-users are usually not concerned about demand limits as that is often not included in their rate structure. As a result, energy cost savings become a priority as that is most impactful to residential end-users during the TOU events. As such system operators can carefully craft out their priorities with consumers in mind when examining the impacts of demand limit enforcement during the TOU pricing

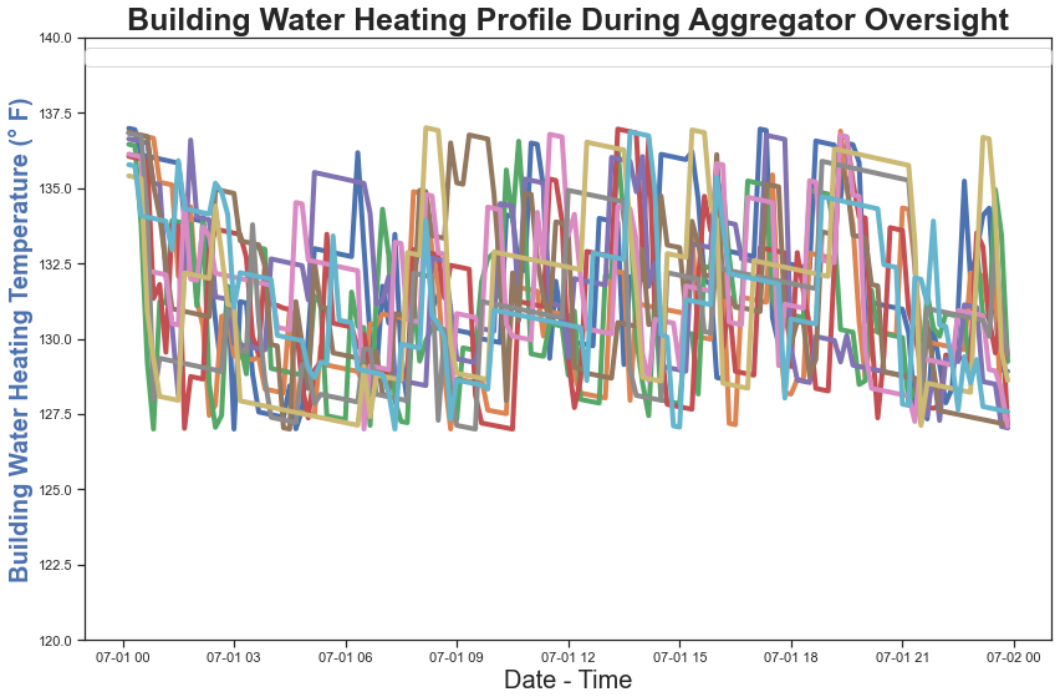

Fig. 6.7: Building Water Heating Profile During Aggregator Oversight

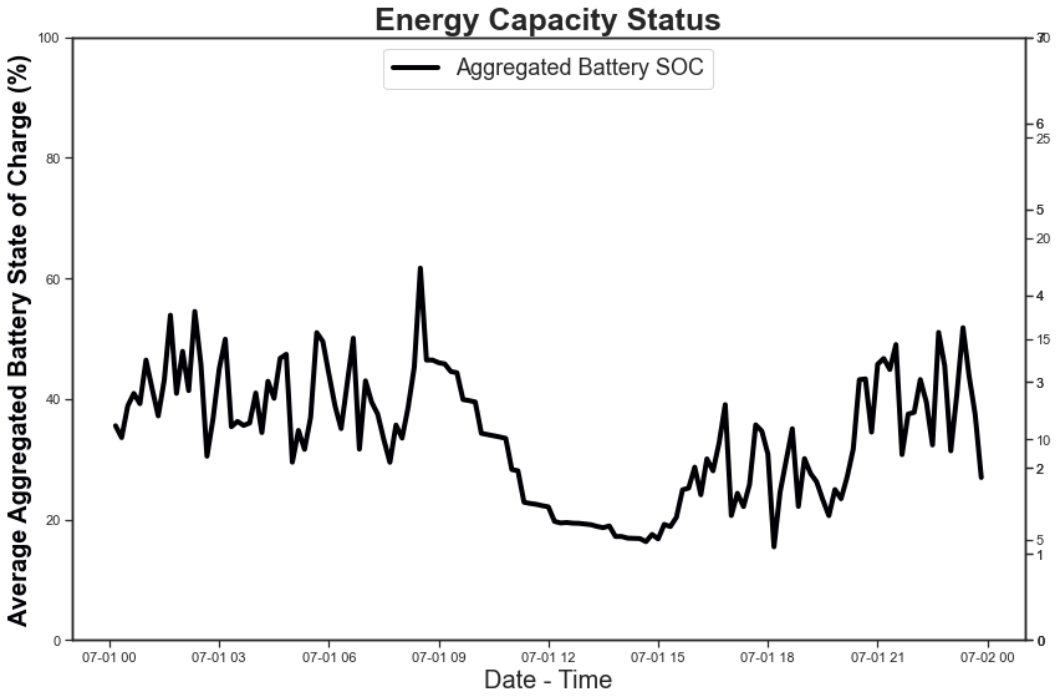

Fig. 6.8: Aggregated Response of charge/discharge operations of the battery

period.

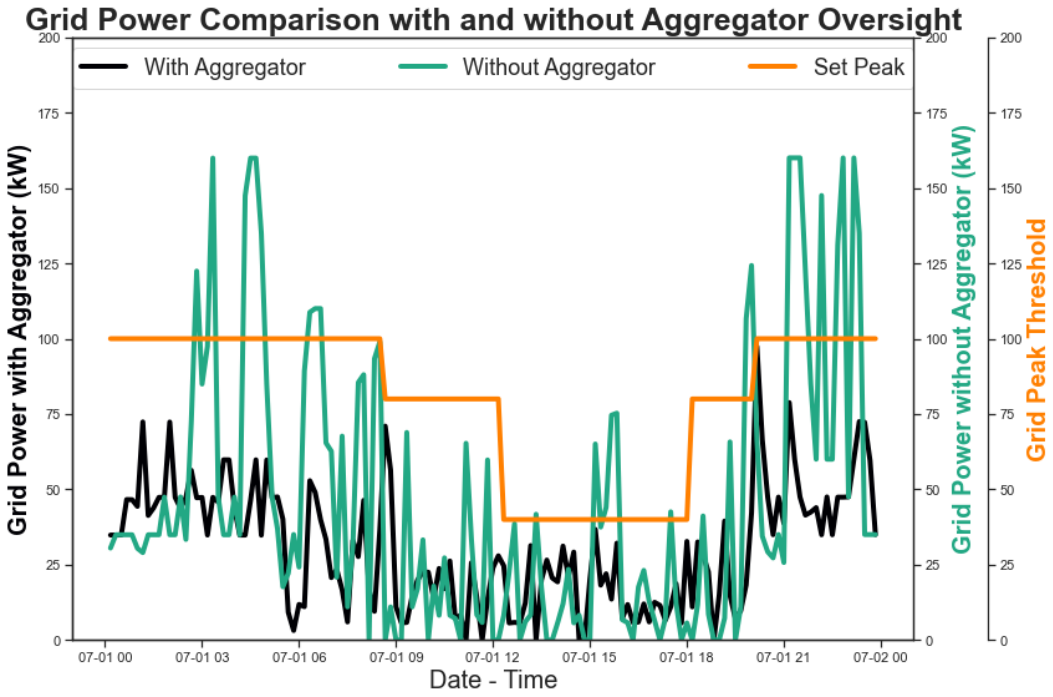

Fig. 6.9: Grid Power Comparison with and without Aggregator Oversight

6.6 Summary

In the presence of N residential building energy end-users geographically co-located in an area and can collectively provide load reduction to influence the grid performance, such service to the grid requires an aggregator that has the capability to unify all the grid resources and enforce certain requirements. The previously discussed models, operation modes, and MPC optimization framework of Chapter 5 were used as a starting point for implementing this aggregator oversight while also characterizing the flexibilities of distributed energy resources across 10 residential passive buildings to reduce peak demand and achieve energy cost savings. A comparison was made to see the benefits of having an aggregator implement the control of the flexible building loads centrally, or allow the building to act on the market information and control their loads independently. It was observed that aggregated control offers additional benefits in achieving 32.4% additional savings in energy costs that impact the end-users while ensuring that no comfort limits violation is recorded

throughout the demand management event period.

CHAPTER 7: CONCLUSIONS AND FUTURE WORK

This dissertation presents an integrated modeling approach with sequential steps in studying the thermal-dynamic operations of passively- designed hybrid ventilated buildings considering their intermittent active power operation. First, the hybrid model, including a procedure for identifying model parameters, was established, and results were compared with EnergyPlus™ counterparts. For this, an average of 4% in CVRMSE error was generated compared with EnergyPlus™ results which is a significant improvement when benchmarking with ASHRAE 14 guidelines requirement that specifies the error to be within 30%.

Second, three distinct functional hybrid operation modes of the developed model for energy management not present in the state-of-the-art were presented and results revealed an average of 70% energy costs reduction impacts on consumers in the evaluated ASHRAE climate zones.

Third, a scalable, generalizable, and extensible energy optimization framework considering all the active energy sources in the building was illustrated, and the results showed that the formulated framework has an intuitive interpretation of prioritizing natural ventilation operation while effectively coordinating building energy resources for a 60% to 65% reduction in peak electricity usage and costs to consumers during the time of use events. Similarly, the model is utilized within Model Predictive Control (MPC) and optimization framework across multiple prediction horizons for evaluating different demand side management events including power reference tracking, and demand response activity with load scheduling capabilities. For this, the results revealed an average of 1.2% error in power reference tracking demonstrating the high accuracy of the developed model and framework in supporting grid services. Also,

49% to 56% gains on incentives to consumers were recorded during load scheduling events in the evaluated zones.

Finally, a distributed energy resource aggregation framework that limits aggregate demand for multiple passive buildings was formulated, to enforce grid limits and simultaneously achieve energy cost savings. The results show that the aggregator framework proves efficient in reducing the aggregate demand of ten passive buildings from 160 kW (without aggregator oversight) to 97.5 kW (with aggregator oversight) while simultaneously providing 34% energy cost savings to end-users.

The future research directions in alignment with this research include:

- The model and controllers including the aggregator framework can be implemented for additional testing of cases or integrated with the IEEE bus systems to solve various grid stability, reliability, and demand-side management problems.

- The hybrid building models and resource clustering formulation of the aggregator algorithms can be further extended for participation in wholesale energy markets.

- The hybrid models can be extended for evaluating different building types, such as commercial buildings and high-rises, considering the variations in dynamics of ventilation across multiple building heights and building components.

- The model can be explored for other extensive applications with hybrid-ventilated buildings, including demand management programs, frequency regulations, ancillary services, real-time resource controls, and other transactive operations.

REFERENCES

[1] U.S. Department of Energy, Energy Information Administration Independent Statistics and Analysis, "Annual Energy Outlook 2022," 2022. https://www.eia.gov/outlooks/aeo/.

[2] U.S. Department of Energy, Energy Information Administration Independent Statistics and Analysis, "Today in Energy:Global energy consumption driven by more electricity in residential, commercial buildings," 2019. https://www.eia.gov/todayinenergy/detail.php?id=41753.

[3] U.S. Department of Energy, Energy Information Administration Independent Statistics and Analysis, "Today in Energy:EIA projects nearly 50% increase in world energy usage by 2050, led by growth in Asia," 2019. https://www.eia.gov/todayinenergy/detail.php?id=41433.

[4] Worldwatch Institute, "State of the World â Into a Warming World," 2019. http://www.worldwatch.org/files/pdf/SOW09_chap3.pdf.

[5] U.S. Department of Energy, Energy Information Administration Independent Statistics and Analysis, "Today in Energy. EIA forecasts renewables will be fastest growing source of electricity generation," 2019. https://www.eia.gov/todayinenergy/detail.php?id=38053.

[6] R. Dunlap, "Sustainable energy: Second edition," *Boston: Cengage*, 2017.

[7] U.S. Department of Energy, Energy Information Administration Independent Statistics and Analysis, "How much energy is consumed in U.S. buildings?," 2022. https://www.eia.gov/tools/faqs/faq.php?id=86&t=1.

[8] I. Yuksek and T. Karadayi, "Energy-efficient building design in the context of building life cycle," *Energy Efficient Buildings*, pp. 52–62, 2017.

[9] A. Ipakchi and F. Albuyeh, "Grid of the future," *IEEE power and energy magazine*, vol. 7, no. 2, pp. 52–62, 2009.

[10] H. Wang, S. Wang, and R. Tang, "Development of grid-responsive buildings: Opportunities, challenges, capabilities and applications of hvac systems in non-residential buildings in providing ancillary services by fast demand responses to smart grids," *Applied Energy*, vol. 250, no. 2, pp. 697–712, 2019.

[11] Passive House Institute, "Criteria for the Passive House," *EnerPHit and PHI Low Energy Building Standard,Rheinstr, Germany*, no. 64283, pp. 44–46, 2015.

[12] B. Wachenfeldt, "Natural ventilation in buildings. detailed prediction of energy performance," *Electronic Theses and Dissertations*, Jun 2003.

[13] U.S. Department of Energy, Energy Information Administration Independent Statistics and Analysis, "Annual Energy Outlook 2022:Electricity," 2022. https://www.eia.gov/outlooks/aeo/narrative/electricity/sub-topic-01.php.

[14] R. Adhikari, "Algorithms and simulation framework for residential demand response," *Electronic Theses and Dissertations*, 2019.

[15] SmartGrid Consumer Collaborative, "Consumer Pulse and Market Segment Study-Wave 6," 2017 (accessed April , 2021). https://smartenergycc.org/consumer-pulse-wave-6-report/.

[16] A. Afram and F. Janabi-Sharifi, "Black-box modeling of residential hvac system and comparison of gray-box and black-box modeling methods," *Energy and Buildings*, vol. 94, pp. 124–129, 2015.

[17] F. Amara, K. Agbossou, A. Cárdenas, Y. Dubé, and S. Kelouwani, "Comparison and simulation of building thermal models for effective energy management," *Smart Grid and Renewable Energy*, vol. 06, pp. 95–112, 2015.

[18] Z. Yang, X. Li, C. P. Bowers, T. Schnier, K. Tang, and X. Yao, "An efficient evolutionary approach to parameter identification in a building thermal model," *IEEE Transactions on Systems, Man, and Cybernetics, Part C (Applications and Reviews)*, vol. 42, no. 6, pp. 957–969, 2012.

[19] Z. Afroz, G. Shafiullah, T. Urmee, and G. Higgins, "Modeling techniques used in building HVAC control systems: A review," *Renewable and Sustainable Energy Reviews*, vol. 83, no. C, pp. 64–84.

[20] P. Bacher and H. Madsen, "Identifying suitable models for the heat dynamics of buildings," *Energy and Buildings*, vol. 43, no. 7, pp. 1511–1522, 2011.

[21] A. Kathirgamanathan, M. De Rosa, E. Mangina, and D. P. Finn, "Data-driven predictive control for unlocking building energy flexibility: A review," *Renewable and Sustainable Energy Reviews*, vol. 135, pp. 110–120, 2021.

[22] X. Li and R. Yao, "Modelling heating and cooling energy demand for building stock using a hybrid approach," *Energy and Buildings*, vol. 235, pp. 110–740, 2021.

[23] B. Tashtoush, M. Molhim, and M. Al-Rousan, "Dynamic model of an hvac system for control analysis," *Energy*, vol. 30, no. 10, pp. 1729–1745, 2005.

[24] M. Wetter, "A view on future building system modeling and simulation," *Lawrence Berkeley National Laboratory Technical Report*, 2011.

[25] S. Zhan and A. Chong, "Data requirements and performance evaluation of model predictive control in buildings: A modeling perspective," *Renewable and Sustainable Energy Reviews*, vol. 142, p. 110835, 2021.

[26] X. Li and J. Wen, "Review of building energy modeling for control and operation," *Renewable and Sustainable Energy Reviews*, vol. Volume 37, pp. 517–537, 2014.

[27] H. Hao, D. Wu, J. Lian, and T. Yang, "Optimal coordination of building loads and energy storage for power grid and end user services," *IEEE Transactions on Smart Grid*, vol. 9, no. 5, pp. 4335–4345, 2018.

[28] R. Ariwoola, "Use of drone and infrared camera for a campus building envelope study," *Electronic Theses and Dissertations*, 2016.

[29] Z. T. Taylor, K. Gowri, and S. Katipamula, "Gridlab-d technical support document: Residential end-use module version 1.0," 7 2008.

[30] U.S. Environmental Protection Agency, "About the U.S. Electricity System and its Impact on the Environment," 2022. `https://www.epa.gov/energy/about-us-electricity-system-and-its-impact-environment`.

[31] U.S. Department of Energy, Energy Information Administration, Independent Statistics Analysis, "Use of energy explained," 2021. `https://www.https://www.eia.gov/energyexplained/use-of-energy/`.

[32] U.S. Department of Energy, Energy Information Administration, Independent Statistics and Analysis, "Residential Energy Consumption Survey - RECS," 2009. `https://www.eia.gov/consumption/residential/reports/2009/air-conditioning.php`.

[33] U.S. Department of Energy, Quadrennial Technology Review, "An assessment of energy Technologies and research Opportunities," 2015. `https://www.energy.gov/sites/prod/files/2017/03/f34/qtr-2015-chapter5.pdf`.

[34] U.S. Environmental Protection Agency, "Electricity Customers," 2022. `https://www.epa.gov/energy/electricity-customers`.

[35] S. Emmerich, W. Dols, and J. Axley, "Natural ventilation review and plan for design and analysis tools," *National institute of Standards and Technology, U.S. Department of Commerce*, 2001.

[36] M. R. Bashir and A. Q. Gill, "Iot enabled smart buildings: A systematic review," pp. 151–159, 2017.

[37] A. A. Khan and H. T. Mouftah, "Energy optimization and energy management of home via web services in smart grid," in *2012 IEEE Electrical Power and Energy Conference*, pp. 14–19, 2012.

[38] S. Ahmadzadeh, G. Parr, and W. Zhao, "A review on communication aspects of demand response management for future 5g iot- based smart grids," *IEEE Access*, vol. 9, pp. 77555–77571, 2021.

[39] G. Wright and K. Klingenberg, "Climate-specific passive building standards," *USDOE Passive House Institute US*, 2015.

[40] Global Alliance for Buildings and Construction, "2020 global status report for buildings and construction," 2020. https://globalabc.org/sites/default/files/inline-files/2020%20Buildings%20GSR_FULL%20REPORT.pdf.

[41] D. Johnston, M. Siddall, O. Ottinger, S. Peper, and W. Feist, "Are the energy savings of the passive house standard reliable? a review of the as-built thermal and space heating performance of passive house dwellings from 1990 to 2018," *Energy Efficiency*, vol. 13, p. 1605â1631, 2020.

[42] S. Peper and H. Bahnstadt, "Minimal monitoring in selected building complexes," *Passive House Institute Interim Report*, 2015.

[43] S. Peper, "Passivhaus BuildTog Bremen-Findorff," 2021. Passivhaus Institut.

[44] M. Krellner, "Annual heat meter readings of four semi-detached houses in nuremberg-wetzdorf," 2015.

[45] Techem Energy Services: Energiekennwerte, "Hilfen fÃŒr den Wohnungswert," 2014 (accessed March , 2023). Eschborn.

[46] Passipedia - The Passive House Resource, "Energy efficiency of the Passive House Standard: Expectations confirmed by measurements in practice," 2022 (accessed March, 2023). https://passipedia.org/operation/operation_and_experience/measurement_results/energy_use_measurement_results#literature.

[47] WHO, "Infection prevention and control during health care when coronavirus disease (COVID-19) is suspected or confirmed," 2020 (accessed March, 2023). https://apps.who.int/iris/handle/10665/332879.

[48] ASHRAE, "ASHRAE Position Document on Infectious Aerosols," 2022 (accessed March, 2023). https://www.ashrae.org/file%20library/about/position%20documents/pd_-infectious-aerosols-2022.pdf.

[49] W. Zheng, J. Hu, Z. Wang, J. Li, Z. Fu, H. Li, J. Jurasz, S. Chou, and J. Yan, "Covid-19 impact on operation and energy consumption of heating, ventilation and air-conditioning (hvac) systems," *Advances in Applied Energy*, vol. 3, 2020.

[50] ASHRAE, "ASHRAE Issues Statements on Relationship Between COVID-19 and HVAC in Buildings," 2020 (accessed March, 2023). https://www.ashrae.org/about/news/2020/ashrae-issues-statements-on-relationship-between-covid-19-and-hvac-in-buildi
~:text=ASHRAE%20officially%20opposes%20the%20advice,the%20spread%20of%20the%20virus.

[51] United States Environmental Protection Agency, "Energy cost and IAQ performance of ventilation systems and controls," 2000 (accessed March, 2023).

[52] S. Dutton and W. Fisk, "Energy and indoor air quality implications of alternative minimum ventilation rates in California offices," *Building and Environment*, vol. 82, pp. 121–127, 2014.

[53] S. Park, Y. Choi, D. Song, and E. Kim, "Natural ventilation strategy and related issues to prevent coronavirus disease 2019 (covid-19) airborne transmission in a school building," *Sci Total Environ*, vol. 789, 2021.

[54] A. Maddie, "Penn State, among other universities, targeted in international hack," 2019 (accessed March, 2023). https://www.collegian.psu.edu/news/penn-state-among-other-universities-targeted-in-international-hack/article_645aaca6-41b7-11e9-af89-ffe0930611fa.html.

[55] Internet of Business, "Hackers used flaws in IoT devices to take down university network," 2017 (accessed March, 2023). https://internetofbusiness.com/hackers-iot-devices-university-network/.

[56] G. Burke and J. Fahey, "AP Investigation: US power grid vulnerable to foreign hacks," 2015 (accessed March, 2023). https://apnews.com/article/technology-iran-san-jose-california-hacking-c8d531ec05e0403a90e9d3ec0b8f83c2.

[57] PHIUS, "Passive House/Building Frequently Asked Questions," 2023 (accessed March, 2023). https://www.phius.org/passive-building/what-passive-building/passive-building-faqs#:~:text=Currently%2C%20a%20passive%20building%20typically,the%20smaller%20the%20cost%20difference.

[58] U.S. Department of Energy, Energy Information Administration Independent Statistics and Analysis, "Electric Utility Demand Side Management - Archive ," 2001. https://www.eia.gov/electricity/data/eia861/dsm/#:~:text=Demand%2Dside%20management%20(DSM),and%20pattern%20of%20electricity%20usage.

[59] Q. Qdr, "Benefits of demand response in electricity markets and recommendations for achieving them," *U.S. Department of Energy*, 2006.

[60] FERC, "National Assessment and Action Plan on Demand Response," 2020 (accessed September 29, 2022). https://www.ferc.gov/electric/industry-activity/demand-response/national-assessment-and-action-plan-demand-response.

[61] U.S. Department of Energy, Energy Information Administration Independent Statistics and Analysis, "Today in Energy:Demand-side management programs save energy and reduce peak demand," 2022. https://www.eia.gov/todayinenergy/detail.php?id=38872.

[62] Duke Energy, "Duke energy carolinas 2020 integrated resource plan," *Duke Energy Carolinas Integrated Resource Plan 2020 Biennial Report*, 2020.

[63] J. McAnany, "2018 demand response operations markets activity report," *PJM Demand Side Response Operations*, 2019.

[64] J. McAnany, "2021 demand response operations markets activity report," *PJM Demand Side Response Operations*, 2022.

[65] M. Parvania and M. Fotuhi-Firuzabad, "Demand response scheduling by stochastic scuc," *IEEE Transactions on Smart Grid*, vol. 1, no. 1, pp. 89–98, 2010.

[66] V. S. K. Murthy Balijepalli, V. Pradhan, S. A. Khaparde, and R. M. Shereef, "Review of demand response under smart grid paradigm," in *ISGT2011-India*, pp. 236–243, 2011.

[67] A. Malik and J. Ravishankar, "A review of demand response techniques in smart grids," in *2016 IEEE Electrical Power and Energy Conference (EPEC)*, pp. 1–6, 2016.

[68] M. S. Behera and S. K. Jain, "A review on different techniques of demand response management and its future scopes," pp. 1–8, 2021.

[69] A. Ailin and T. Kevin, "Optimal use of incentive and price based demand response to reduce costs and price volatility," *Electric Power Systems Research*, vol. 144, pp. 215–223, 2017.

[70] San Diego Gas Electric, "Time of Use Plus (Critical Peak Pricing CPP)," 2022. https://www.sdge.com/businesses/savings-center/energy-management-programs/demand-response/critical-peak-pricing#:~:text=*%20Critical%20Peak%20Pricing%20(CPP),charges%20for%20the%20time%20period.

[71] San Diego Gas Electric, "Base Interruptible Program," 2022. https://www.sdge.com/businesses/savings-center/energy-management-programs/demand-response/base-interruptible-program#:~:text=The%20Base%20Interruptible%20Program%20provides,%246.30%20per%20kW%20are%20available.

[72] San Diego Gas Electric, "Capacity Bidding Program," 2022. https://www.sdge.com/businesses/savings-center/energy-management-programs/demand-response/capacity-bidding-program.

[73] PGE, "Capacity Bidding Program," 2022. https://www.pge.com/en_US/large-business/save-energy-and-money/energy-management-programs/energy-incentives/third-party-programs-capacity-bidding.page.

[74] ClearlyEnergy, "Residential Direct Load Control Programs)," 2022. https://www.clearlyenergy.com/residential-demand-response-programs.

[75] Entergy Arkansas, Inc, "Summer Advantage Program)," 2022. http://www.entergy-arkansas.com/your_home/save_money/EE/summer-advantage.aspx.

[76] what-when-how, "Pricing Programs: Time-of-Use and Real Time (Energy Engineering)," 2008 (accessed September 25, 2022). http://what-when-how.com/energy-engineering/pricing-programs-time-of-use-and-real-time-energy-engineering/.

[77] Energy.gov, "About Building Energy Modeling," 2022. https://www.energy.gov/eere/buildings/about-building-energy-modeling.

[78] NREL, "BEopt: Building Energy Optimization Tool," 2016. https://www.nrel.gov/buildings/beopt.html.

[79] TRACE, "Introduction to TRACE 700," 2022. https://energy-models.com/training/trace-700/introduction.

[80] Designbuilder, "Simulation Made Easy," 2022. https://designbuilder.co.uk/.

[81] eQuest, "eQUEST the QUick Energy Simulation Tool," 2022. https://www.doe2.com/equest/.

[82] TRNSYS, "Transient System Simulation Tool," 2022. https://www.trnsys.com/.

[83] H. Fennel, "Building envelope theory; r-value drift," pp. 1729–1745, 2015. http://www.foam-tech.com/theory/rvaluedrift.htm.

[84] AFM Corporation, "Long-Term Thermal Resistance," 2014. www.afmcorporation.com/wp-content/uploads/downloads//Foam-Control%20EPS%20Update%20-%20LTTR.pdf.

[85] N. Iole, S. Sfarra, and A. Dario, "Quantitative thermography for the estimation of the u-value: state of the art and a case study," *Journal of Physics; Conference series*, vol. 5, no. 47, pp. 4358–4365, 2014.

[86] J. Carmody and K. Haglund, "Measure guideline: Energy-efficient window performance and selection," *The National Renewable Energy Laboratory Technical Report*, 2012.

[87] T. Hong, "Modeling and simulation of human behavior in buildings," *Lawrence Berkeley National Laboratory Technical Report*, 2015.

[88] S. M. Dutton, H. Zhang, Y. Zhai, E. A. Arens, Y. B. Smires, S. L. Brunswick, K. S. Konis, and P. Haves, "Application of a stochastic window use model in energyplus," in *SimBuild 2012, 5th National Conference of IBPSA-USA, August 1-3, 2012*, (Madison, WI), 2012.

[89] Y. CMJ, "Statistical modelling and forecasting schemes for air-conditioning system," *Theses, Ann. Arbor.. Hong Kong Polytechnic University (Hong Kong)*, 2008.

[90] A. Abbas and B. Chowdhury, "A data-driven approach for providing frequency regulation with aggregated residential hvac units," in *2019 North American Power Symposium (NAPS)*, pp. 1–6, 2019.

[91] X. Xu, Y. Jia, Y. Xu, Z. Xu, S. Chai, and C. S. Lai, "A multi-agent reinforcement learning-based data-driven method for home energy management," *IEEE Transactions on Smart Grid*, vol. 11, no. 4, pp. 3201–3211, 2020.

[92] R. Z. Homod, "Review on the hvac system modeling types and the shortcomings of their application," *Hindawi Journal of Energy*, vol. 2013, pp. 1–10, 2009.

[93] K. K. Andersen, H. Madsen and L. H. Hansen, "Modelling the heat dynamics of a building using stochastic differential equations," *Energy and Buildings*, vol. 31, p. 13â24, Jul. 2000.

[94] Z. Vána, J. Kubecek, and L. Ferkl, "Notes on finding black-box model of a large building," *2010 IEEE International Conference on Control Applications*, pp. 1017–1022, 2010.

[95] A. Abbas, R. Ariwoola, S. Kamalasadan and B. Chowdhury, "Evaluation of hybrid commercial building models for grid interactive building simulations," in *53rd North American Power Symposium*, pp. 1–6, 2021.

[96] C. Jianli, A. Godfried, and S. Xinyi, "Evaluating the potential of hybrid ventilation for small to medium sized office buildings with different intelligent controls and uncertainties in us climates," *Energy and Buildings*, vol. 158, pp. 1648–1661, 2018.

[97] H. Hao, B. M. Sanandaji, K. Poolla, and T. L. Vincent, "A generalized battery model of a collection of thermostatically controlled loads for providing ancillary service," in *51st Annual Allerton Conference on Communication, Control, and Computing (Allerton)*, pp. 551–558, 2013.

[98] A. Akintonde, R. Ariwoola, C. Badrul, and S. Kamalasadan, "Evaluation of equivalent battery model representations for thermostatically controlled loads in commercial buildings," in *In Print:2022 IEEE Industry Applications Society Annual Meeting (IAS)*, pp. 1–8, IEEE, 2021.

[99] E. T. Maddalena, Y. Lian, and C. N. Jones, "Data-driven methods for building control â A review and promising future directions," *Control Engineering Practice*, vol. 95, p. 104211, 2020.

[100] S. Soyguder and H. Alli, "An expert system for the humidity and temperature control in hvac systems using anfis and optimization with fuzzy modeling approach," *Energy and Buildings*, vol. 41, no. 8, pp. 814–822, 2009.

[101] J. W. Moon, J. C. Park, and S. Kim, "Development of control algorithms for optimal thermal environment of double skin envelope buildings in summer," *Building and Environment*, vol. 144, pp. 657–672, 2018.

[102] M. Toub, M. Shahbakhti, R. D. Robinett, and G. Aniba, "MPC-trained ANFIS for Control of MicroCSP Integrated into a Building HVAC System," in *2019 American Control Conference*, pp. 241–246, 2019.

[103] R. Ariwoola and S. Kamalasadan, "Integrated hybrid thermal dynamics model for residential building," in *2021 IEEE Industry Applications Society Annual Meeting (IAS)*, pp. 1–8, IEEE, 2021.

[104] EnergyPlus™ 2022. `https://energyplus.net/`.

[105] S. J. Hossain, T. Paul, R. Bisht, A. Suresh, and S. Kamalasadan, "An integrated battery power dispatch architecture for end-user-driven microgrid in islanded and grid-connected mode of operation," *IEEE Transactions on Industry Applications*, vol. 54, pp. 3806–3819, 2018.

[106] M. Deru, K. Field, D. Benne, B. Griffith, P. Torcellini, B. Liu, M. Halverson, D. Winiarski, and et. al, "U.S. Department of Energy residential reference building models of the national building stock," 2011.

[107] ArchDaily, "How Does a Trombe Wall Work?," 2022. `https://www.archdaily.com/946732/how-does-a-trombe-wall-work`.

[108] ANSI/ASHRAE Standard 55: 2017, "Thermal Environmental Conditions for Human Occupancy," 2017.

[109] B. M. Wilamowski and H. Yu, "Improved computation for levenbergâmarquardt training," *IEEE Transactions on Neural Networks*, vol. 21, no. 6, pp. 930–937, 2010.

[110] M. I. A. Lourakis, "A brief description of the levenberg-marquardt algorithm implemented by levmar," *Institute of Computer Science Foundation for Research and Technology - Hellas (FORTH)*, 2005.

[111] ASHRAE Standard 14: 2014, "Measurement of Energy and Demand Savings; Technical Report; American Society of Heating, Ventilating, and Air Conditioning Engineers," 2014.

[112] ASHRAE Standard 14: 2002, "Measurement of Energy and Demand Savings; Technical Report; American Society of Heating, Ventilating, and Air Conditioning Engineers," 2002.

[113] Rheem, "Water Heater Datasheet," 2022. https://s3.amazonaws.com/WebPartners/ProductDocuments/8EA53647-1458-4512-BCAB-2A28BCC3572D.pdf.

[114] TESLA Power Wall II, "Powerwall 2 AC Datasheet," 2022. https://www.tesla.com/sites/default/files/pdfs/powerwall/Powerwall_2_AC_Datasheet_EN_NA.pdf.

[115] F. David, V. Ramasamy, R. Fu, A. Ramdas, J. Desai, and R. Margolis, "U.S. Solar Photovoltaic System Cost Benchmark: Q1 2020," *National Renewable Energy Laboratory*, 2021.

[116] S. Matasci, "What is the average solar panel size and weight?," 2020. https://news.energysage.com/average-solar-panel-sizeweight/.

[117] NREL, "Best Research-Cell Efficiency Chart," 2021. https://www.nrel.gov/pv/cell-efficiency.html.

[118] ANSI/ASHRAE Standard 90.2: 2018, "Energy Efficient Design of Low-Rise Residential Buildings," 2018.

[119] National Oceanic and Atmospheric Administration, "U.S. Climate Normals," 2022. https://www.ncei.noaa.gov/products/land-based-station/us-climate-normals.

[120] R. Ariwoola and S. Kamalasadan, "A simplified functional hybrid operation mode for grid-interactive building energy management," in *2022 IEEE International Conference on Power Electronics, Smart Grid, and Renewable Energy (PESGRE)*, pp. 1–6, 2022.

[121] R. de Dear and G. Brager, "Thermal comfort in naturally ventilated buildings: revisions to ashrae standard 55," *Energy and Buildings*, vol. 34, pp. 549–561, 2002.

[122] R. Ariwoola and S. Kamalasadan, "An integrated hybrid thermal dynamics model and energy aware optimization framework for grid-interactive residential building management," *IEEE Transactions on Industry Applications*, pp. 1–12, 2022.

[123] Gurobi Optimization, LLC, "Gurobi Optimizer Reference Manual," 2021.

[124] Time-Of-Use Rate Plans. PG and E. Retrieved July 12, 2021 from https://www.pge.com/en-US/residential/rate-plans.

[125] Rocky Mountain Power, "Time-based pricing," 2023 (accessed March, 2023). https://www.rockymountainpower.net/savings-energy-choices/time-of-day.html.

[126] Duke Energy Carolinas, "Residential Time-of-Use Rate Program," 2023 (accessed March, 2023). https://www.duke-energy.com/home/billing/time-of-use.

[127] R. Lv, Z. Yuan, B. Lei, J. Zheng, and X. Luo, "Model Predictive Control with Adaptive Building Model for Heating Using the Hybrid Air-Conditioning System in a Railway Station," *Energies*, vol. 14, no. 7, 2021.

[128] Bonneville Power Administration, "Integrating renewables into the generation mix: challenges and unknowns," *Tech. rep. Docket 11-IEP-1N, PSI Media*, 2011.

[129] A. Bhattacharya, J. Hansen, K. Kalsi, J. Lian, S. P. Nandanoori, H. Reeve, V. Adetola, F. Lin, T. Leichtman, S. N. Gourisetti, W. Hofer, S. Kundu, L. Marinovici, S. Niddodi, D. Vrabie, M. Chiodo, S. Yuan, and D. Wright, "Incentive-based control and coordination of distributed energy resources,"

[130] A. Abbas, R. Ariwoola, B. Chowdhury, S. Kamalasadan, and Y. Lin, "Evaluation of equivalent battery model representations for thermostatically controlled loads in commercial buildings," in *2022 IEEE Industry Applications Society Annual Meeting (IAS)*, pp. 1–6, 2022.

[131] PGE, "Commercial/Industrial Electric Rates," 2023. https://www.pge.com/en_US/small-medium-business/your-account/rates-and-rate-options/time-of-use-rates.page.

[132] Redis, "A vibrant, open source database," 2023. https://redis.io/.

[133] X. Kou, F. Li, J. Dong, M. Starke, J. Munk, T. Kuruganti, and H. Zandi, "A distributed energy management approach for residential demand response," in *2019 3rd International Conference on Smart Grid and Smart Cities (ICSGSC)*, pp. 170–175, 2019.